宇宙線観測で探る宇宙の進化

藤井 俊博（京都大学）fujii@cr.scphys.kyoto-u.ac.jp

「相対論的現象で探る宇宙の進化 I 」

ホテルサザンコースト宮古島　2020年3月28日

宇宙線観測で探る宇宙の進化

- 極高エネルギー(E > 10^{18} eV) 宇宙線観測
  - 観測量：エネルギー、粒子種（の指標となる値）、到来方向
    - Energy spectrum, mass/chemical composition, anisotropy
- 宇宙線観測で探る宇宙の進化
  - ソース密度が遠方でどのように変化しているか？ $Q(E,z) \propto E^{-p}(1+z)^m$
    - エネルギースペクトルの形に影響する
- 来年度の学術変革領域（B）へ向けたアイディアの検討
  - 学問分野に新たな変革や転換をもたらし、既存の学問分野の枠に収まらない新興・融合領域の創成が期待できる基礎的研究 (基礎から応用への展開を目指すものを含む)

エネルギースペクトル

$E^{2.6}\ F(E)$

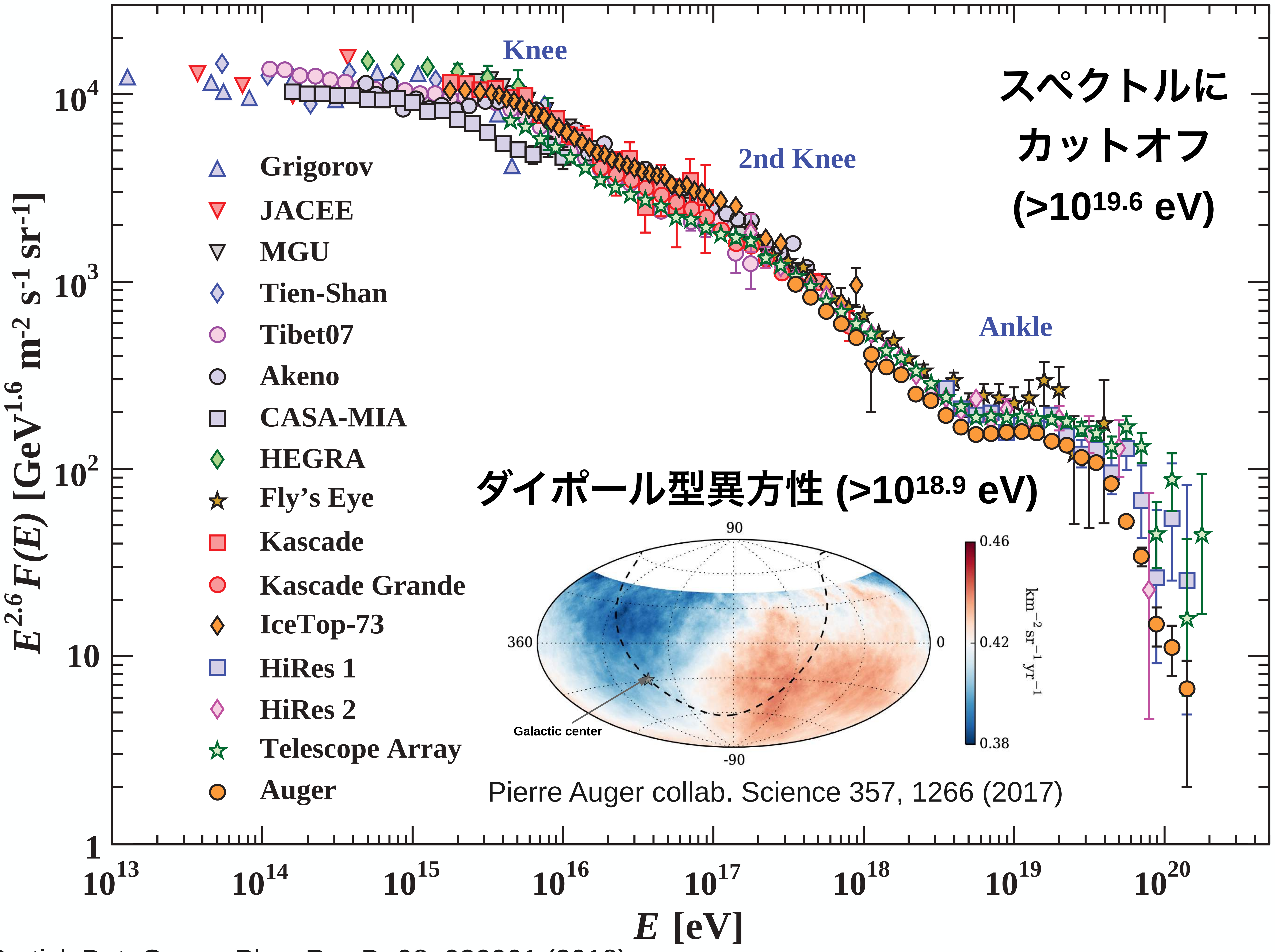

ParticleDataGroup, Phys.Rev.D, 98, 030001 (2018)

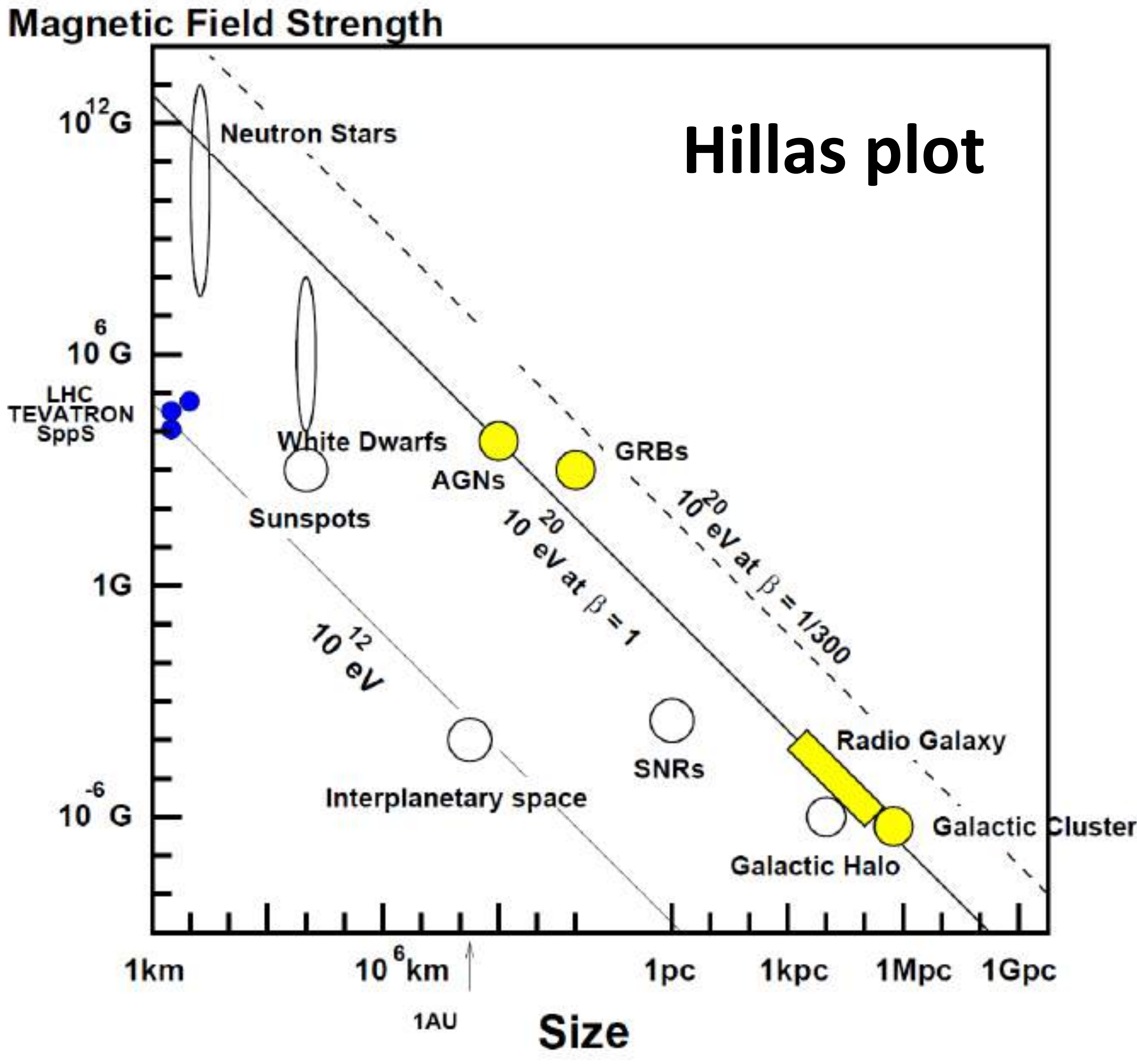

$$E_{\max} \leq \gamma e Z B R$$

γ : ローレンツ因子, Z : 原子番号

B : 磁場の強さ, R : 大きさ

A. M. Hillas, Astron. Astrophys., 22, 425 (1984)

スペクトルの細部構造

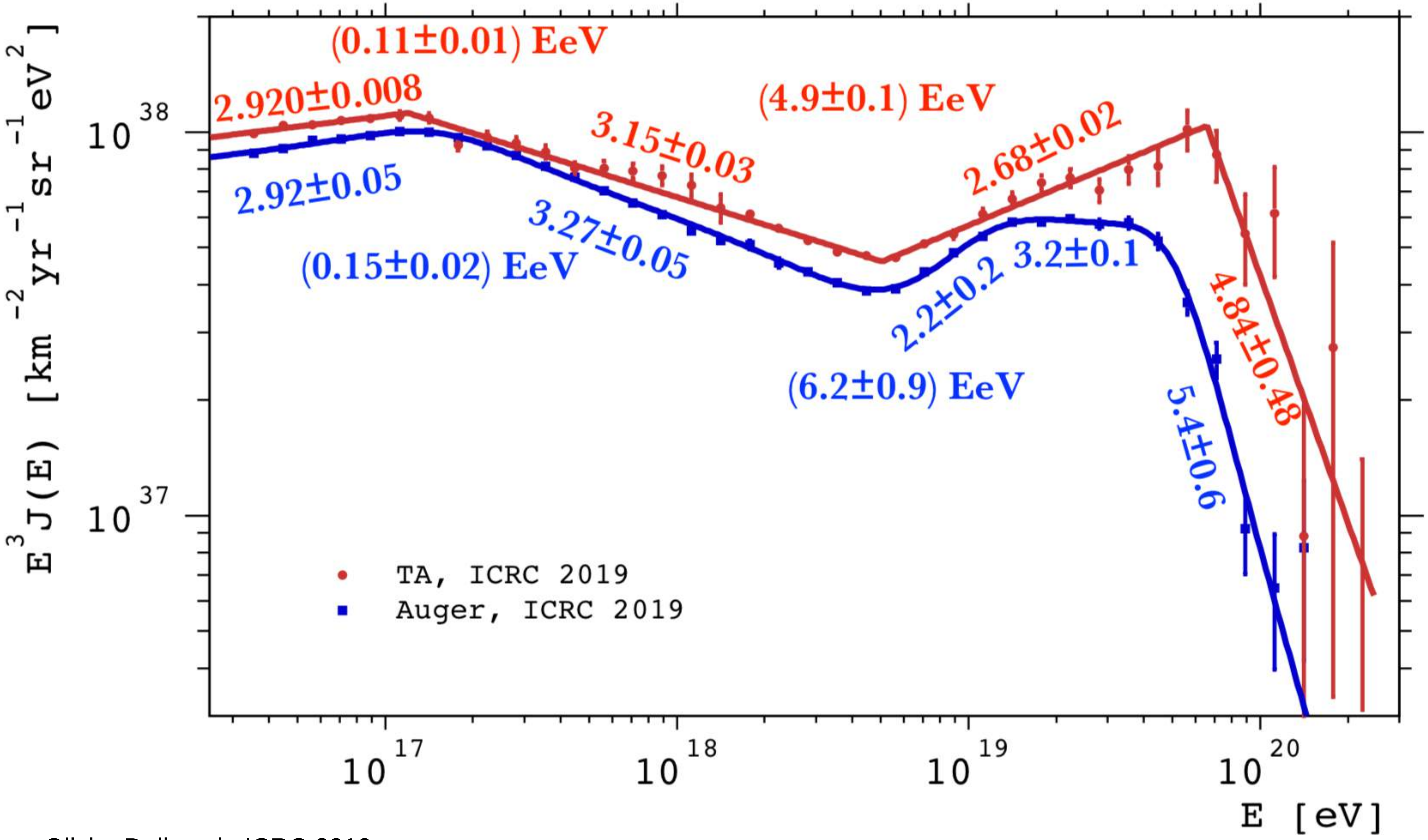

Olivier Deligny in ICRC 2019

スペクトルをソースモデルでFit

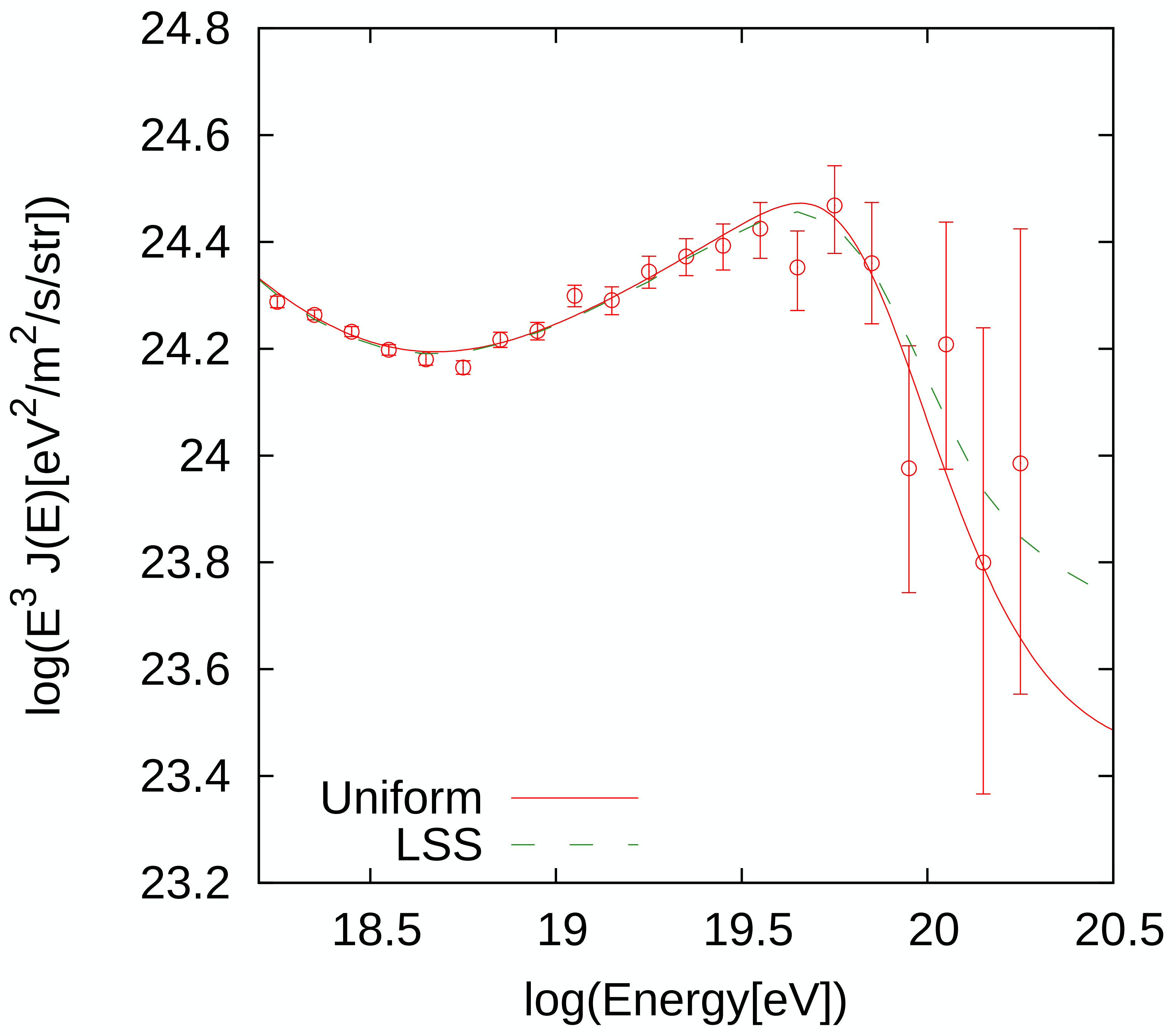

Figure 1: The red data points denote the energy spectrum measured by TA SD. The red solid line denotes the best-fit expected energy spectrum with $p = 2.21$, $m = 6.7$, $\Delta \log E = -0.03$ for a uniform distribution of UHECR sources. χ^2/d.o.f. is 12.4/17. In this figure, the energy scale of the data points is fixed and the energy scale of the model is shifted by $\Delta \log E = +0.03$. The green dashed line denotes the best-fit expected energy spectrum when UHECRs are distributed along the LSS.

$$Q(E, z) \propto E^{-p}(1+z)^m$$

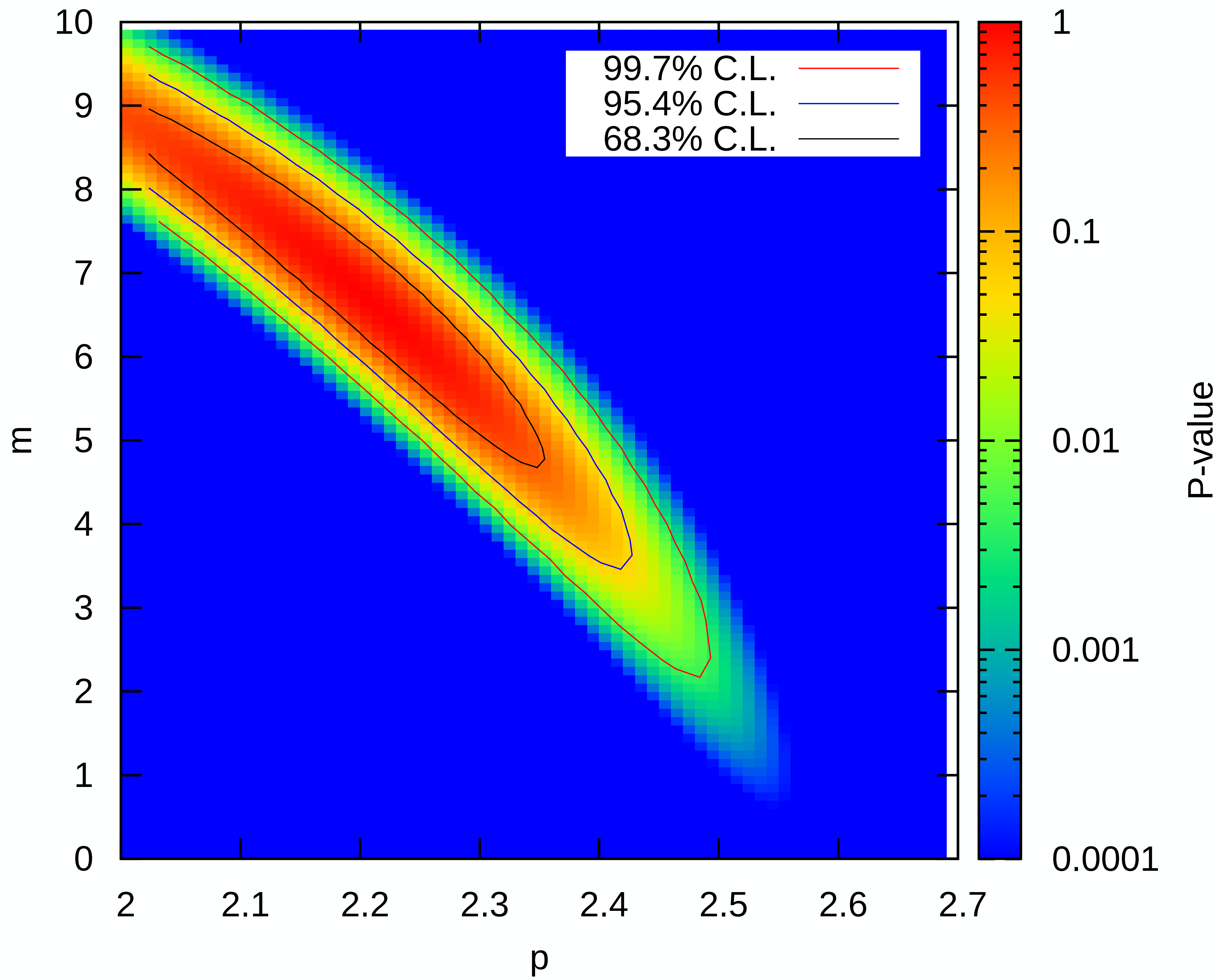

E. Kido in ICRC 2015

ニュートリノの上限値と矛盾する

JH, Boncioli, Bustamante, Winter
ApJ 825:122 (2016)

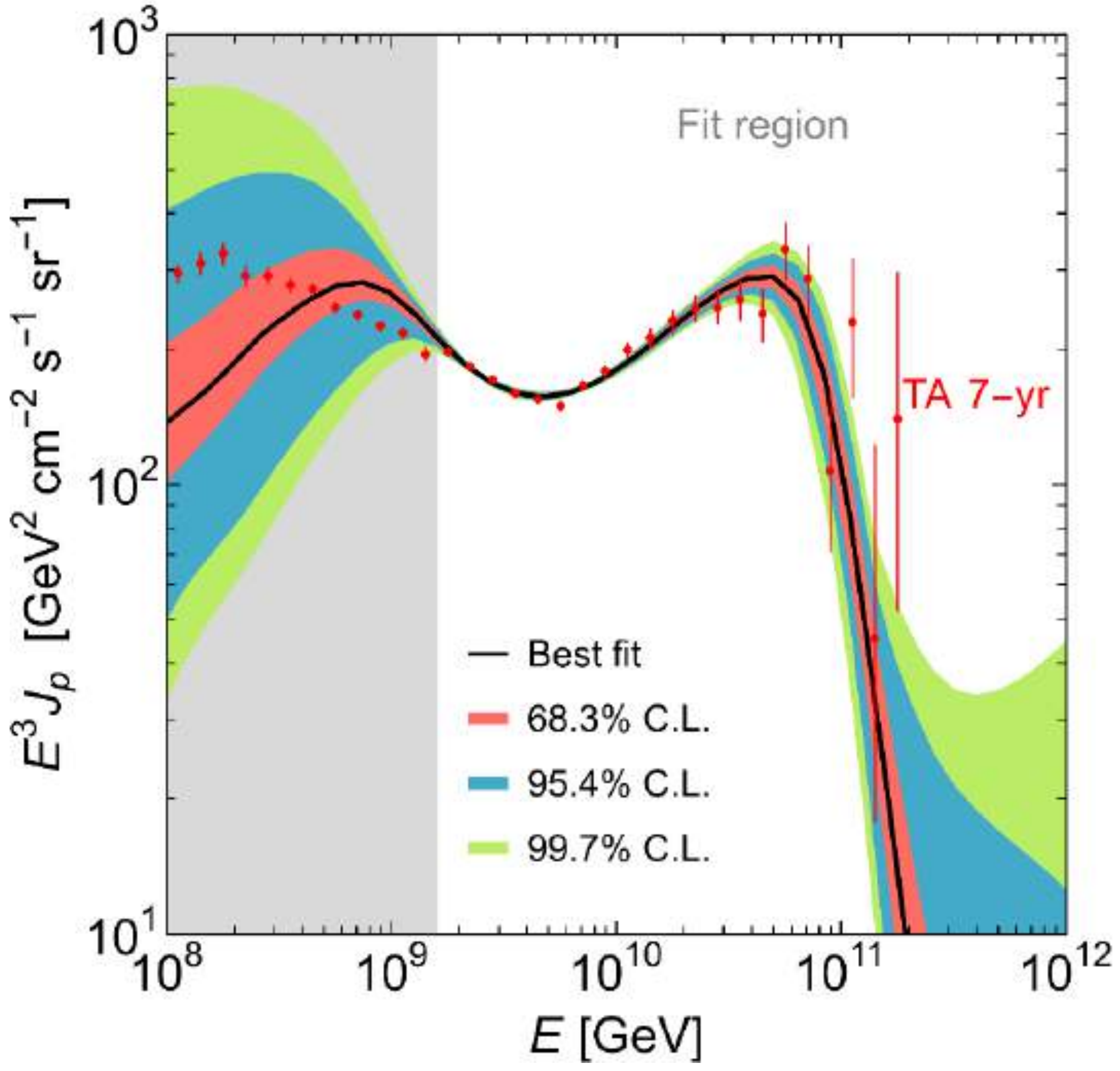

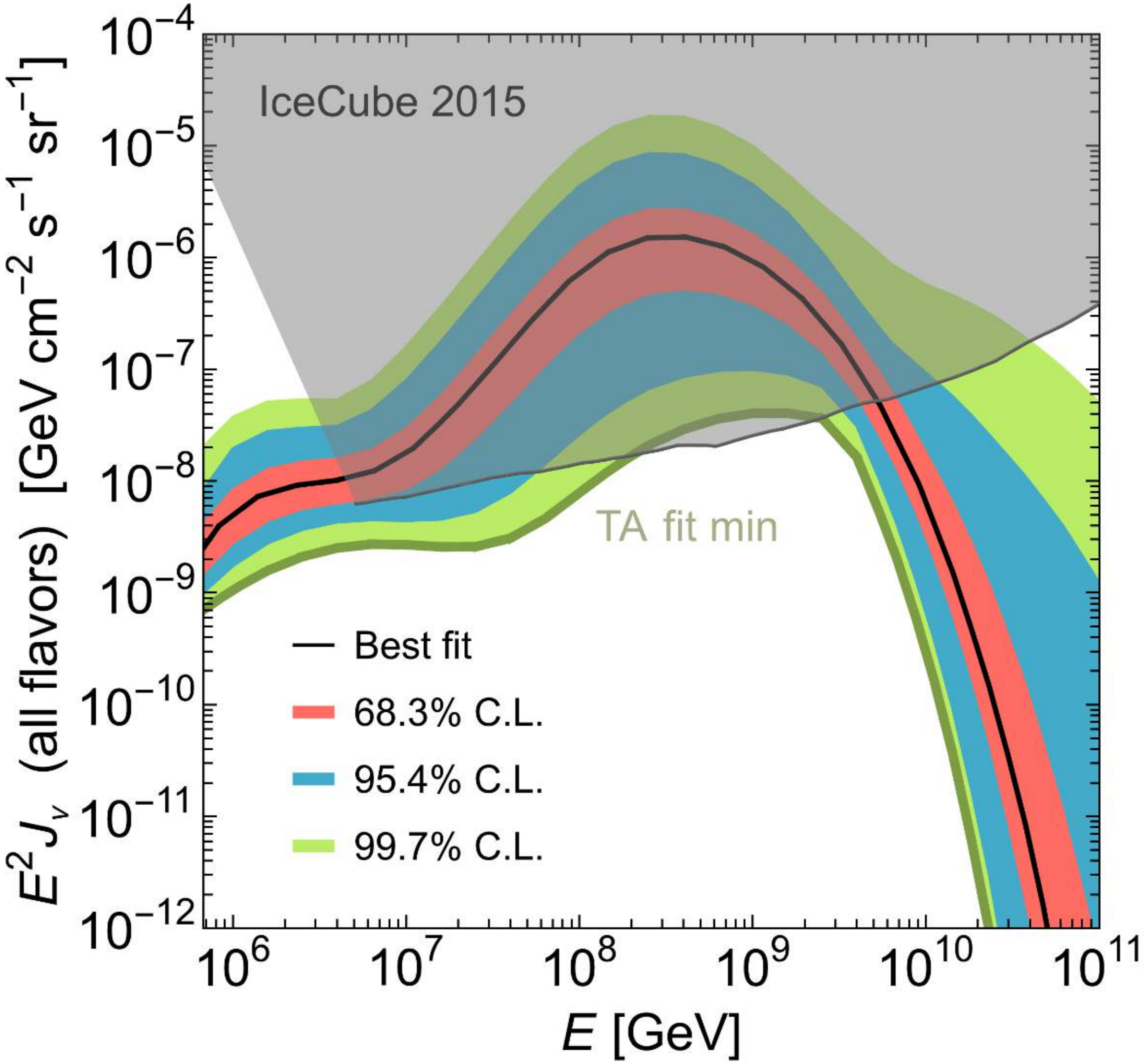

- Low statistics cannot distinguish source- or GZK effect
- Fit driven by ankle region
  - Favours hard spectra....
  - …and strong source evolution

陽子だけではなさそう

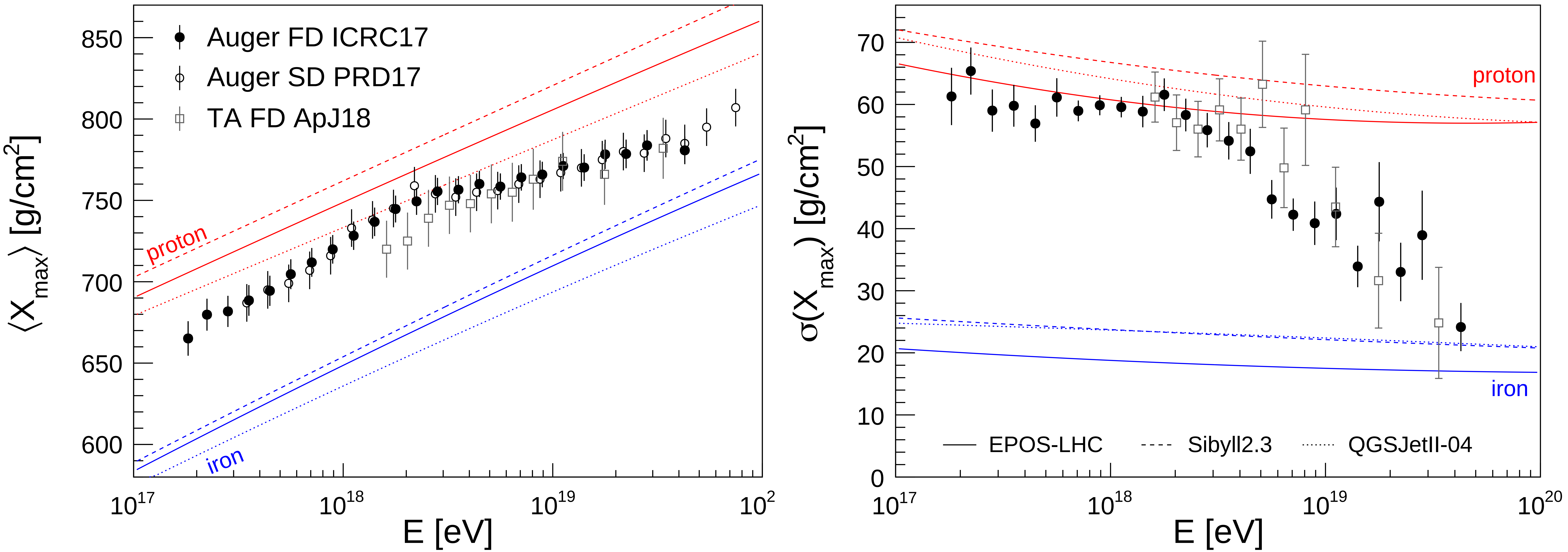

陽子

鉄

R.A. Batista et al., Front.Astron.Space Sci. 6 (2019) 23

Xmaxの分布

Augerの測定結果

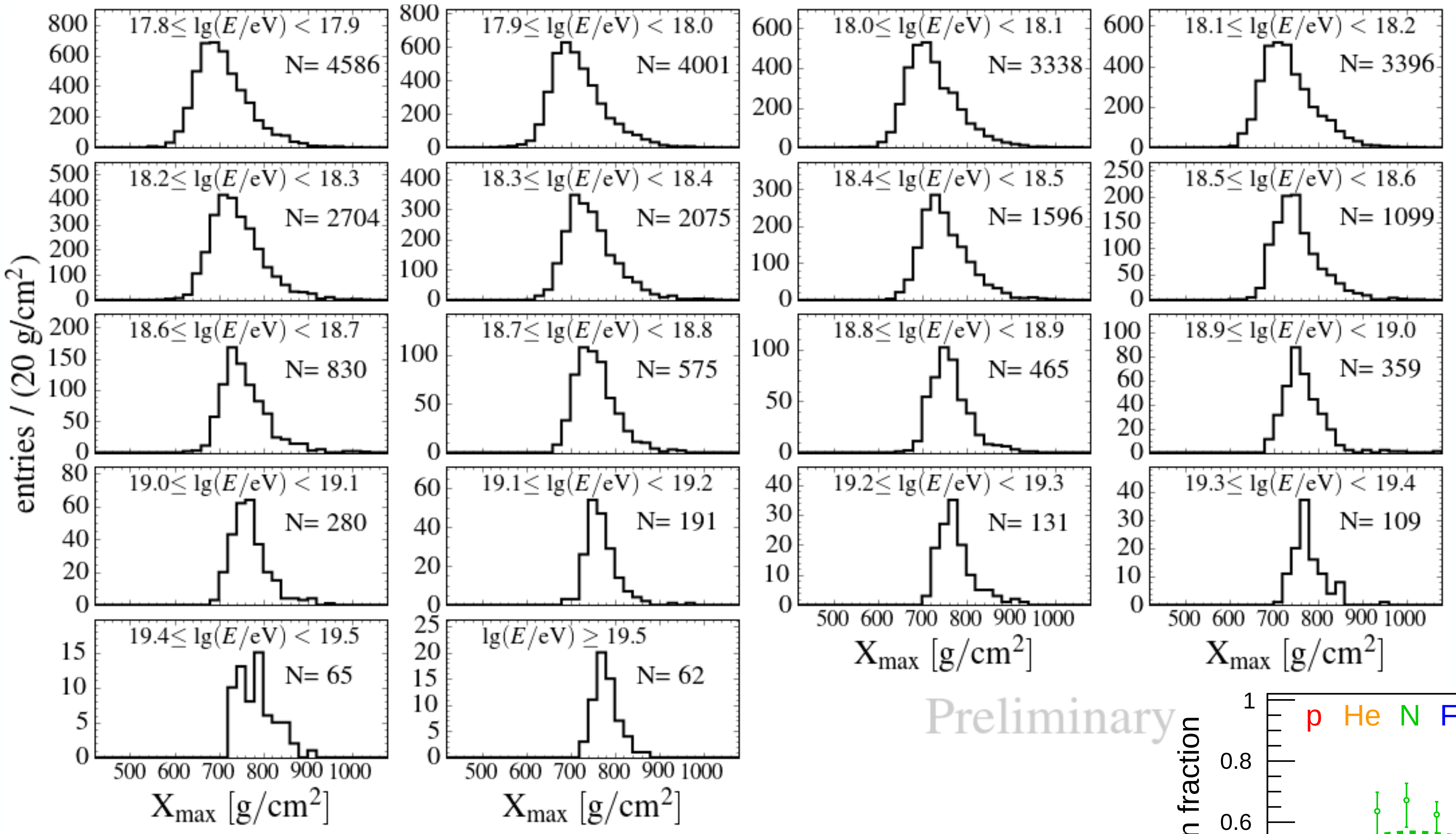

J. Bellido, ICRC 2017

期待値

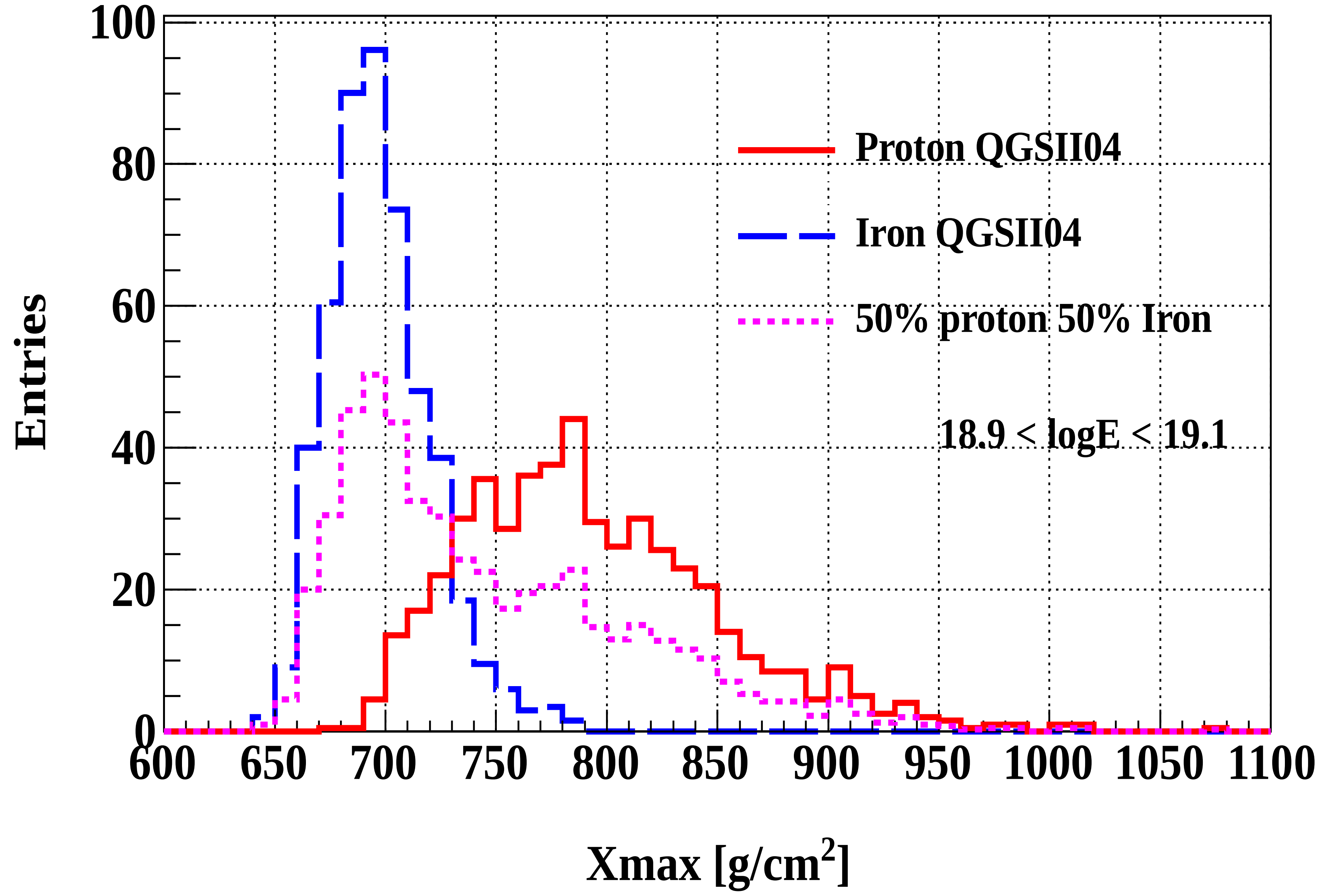

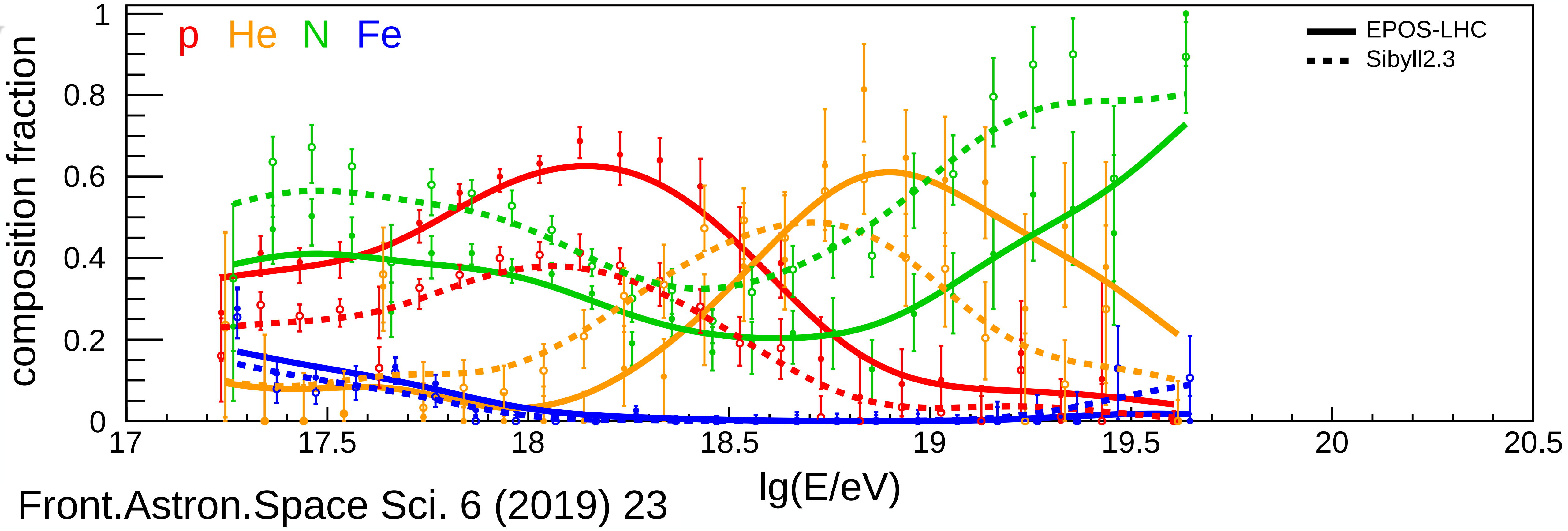

R.A. Batista et al., Front.Astron.Space Sci. 6 (2019) 23

銀河系内/系外の磁場で曲げられる

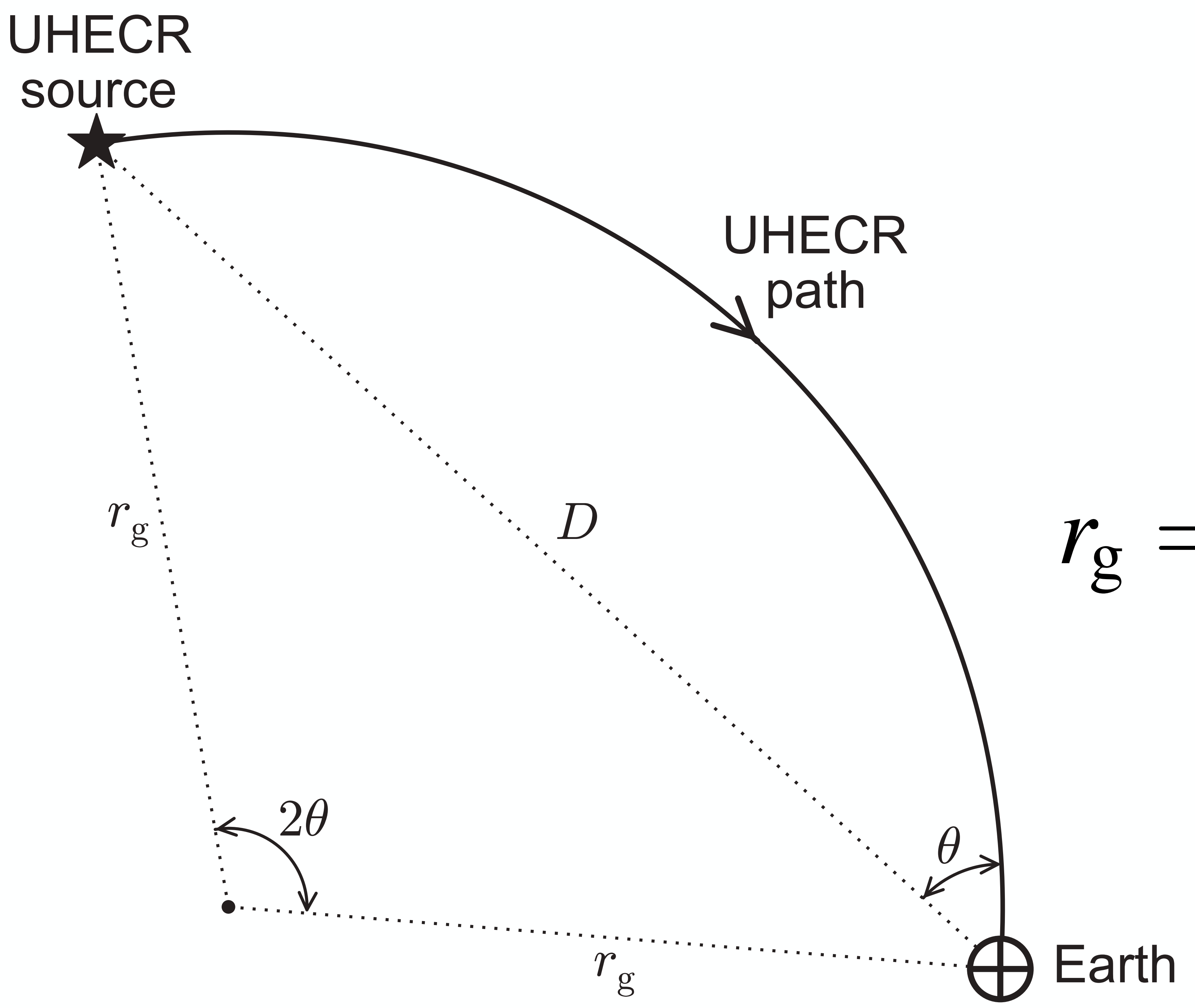

$$r_g = \frac{E}{ZecB_\perp},$$

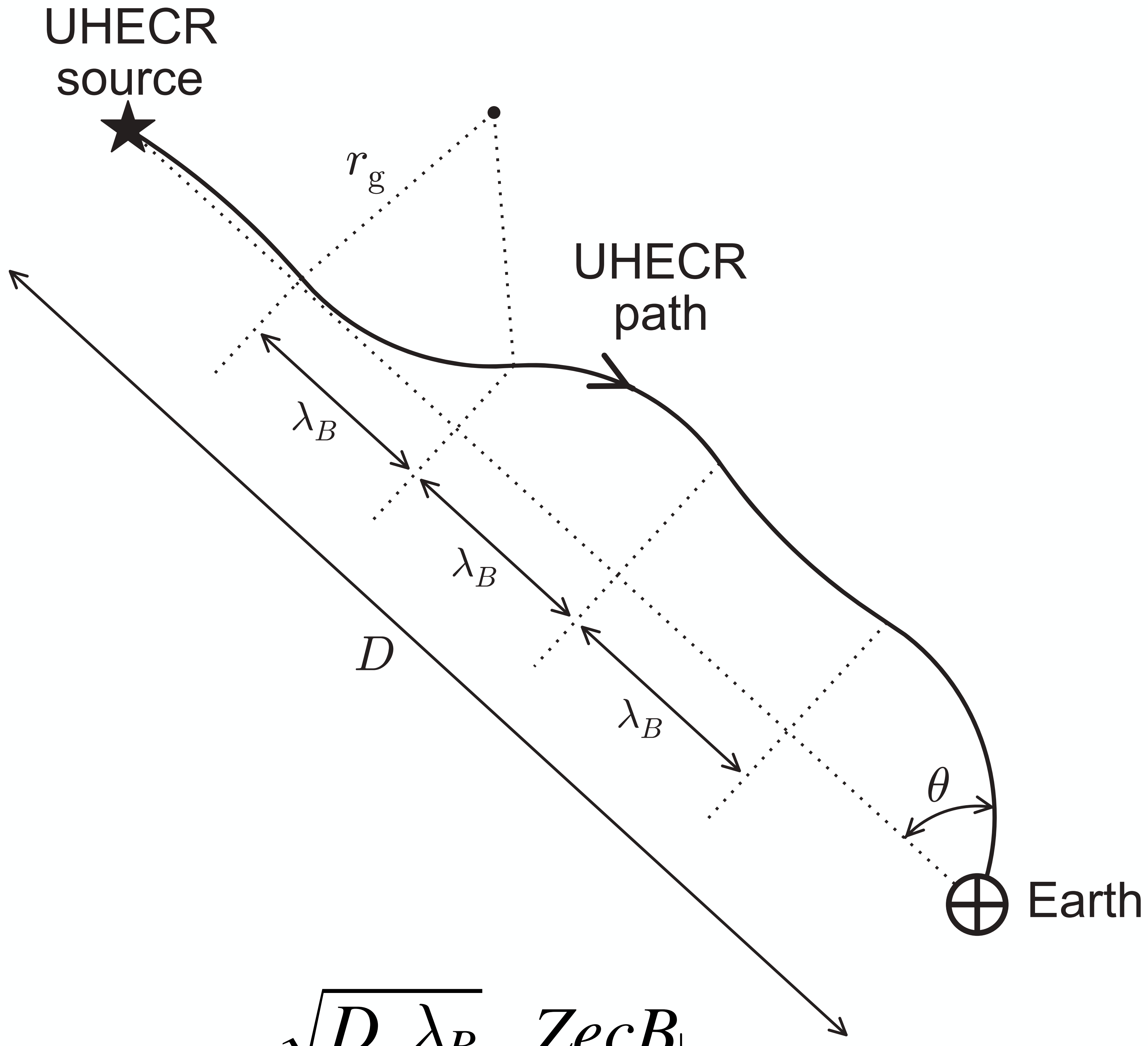

$$\sin\theta = \frac{D}{2}\frac{ZecB_\perp}{E}$$

$$\theta_{\rm rms} \approx \frac{\sqrt{D\ \lambda_B}}{2}\ \frac{ZecB_\perp}{E}$$

$$=2^\circ\!\!.65 Z\left(\frac{D}{10\ \mathrm{Mpc}}\right)\left(\frac{B_\perp}{10^{-9}\ \mathrm{G}}\right)\left(\frac{E}{10^{20}\ \mathrm{eV}}\right)^{-1}.$$

$$\approx 0^\circ\!\!.84 Z\left(\frac{D}{10\ \mathrm{Mpc}}\right)^{\frac{1}{2}}\left(\frac{\lambda_B}{1\ \mathrm{Mpc}}\right)^{\frac{1}{2}} \times \left(\frac{B_\perp}{10^{-9}\ \mathrm{G}}\right)\left(\frac{E}{10^{20}\ \mathrm{eV}}\right)^{-1}$$

J. D. Bray and A. M. M. Scaife, The Astrophysical Journal, 861:3 (7pp), 2018 July 1

銀河系内磁場

銀河系内磁場

$$\theta = 10^\circ Z \left(\frac{E}{10\,\mathrm{EeV}} \right)^{-1}$$

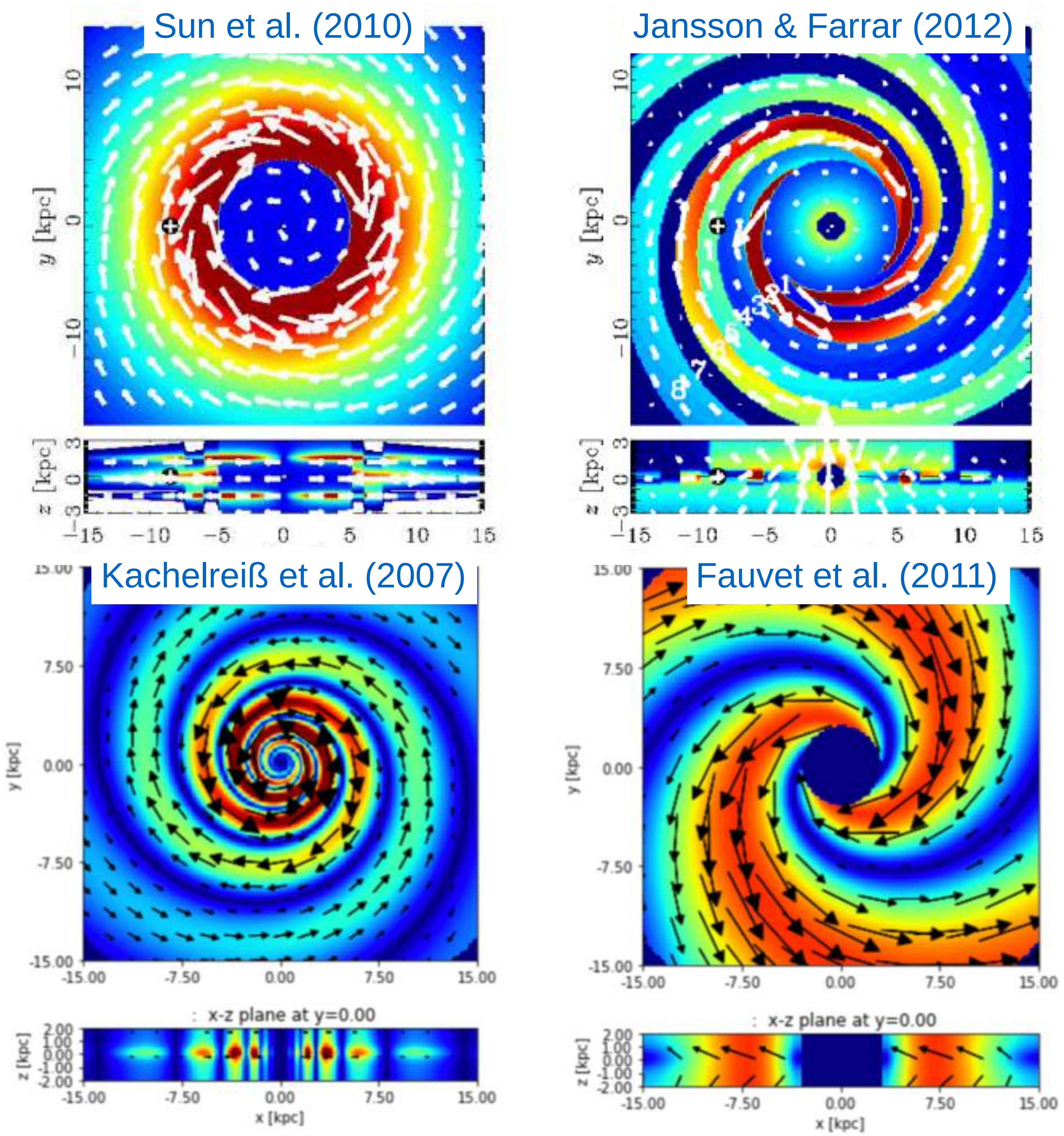

Tess Jaffe in 20-years Auger symposium, IMAGINE project, arXiv: 1801.04341

1 EeV proton	10 EeV proton	100 EeV proton
= O(8 EeV), Fe(26 EeV)	= O(80 EeV), Fe(260 EeV)	= O(800 EeV), Fe(2600 EeV)

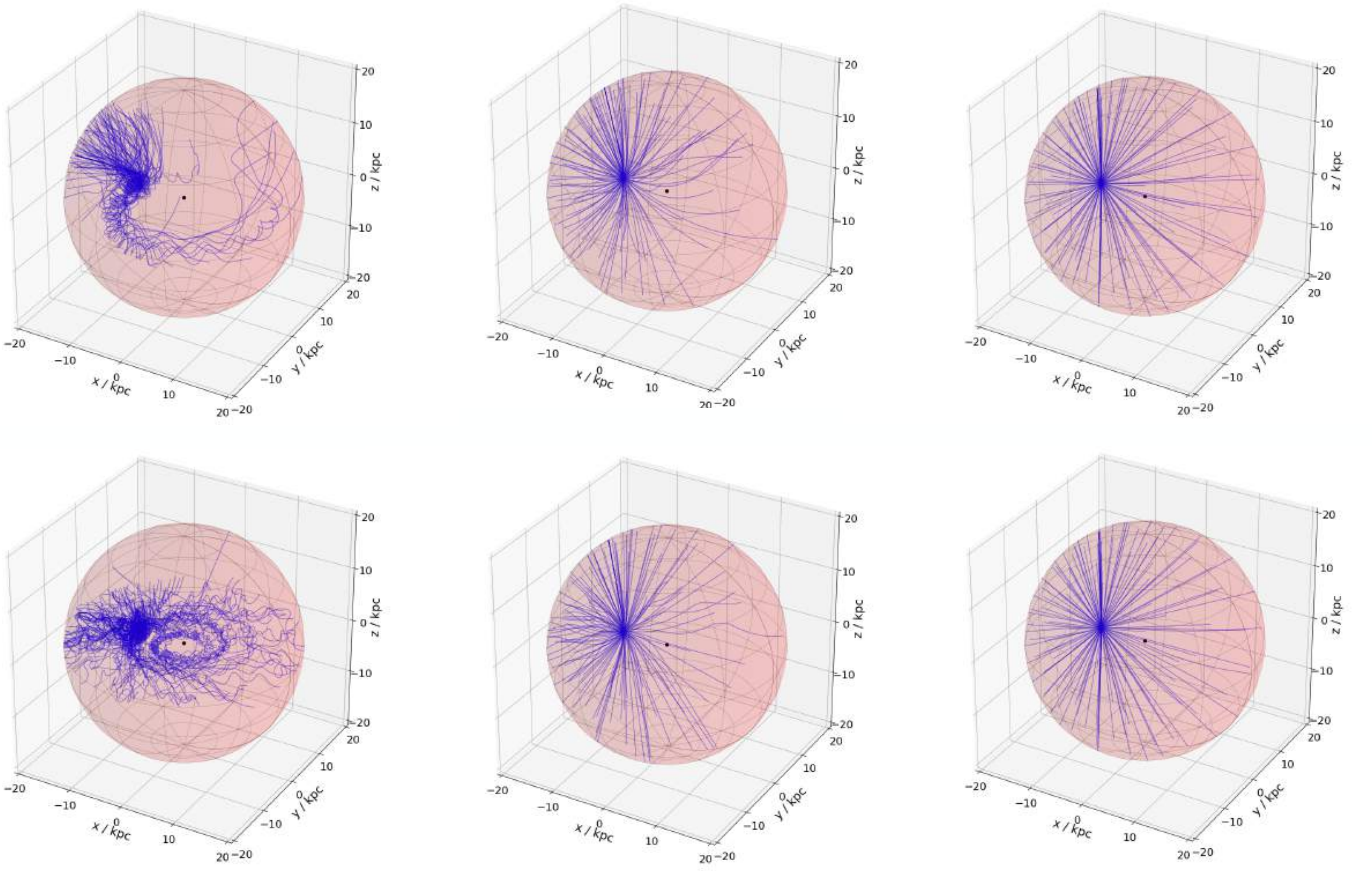

R. Higuchi using CRPropa

Observation of dipole above 8 EeV

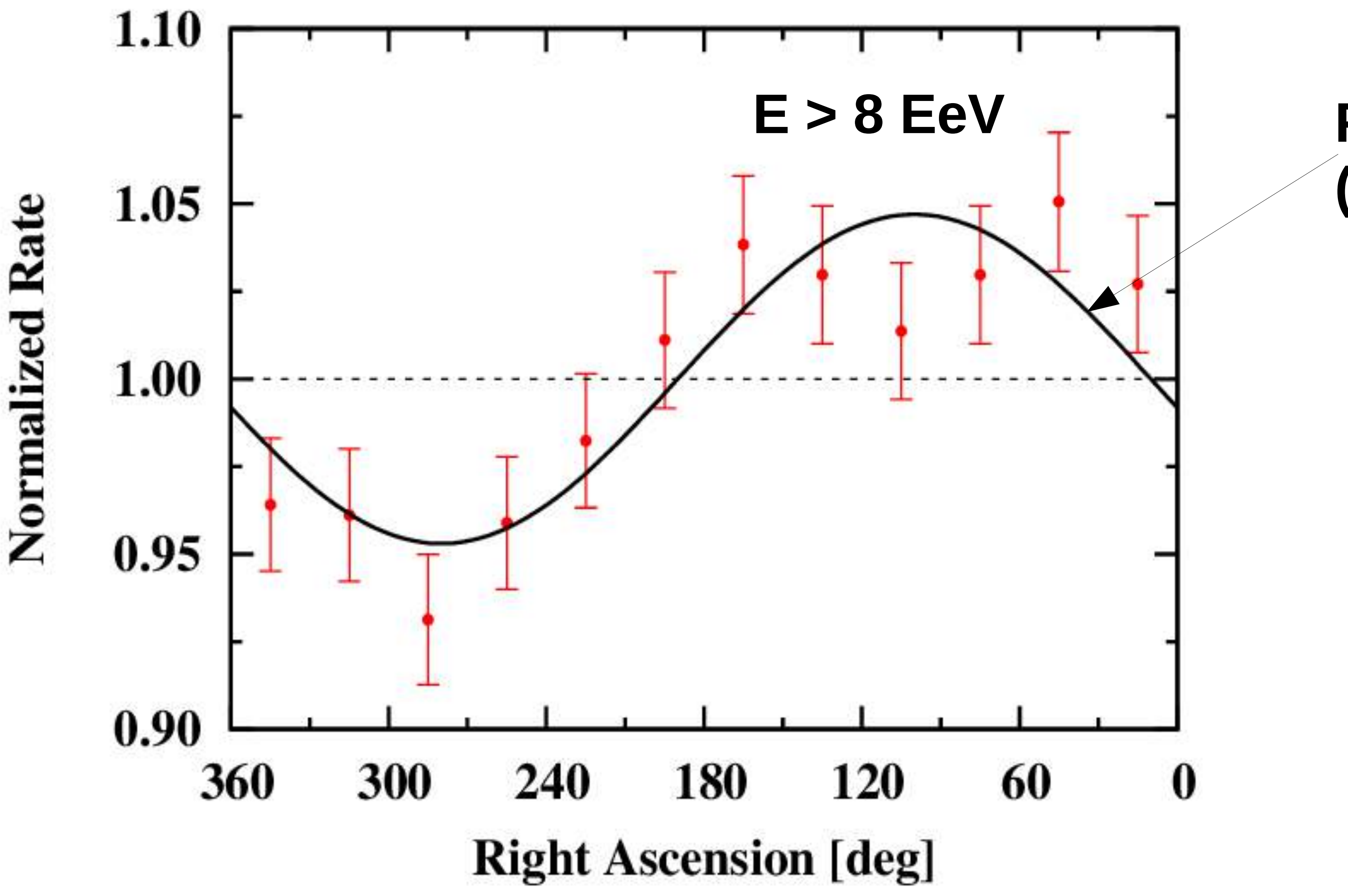

Harmonic analysis in right ascension α

E [EeV]	events	amplitude r	phase [deg.]	$P(\geq r)$
4-8	81701	$0.005^{+0.006}_{-0.002}$	80 ± 60	0.60
> 8	32187	$0.047^{+0.008}_{-0.007}$	100 ± 10	2.6×10^{-8}

significant modulation at 5.2σ (5.6σ before penalization for energy bins explored)

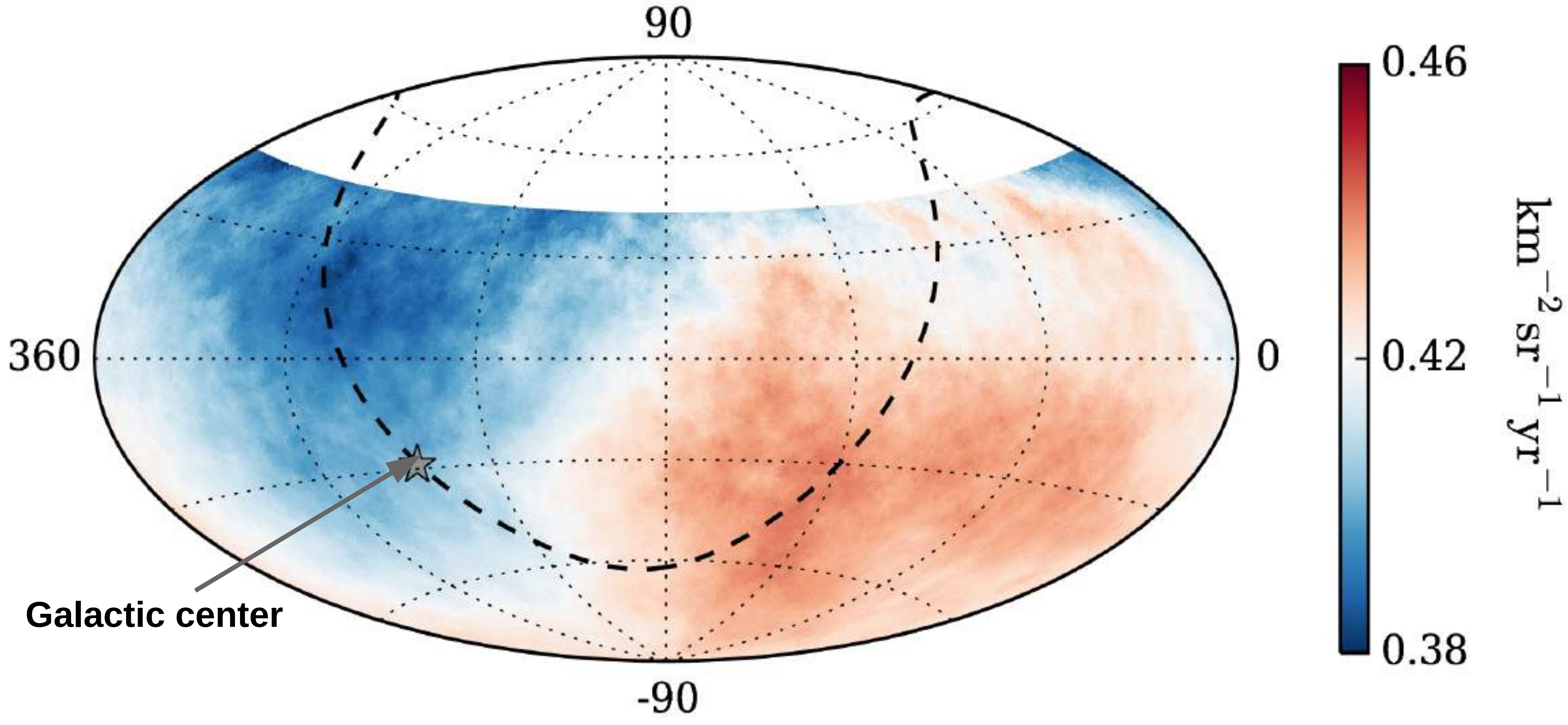

Pierre Auger Collab. Science 357, 1266 (2017)

A directional reconstruction of the dipole

E [EeV]	d_z [%]	$d_\perp$ [%]	d [%]	δ_d[°]	α_d[°]
4 - 8	-2.4 ± 0.9	$0.6^{+0.7}_{-0.3}$	$2.5^{+1.0}_{-0.7}$	-75^{+17}_{-8}	80 ± 60
≥ 8	-2.6 ± 1.5	$6.0^{+1.1}_{-1.0}$	$6.5^{+1.3}_{-0.9}$	-24^{+12}_{-13}	100 ± 10

6.5% dipole amplitude
Equatorial (α_d, δ_d)=(100°, -24°)
Galactic (l, b)=(233°, -13°)

2 micron all-sky redshift survey (2MRS)

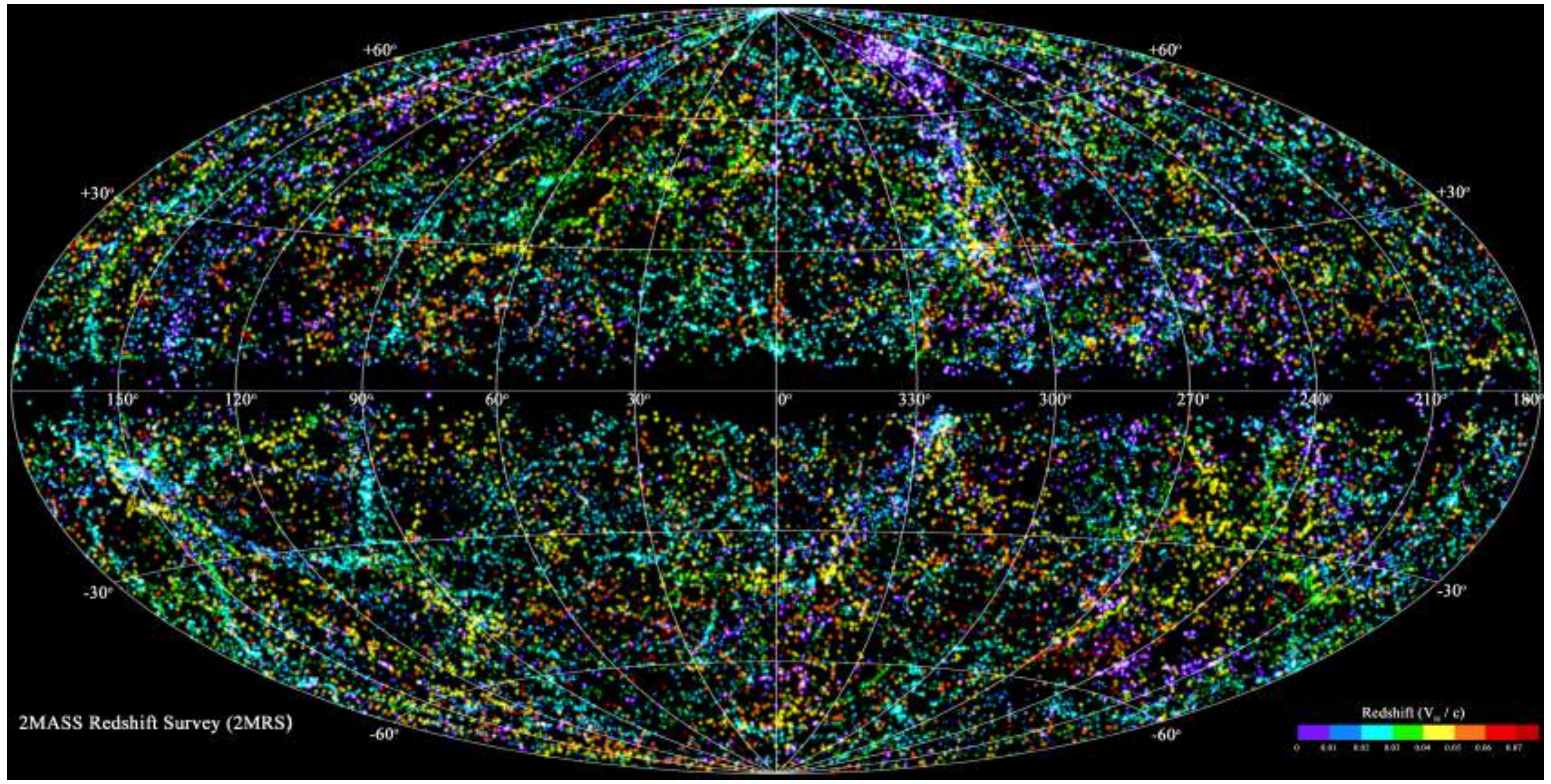

O. Taborda et al., ICRC 2017

The flux-weighted dipole from IR galaxy distribution in 2MRS points to (l,b)=(251º,38º) → ~55º from observed

[Erdogdu et al. 2006]

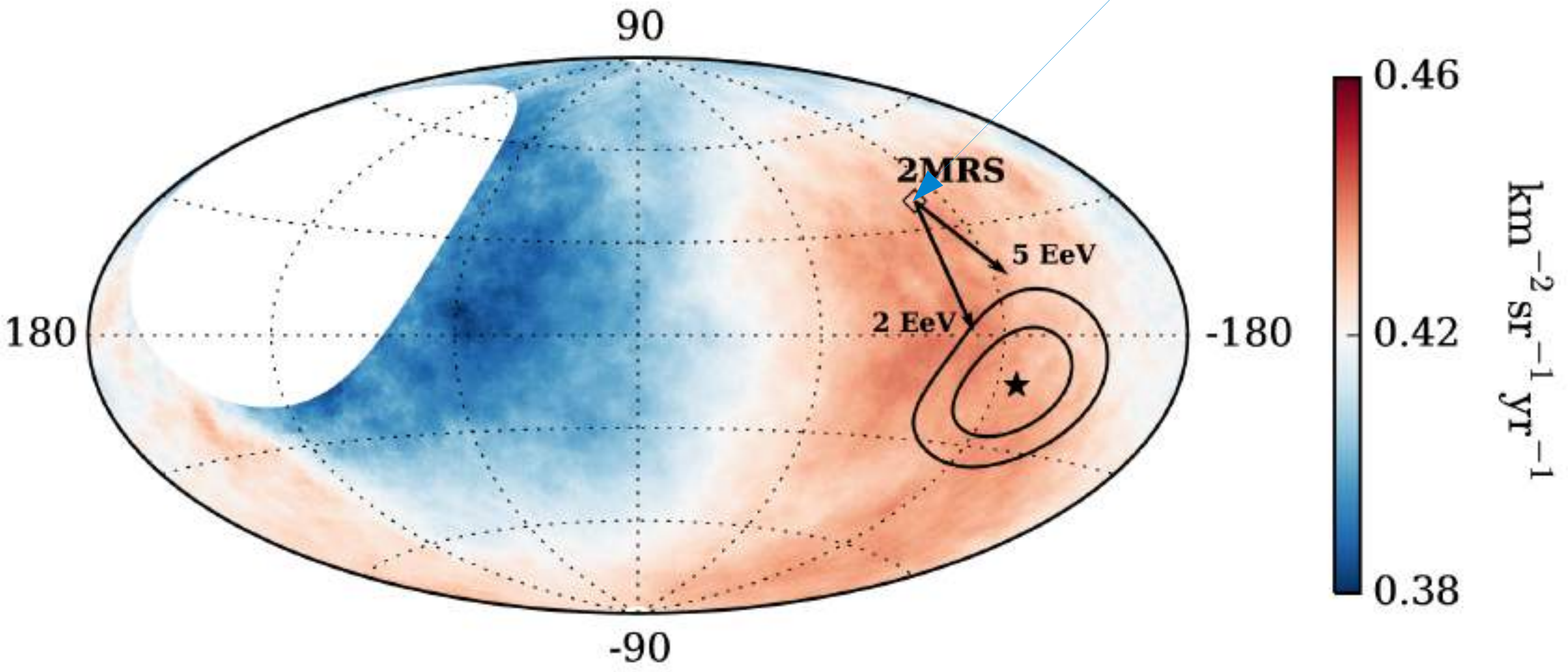

Accounting GMF deflections

[Jansson and Farrar ApJ 757 (2012) 14]

Z ~ 1.7 – 5 at 10 EeV → E/Z ~ 2 – 5 EeV

[Auger Coll. PRD 90 (2014) 122006]

Improves agreement observation ↔ 2MRS

Pierre Auger collab. Science 357, 1266 (2017)

Local void 方向からの宇宙線が少ない

Ankle (E_{TA}>10 EeV, E_{Auger}>8.86 EeV) 45° circle

Confidential

EPJ Web of Conferences **210**, 01005 (2019) using a different color contour

Nearby Prominent Sources

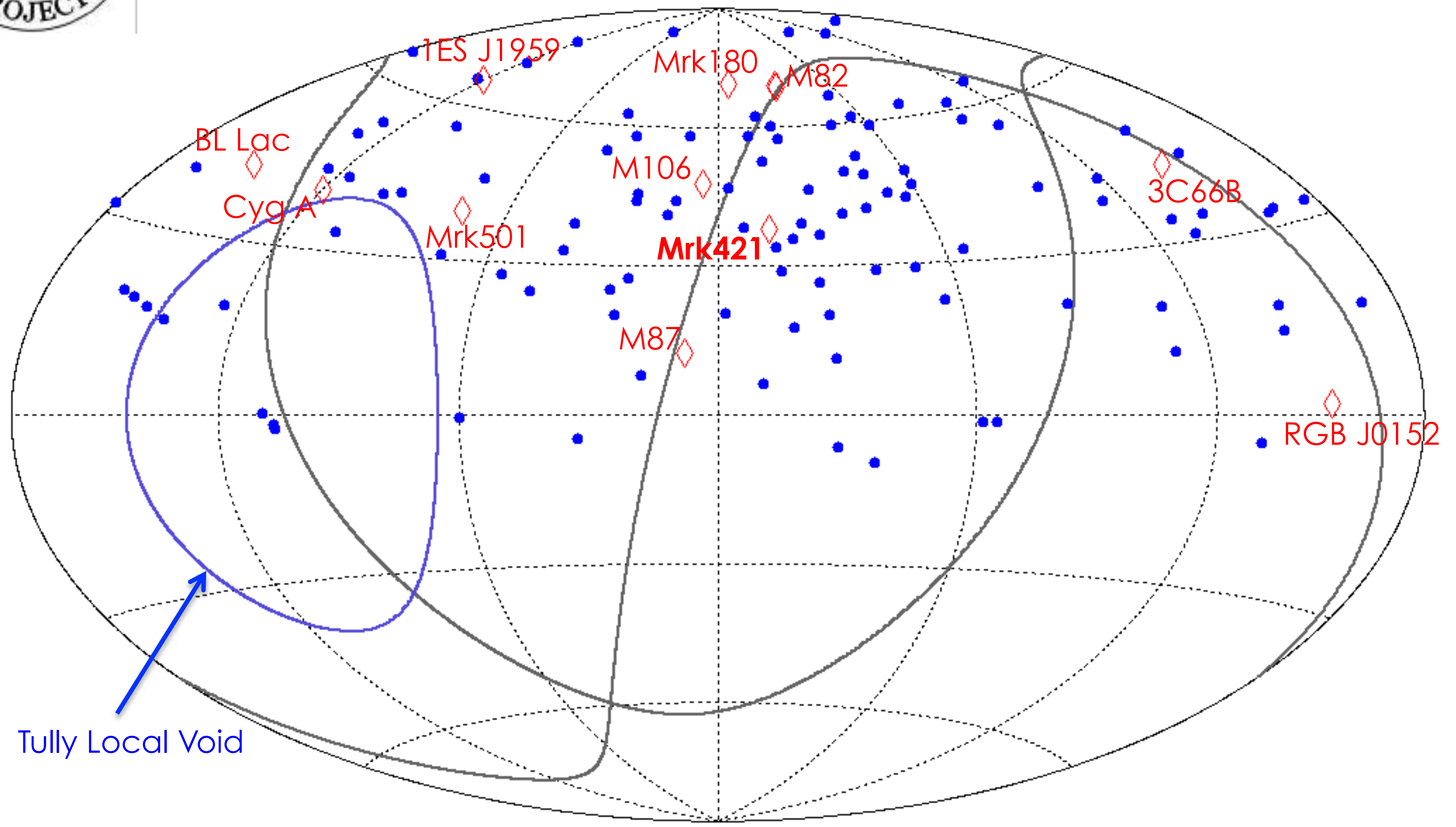

The blazar Mrk421, Mrk180 and starburst galaxy M82 are candidates?

K. Fang, et al., ApJ, 794, 126 (2014)
H.-N. He, et al., arXiv:1411.5273 (2014)

K. Kawata in ICRC 2015

エネルギー依存性

The Astrophysical Journal, 891:142 (10pp), 2020 March 10 Aab et al.

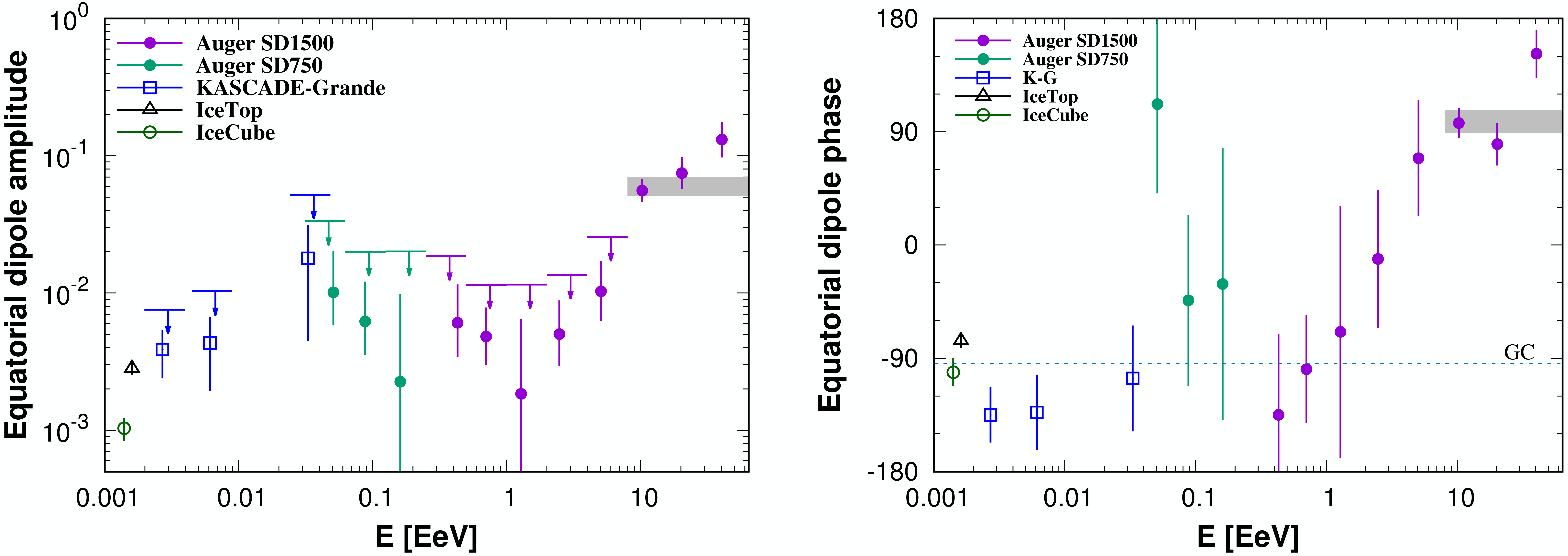

Figure 1. Reconstructed equatorial dipole amplitude (left) and phase (right). The upper limits at 99% CL are shown for all the energy bins in which the measured amplitude has a chance probability greater than 1%. The gray bands indicate the amplitude and phase for the energy bin $E \geqslant 8$ EeV. Results from other experiments are shown for comparison (IceCube Collaboration 2012, 2016; KASCADE-Grande Collaboration 2019).

極高エネルギー宇宙線の到来方向 (2005)

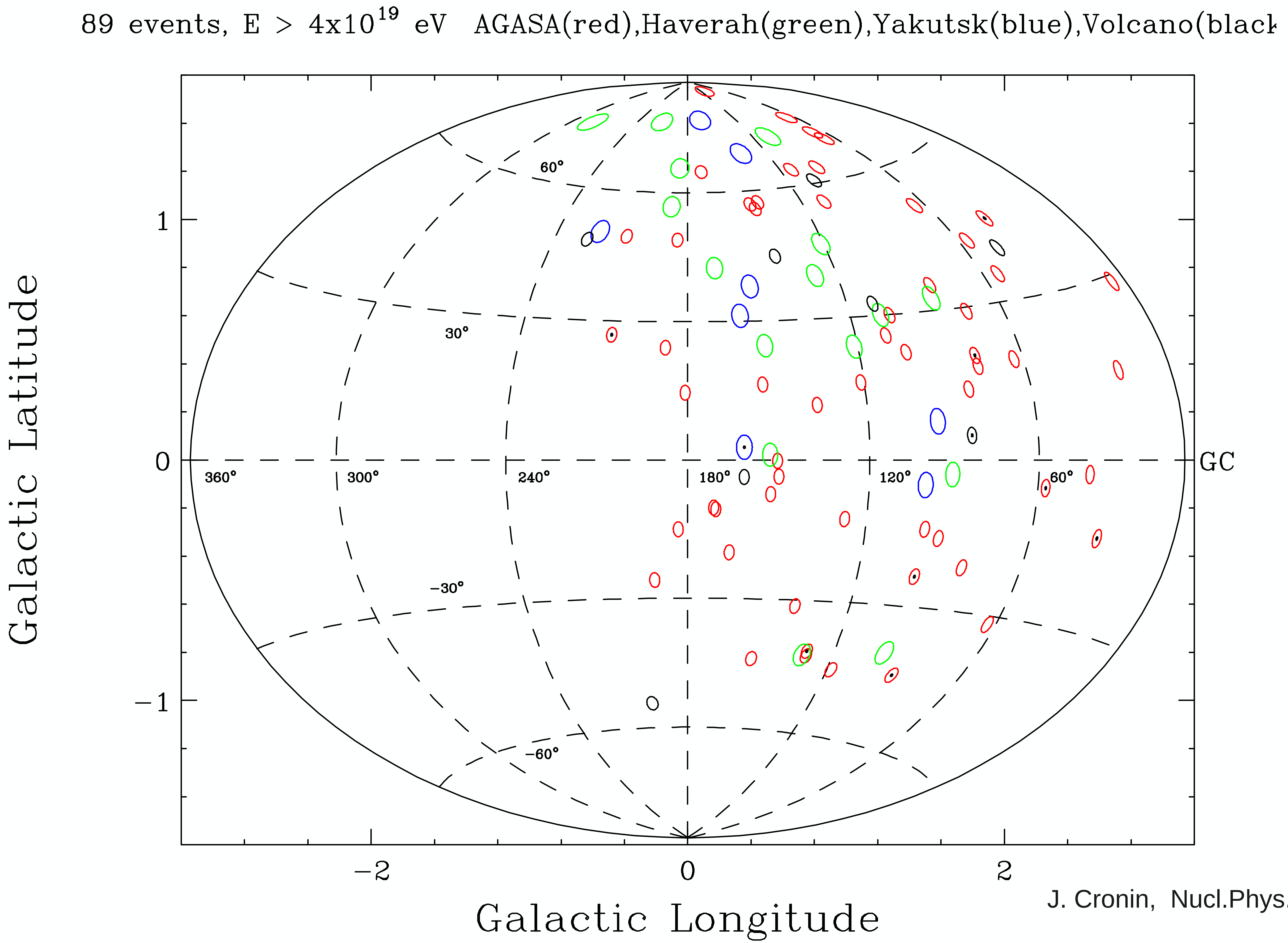

J. Cronin, Nucl.Phys.Proc.Suppl. 138:465 (2005)

極高エネルギー宇宙線の到来方向

E_{TA}>52.3 EeV, E_{Auger}>40 EeV

Confidential

Data from EPJ Web of Conferences **210**, 01005 (2019)

有意度map

E_{TA}>52.3 EeV, E_{Auger}>40 EeV

Confidential

EPJ Web of Conferences 210, 01005 (2019) using a different color contour

"Hotspot" update from 11 years of data

K. Kawata

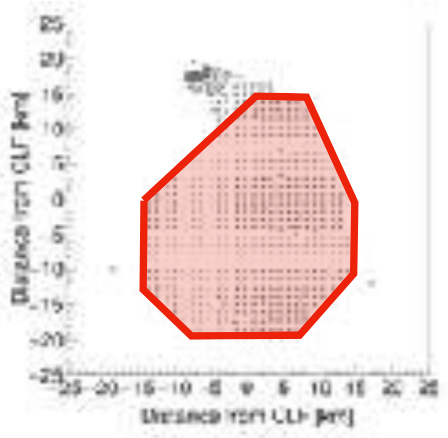

There is a marginal excess is seen along the SGP (around the Perseus-Pisces Supercluster) at the local significance of ~ 3σ

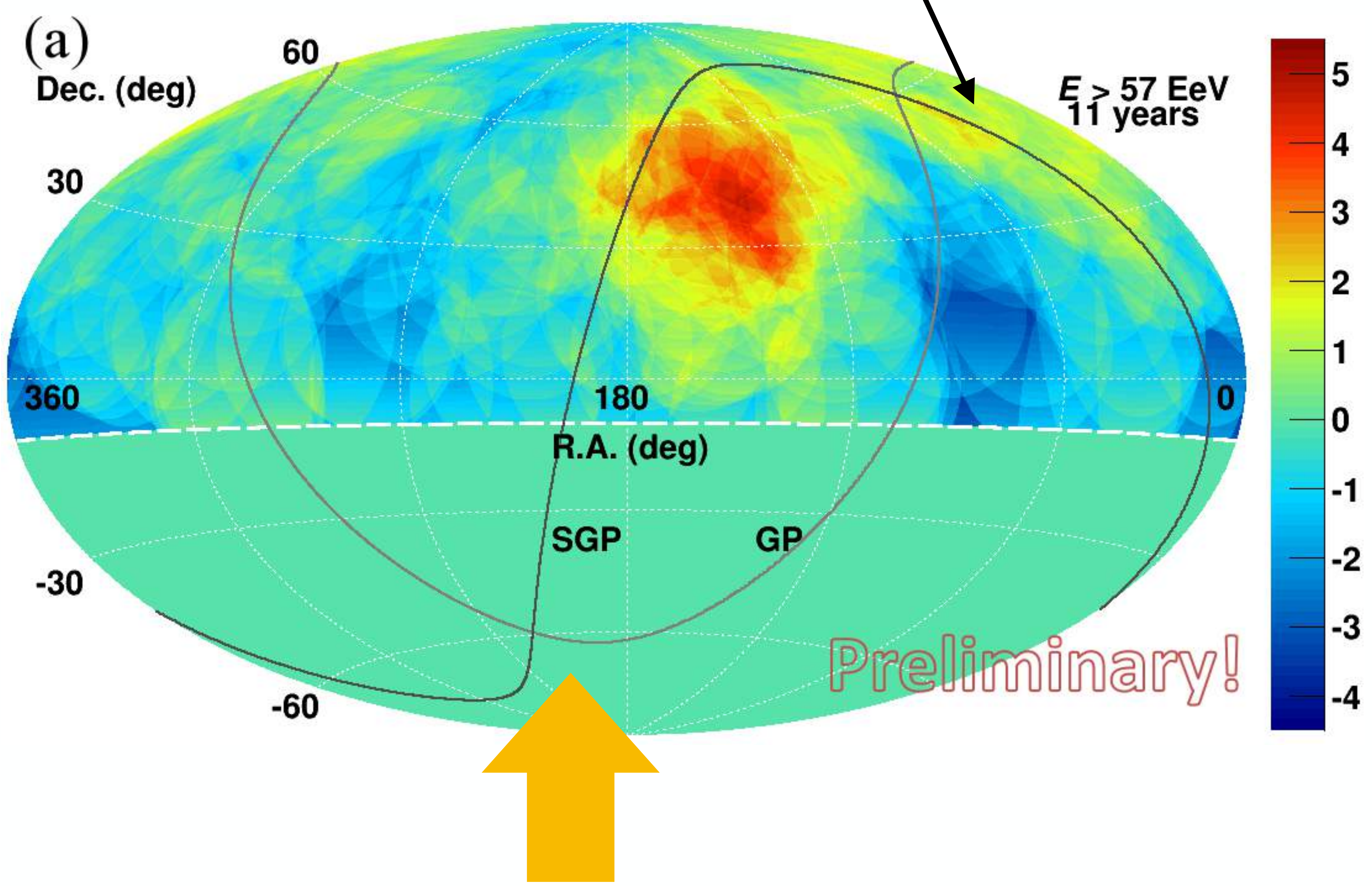

The increase rate of the events inside the hotspot circle is consistent with a constant within ±1σ fluctuation

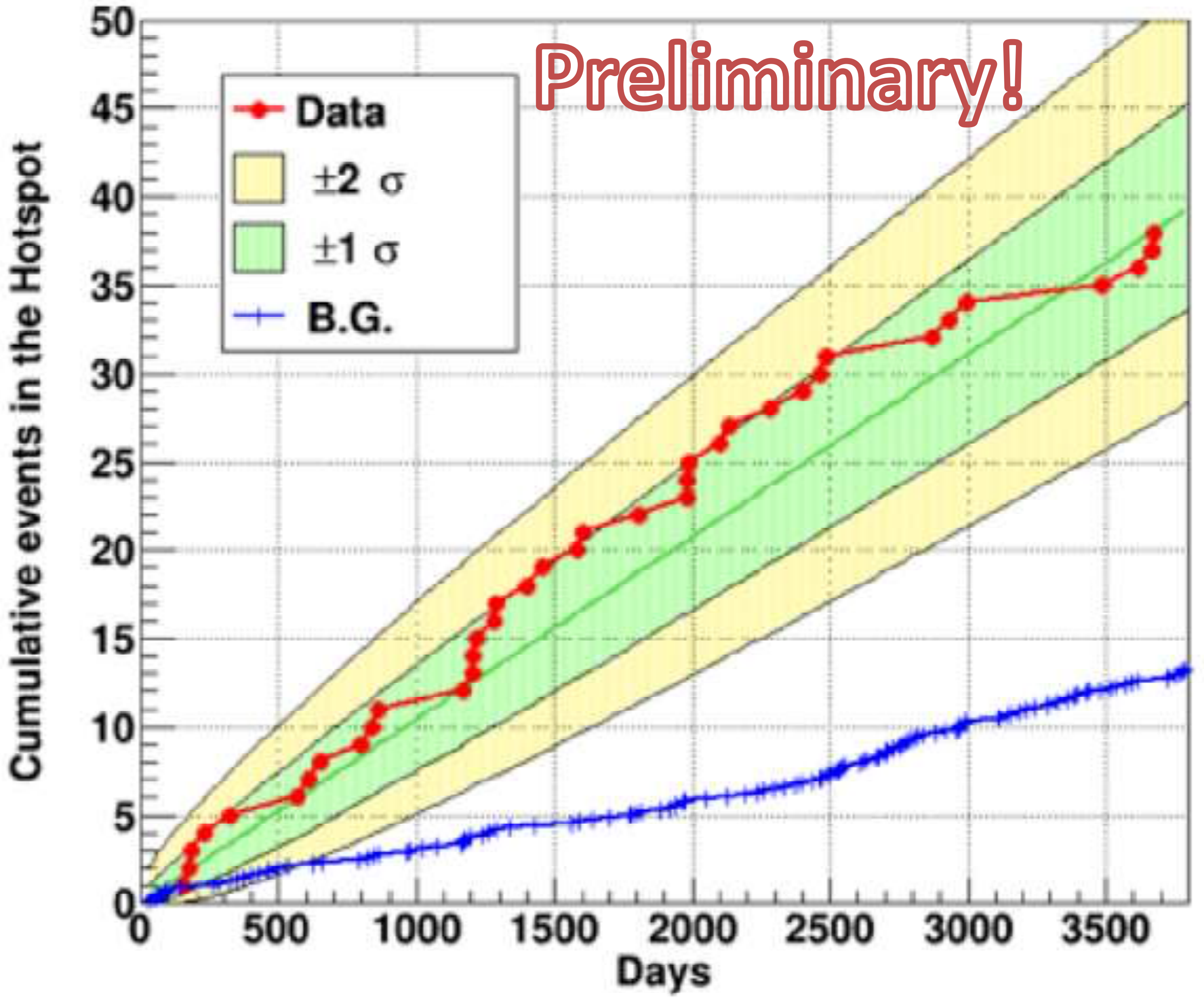

Hotspot from 11 years of TA SD data, from May 11, 2008 to May 11, 2019

E > 57 EeV, in total 168 events
38 events fall in Hotspot (α=144.3°, δ=40.3°, 25° radius, 22° from SGP), expected=14.2 events
local significance = 5.1 σ, chance probability → 2.9σ
25° over-sampling radius shows the highest local significance (scanned 15° to 35° with 5° step)

Shoichi Ogio in ICRC 2019

Centaurus A 方向から3.9σの有意度の異方性

Intermediate anisotropy

Total SD events with E>32 EeV : 2157
Total exposure 101,400 km² sr yr

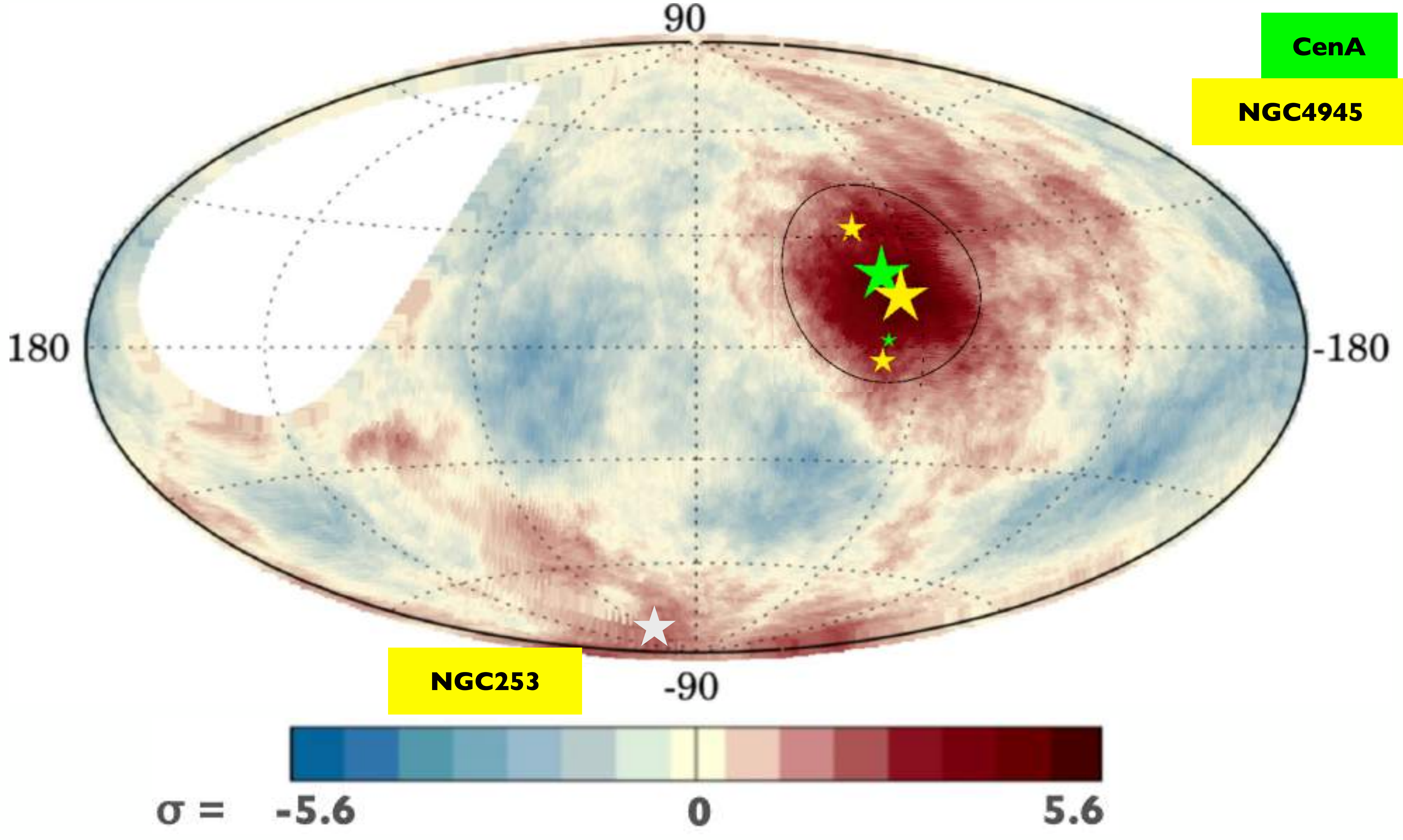

Blind search

Scan ranges:
32 EeV ≤ Eth ≤ 80 EeV (1 EeV steps)
1° ≤ ψ ≤ 30° (1° steps)

Most significant excess for E>38 EeV
(α=202°, δ= -45°) ~2° from CenA

Centaurus A

3.9 σ effect (post-trial)
for E>37 EeV, 28° window

L.Caccianiga #206

Antonella Castellina in ICRC 2019

近傍天体とFlux pattern解析

Pierre Auger collab., ApJL 853:L29 (2018)

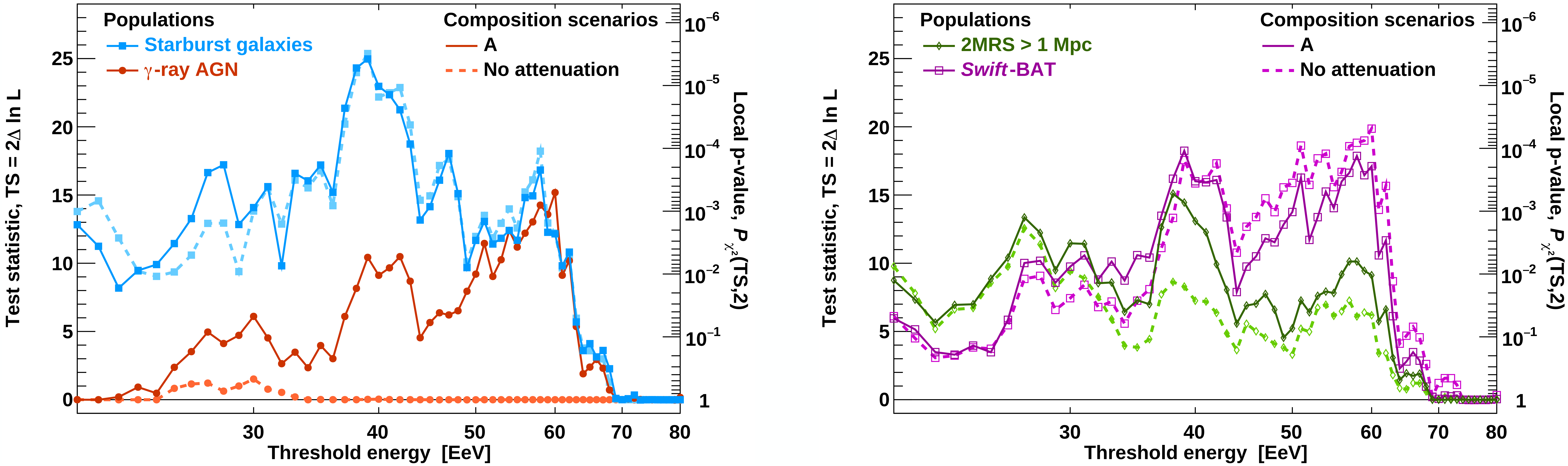

Figure 1. TS scan over the threshold energy for SBGs and AGNs (*Left*) and *Swift*-BAT and 2MRS sources (*Right*), including attenuation (light-dashed lines) or not (darker-solid lines).

- 40 EeV付近でどのカタログも相関が強くなる
- AGNとの相関は減衰を考慮すると、近傍のCen Aに限定されて相関が強くなる。
  - それ以外の銀河も含めると(2MRS, Swift-BAT)、相関は小さいが存在する(2.7σ ~ 3.2σ)

Auger best-fit flux pattern

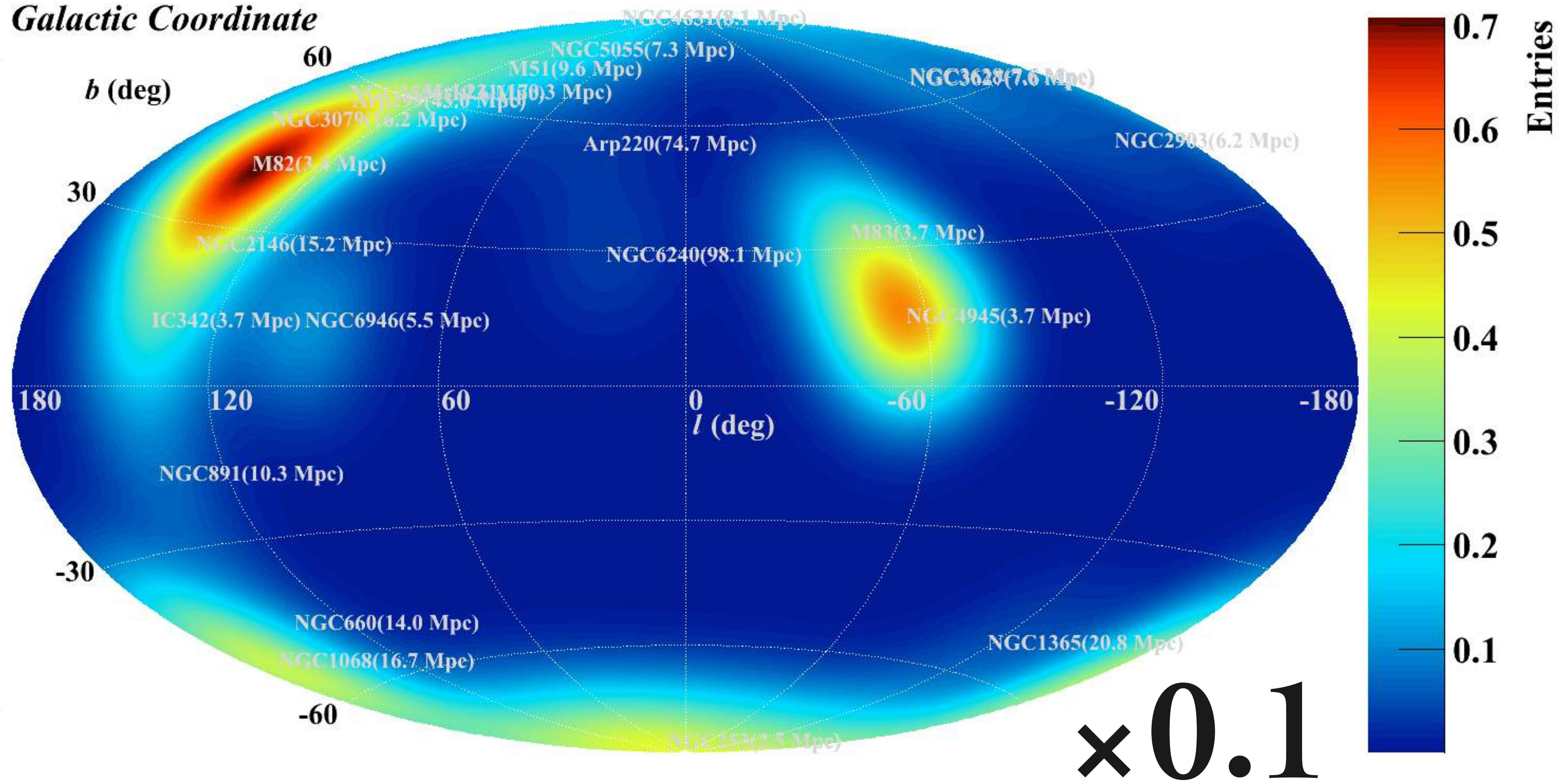

×0.1

+

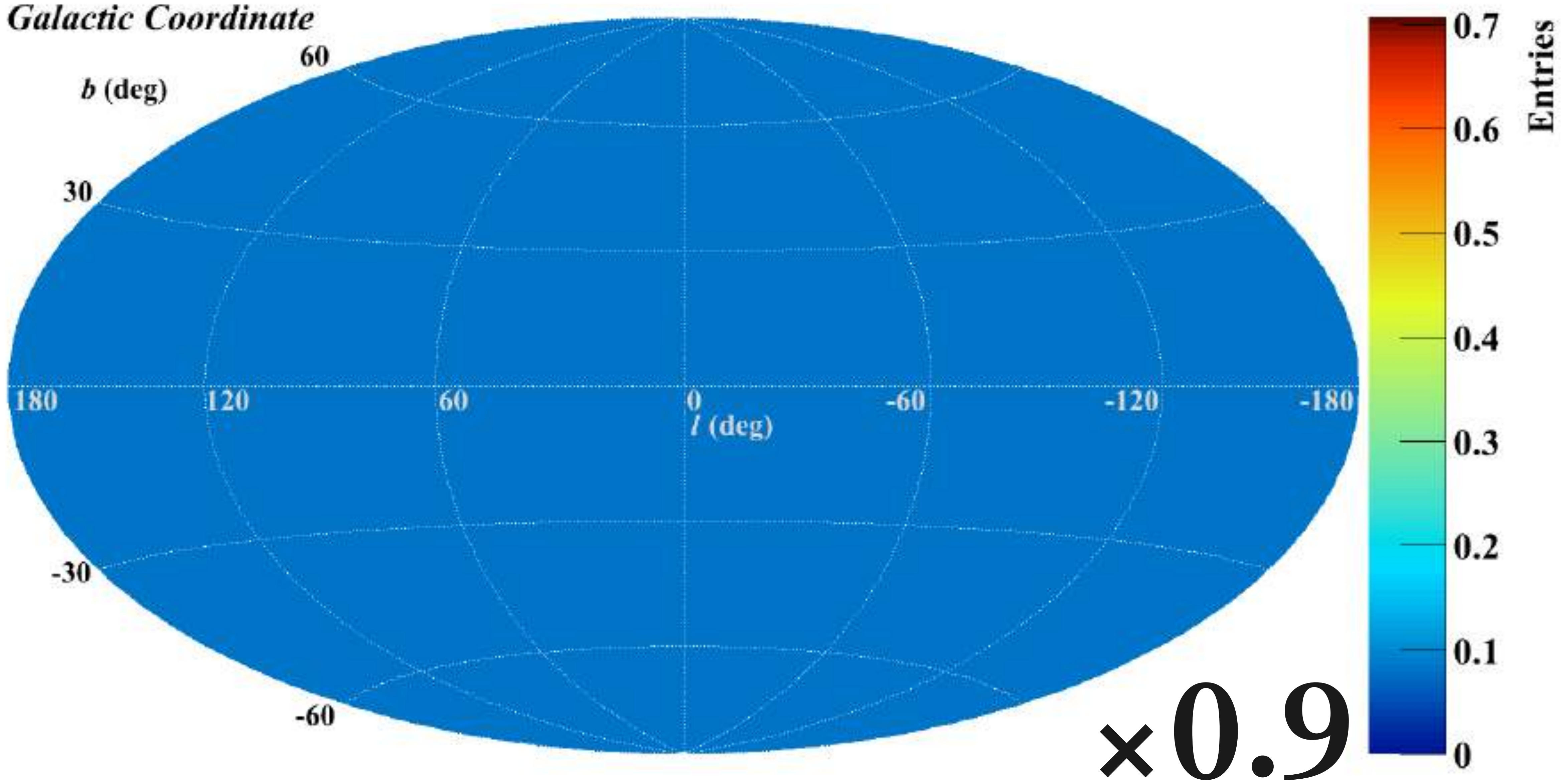

×0.9

=

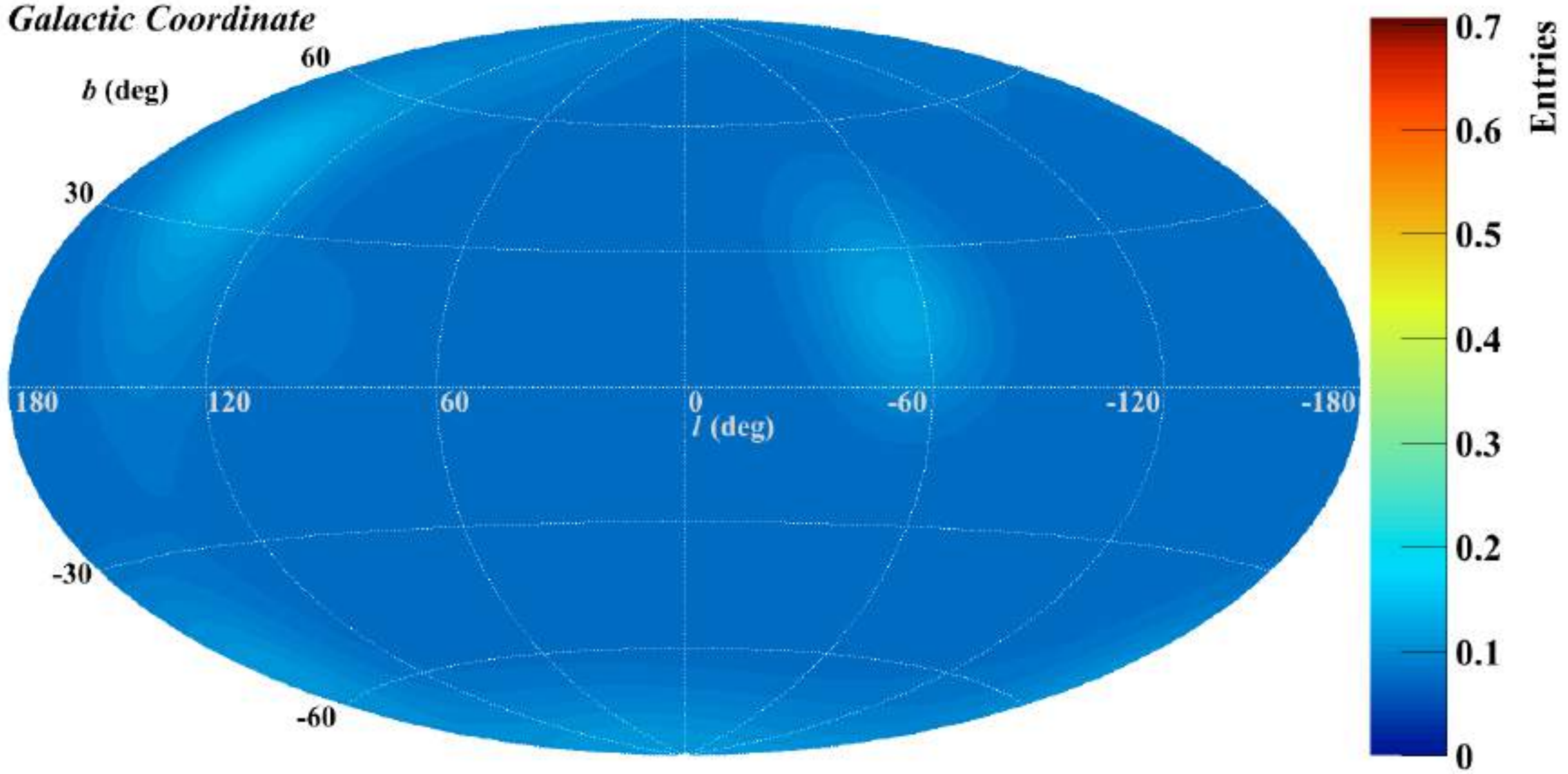

- ✦ほとんど(90.3%)の宇宙線は等方的である
- ✦一部(9.7%)の宇宙線の起源が近傍のスターバースト銀河と関係しているかもしれない
- ✦超銀河面に天体が多いのはどのカタログでも共通なため、スターバースト銀河だけに有意な相関があるわけではない

4.5σに増加 (ICRC 2019)

Intermediate anisotropy

γ AGNs
- 3FHL catalog < 250 Mpc
- 33 sources (CenA, Fornax A, M87…)
- Flux proxy ϕ(>10 GeV)

Starburst Galaxies
- 32 sources (Circinus, M82, M83,…)
- <250 Mpc
- Flux proxy ϕ(>1.4 GHz), > 0.3 Jy

Swift-BAT
- >300 radio loud and quiet sources
- <250 Mpc
- $\phi > 13.4\ 10^{-12}$ erg cm^{-2} s^{-1}

2MRS
- ~10^4 sources with D>1 Mpc
- <250 Mpc
- Flux proxy ϕ(14-195 keV)

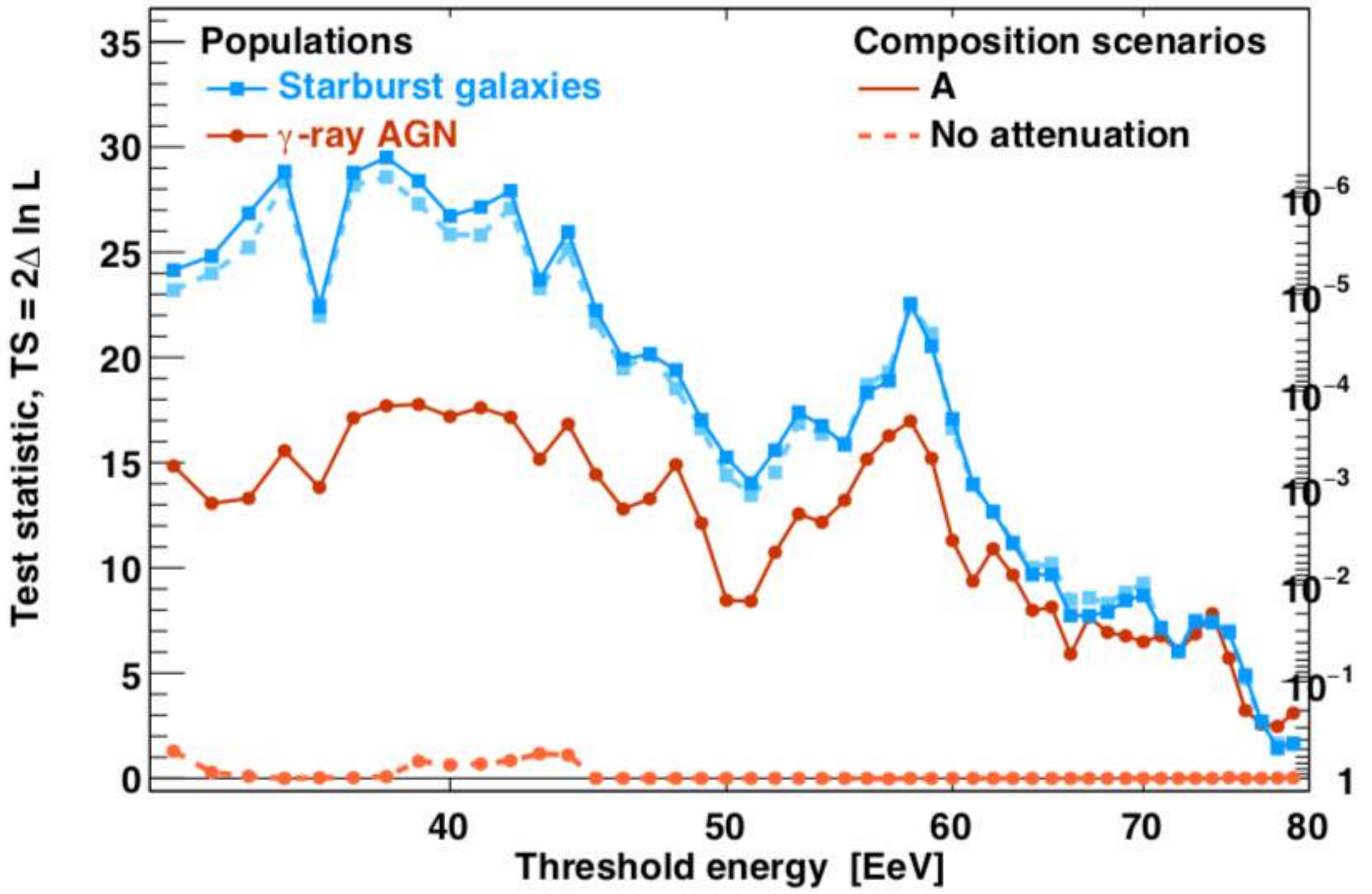

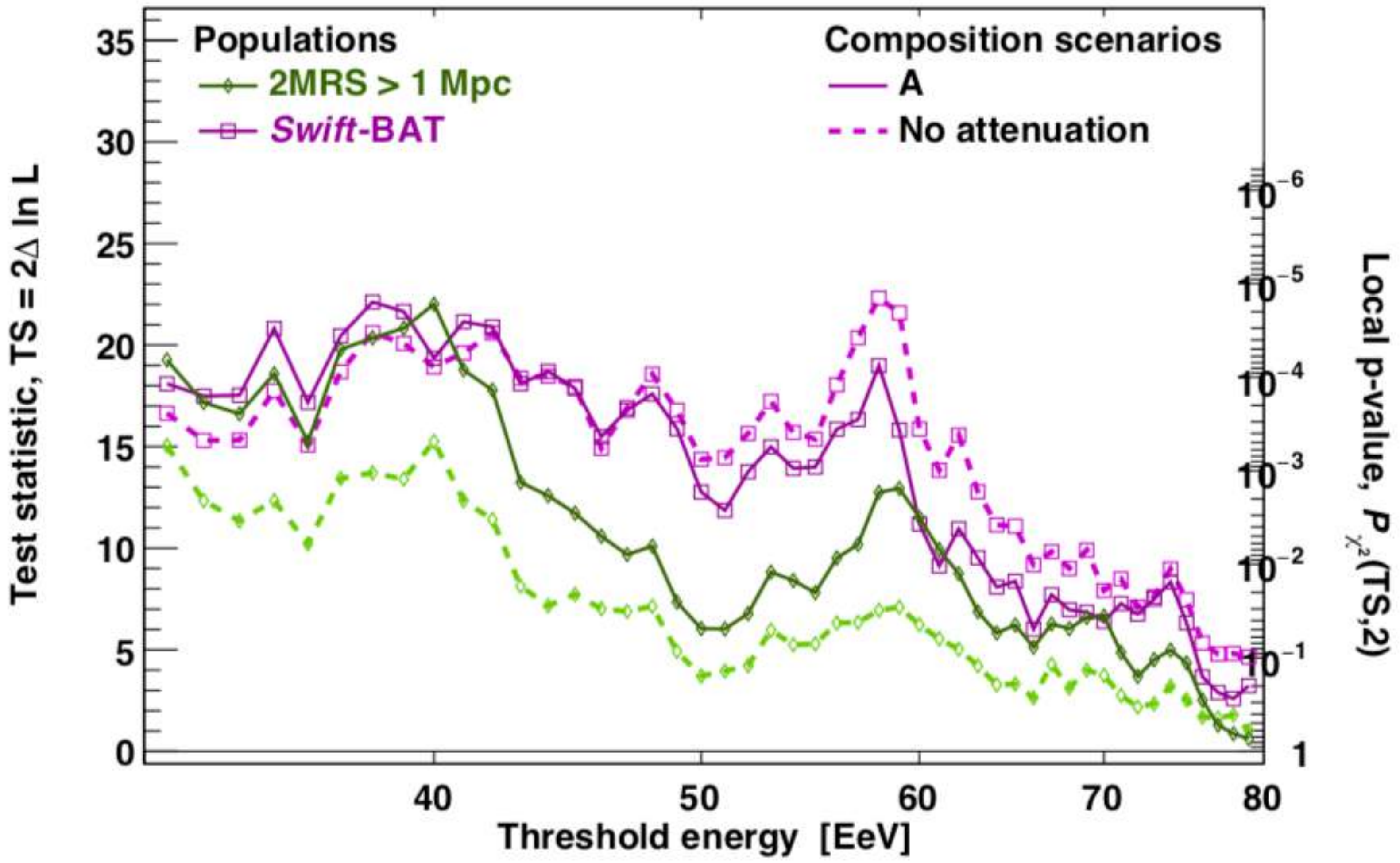

Likelihood analysis $TS = 2Log\left[L(\psi, f_{anis})/L(f_{anis}=0)\right]$

Catalog	E_{th}	TS	Local p-value	post-trial	f_{aniso}	θ
Starburst	38 EeV	29.5	4×10^{-7}	4.5 σ	$11^{+5}_{-4}\%$	$15^{+5}_{-4}{}^\circ$
γ–AGN	39 EeV	17.8	1×10^{-4}	3.1 σ	$6^{+4}_{-3}\%$	$14^{+6}_{-4}{}^\circ$
Swift-BAT	38 EeV	22.2	2×10^{-5}	3.6 σ	$8^{+4}_{-3}\%$	$15^{+6}_{-4}{}^\circ$
2MRS	40 EeV	22.0	2×10^{-5}	3.6 σ	$19^{+10}_{-7}\%$	$15^{+7}_{-4}{}^\circ$

他分野への波及効果

銀河系外磁場をUHECRから制限

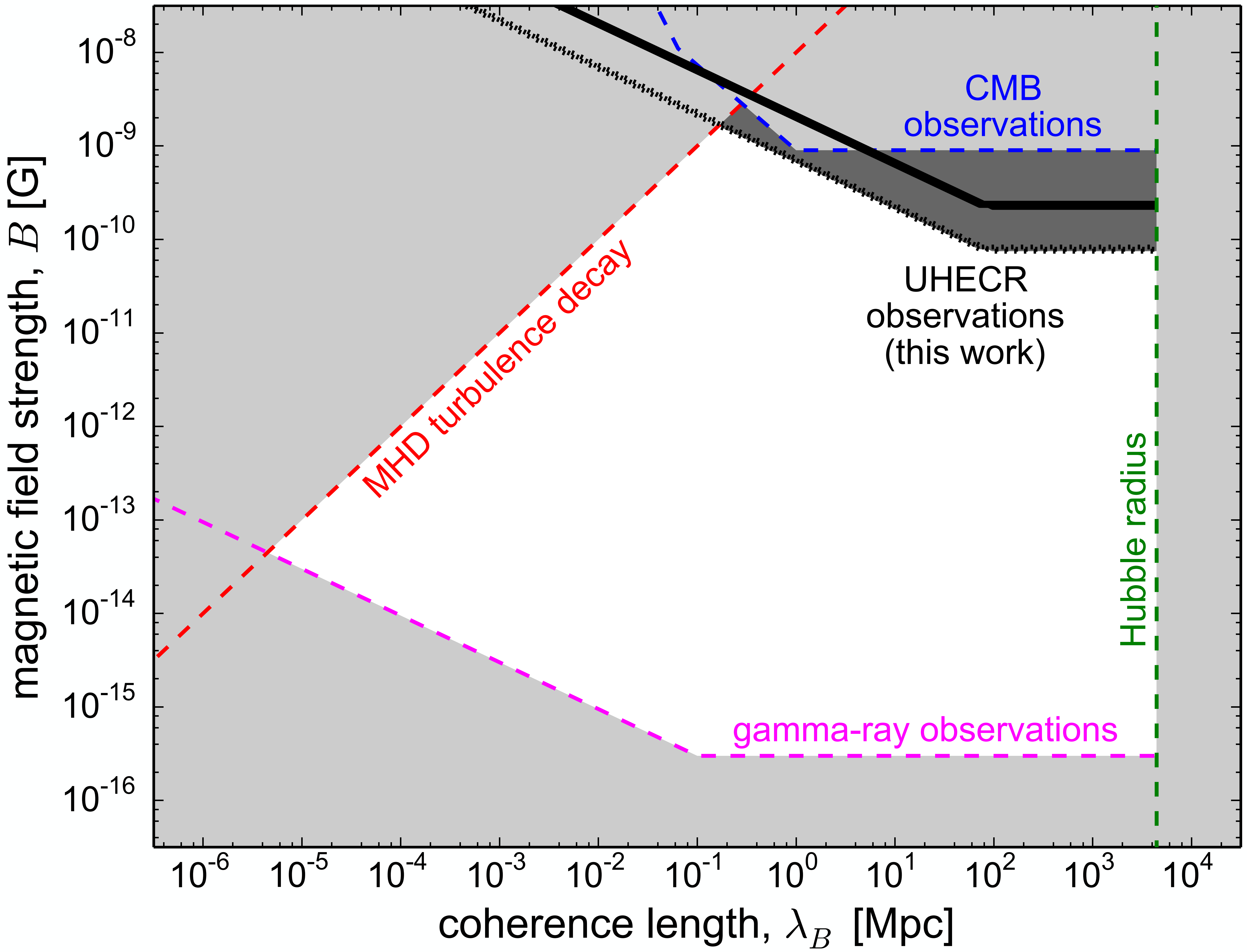

Figure 3. Parameter space for the strength B and coherence length λ_B of the EGMF in voids, showing regions excluded by past limits (light shaded) and this work (dark shaded). The near-identical limits placed in this work, based on UHECR observations, have a substantial uncertainty associated with the mean UHECR atomic number Z; solid and dotted lines show respectively the cases $Z = 1.7$ and $Z = 5$, which represent the range permitted by current composition measurements. Theoretical constraints are set by MHD turbulence, which causes the decay of short-scale modes in magnetic fields (Durrer & Neronov 2013), and by the Hubble radius, which places an upper limit to the size of any observable structure. The lower limit is set by the non-detection of gamma-ray cascades (Neronov & Vovk 2010). The upper limit shown from CMB observations is a projection from Paoletti & Finelli (2011), as represented by Durrer & Neronov (2013), and compatible with the limit $B < 9 \times 10^{-10}$ G established with Planck data (Ade et al. 2016).

$$B < 0.7\text{–}2.2 \times 10^{-9}(\lambda_B/1\ \mathrm{Mpc})^{-1/2}\ \mathrm{G}$$

J. D. Bray and A. M. M. Scaife, The Astrophysical Journal, 861:3 (7pp), 2018 July 1

スターバースト銀河からの放射とUHECRの明るいところが似ている

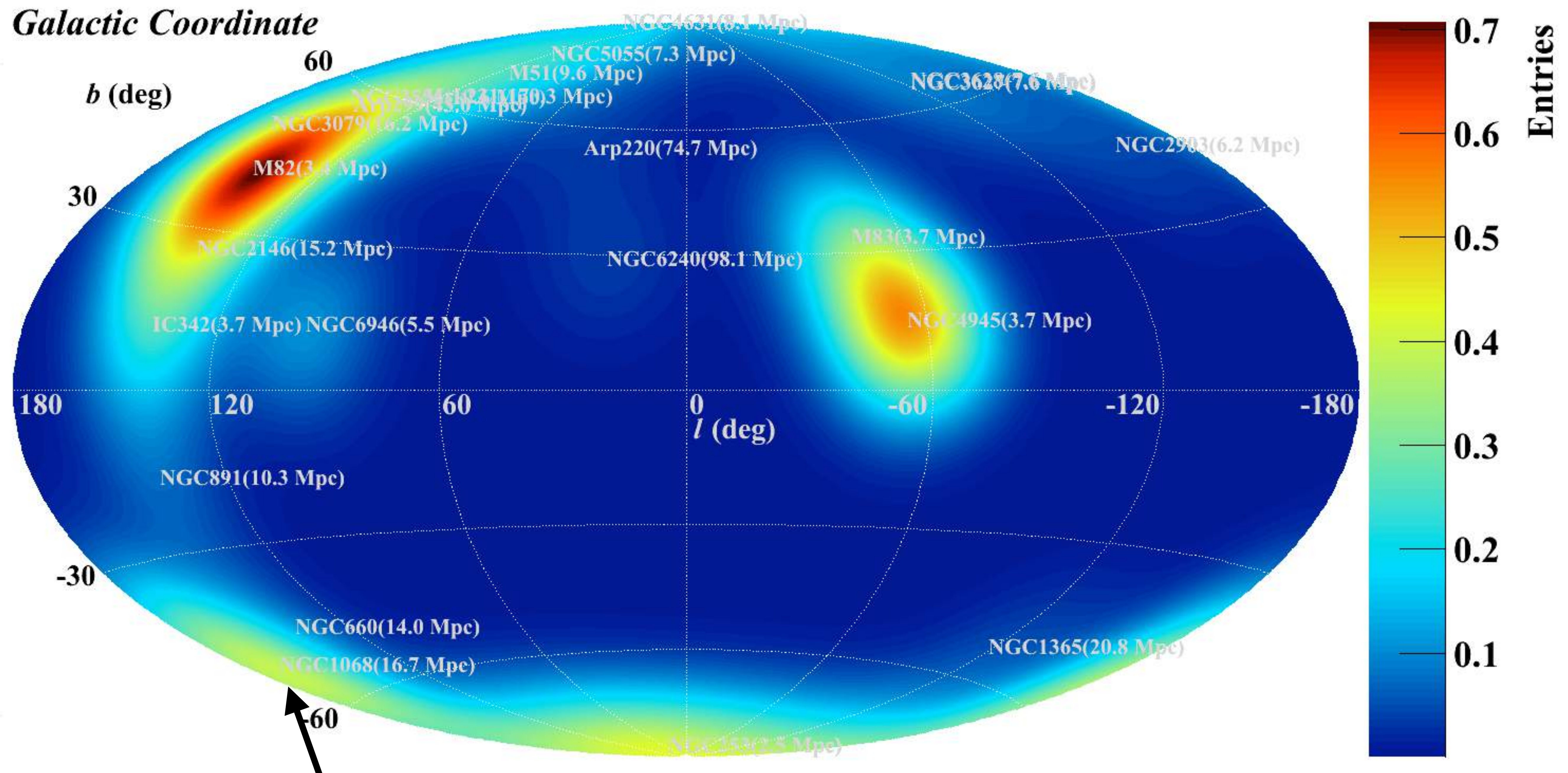

NGC 1068

Flux pattern

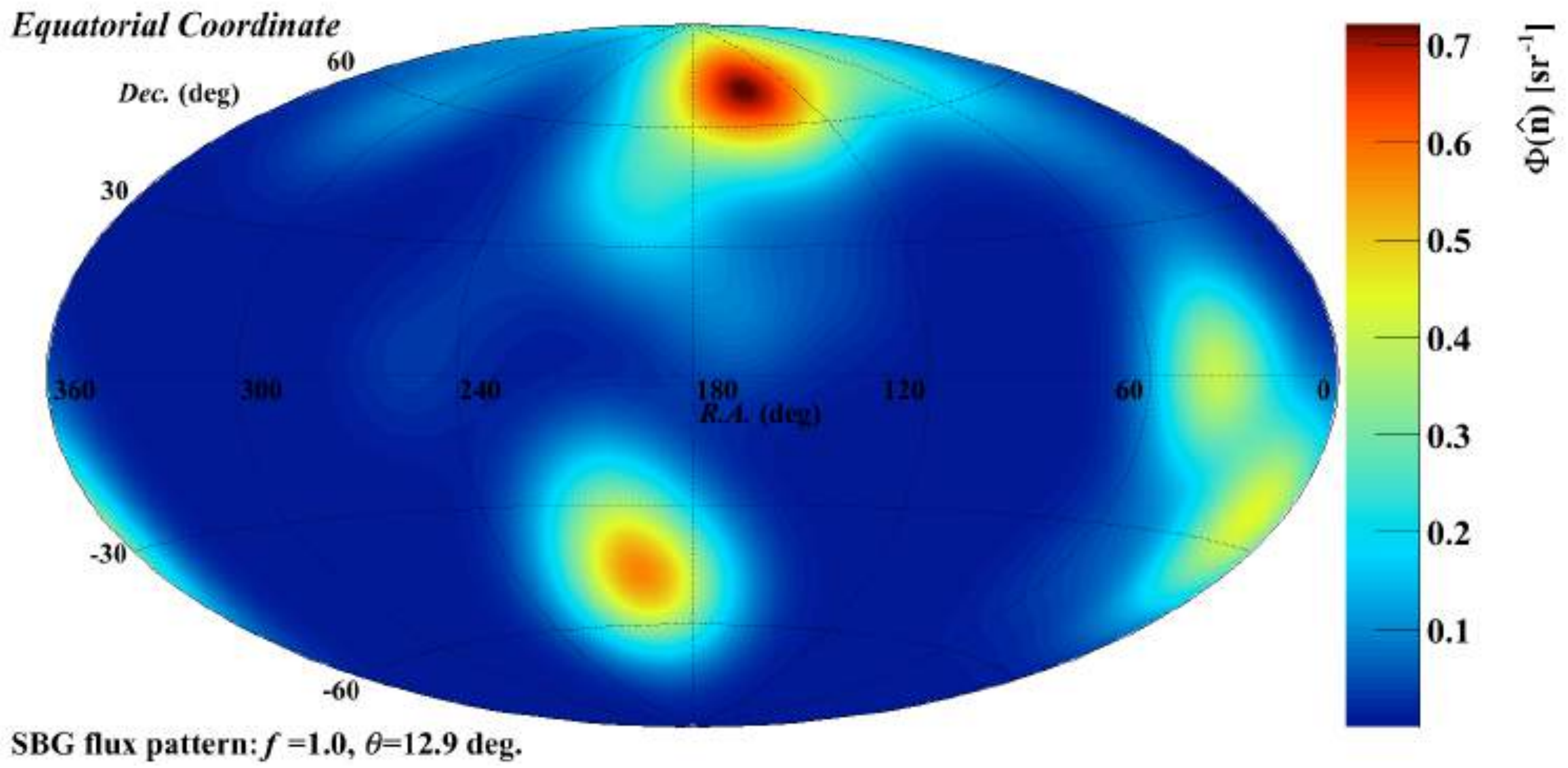

Data (TA + Auger, ICRC 2015)

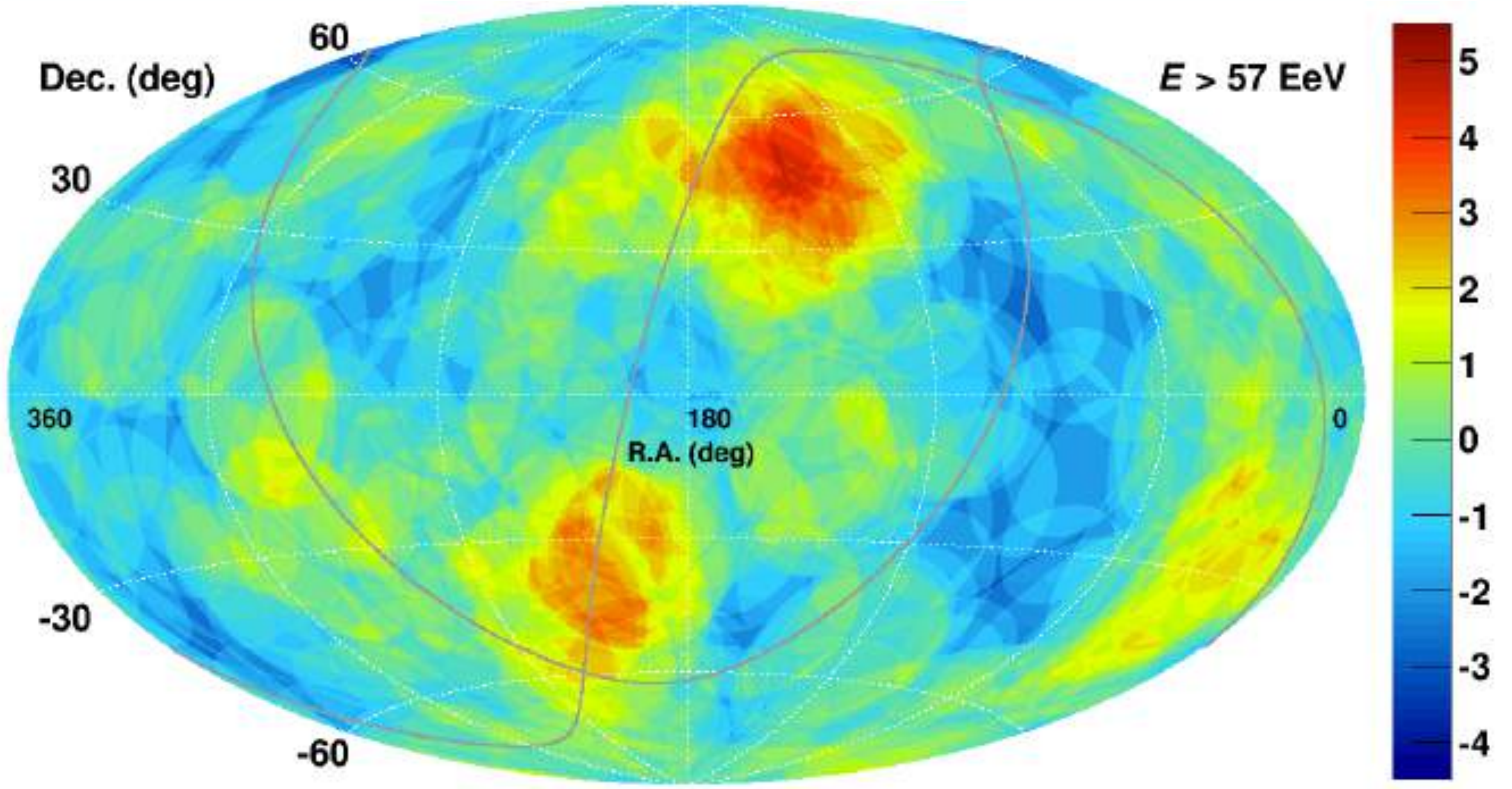

IceCube neutrino hotspot?

ニュートリノのホットスポット (2.9σ)

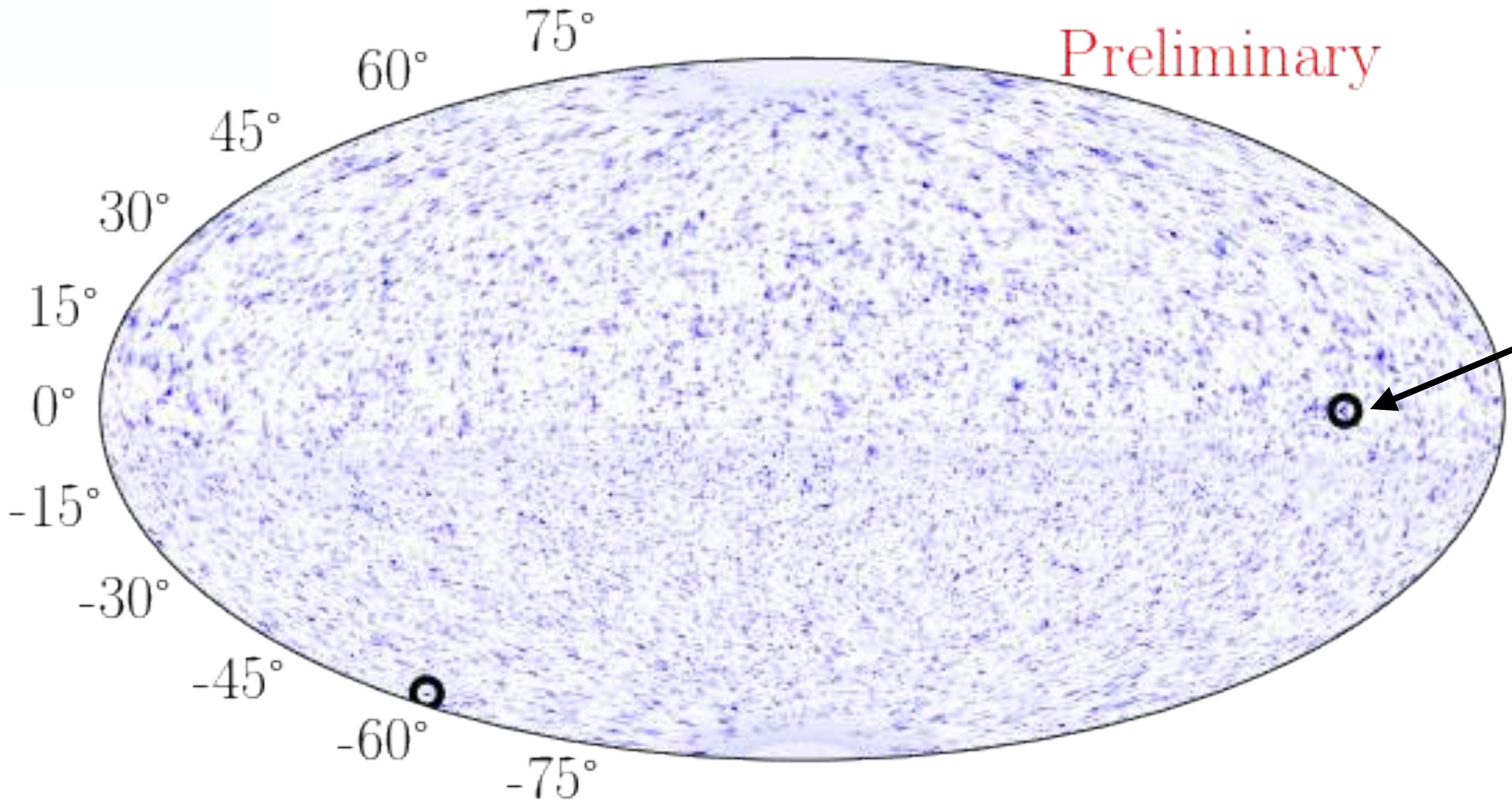

NGC 1068から0.35°

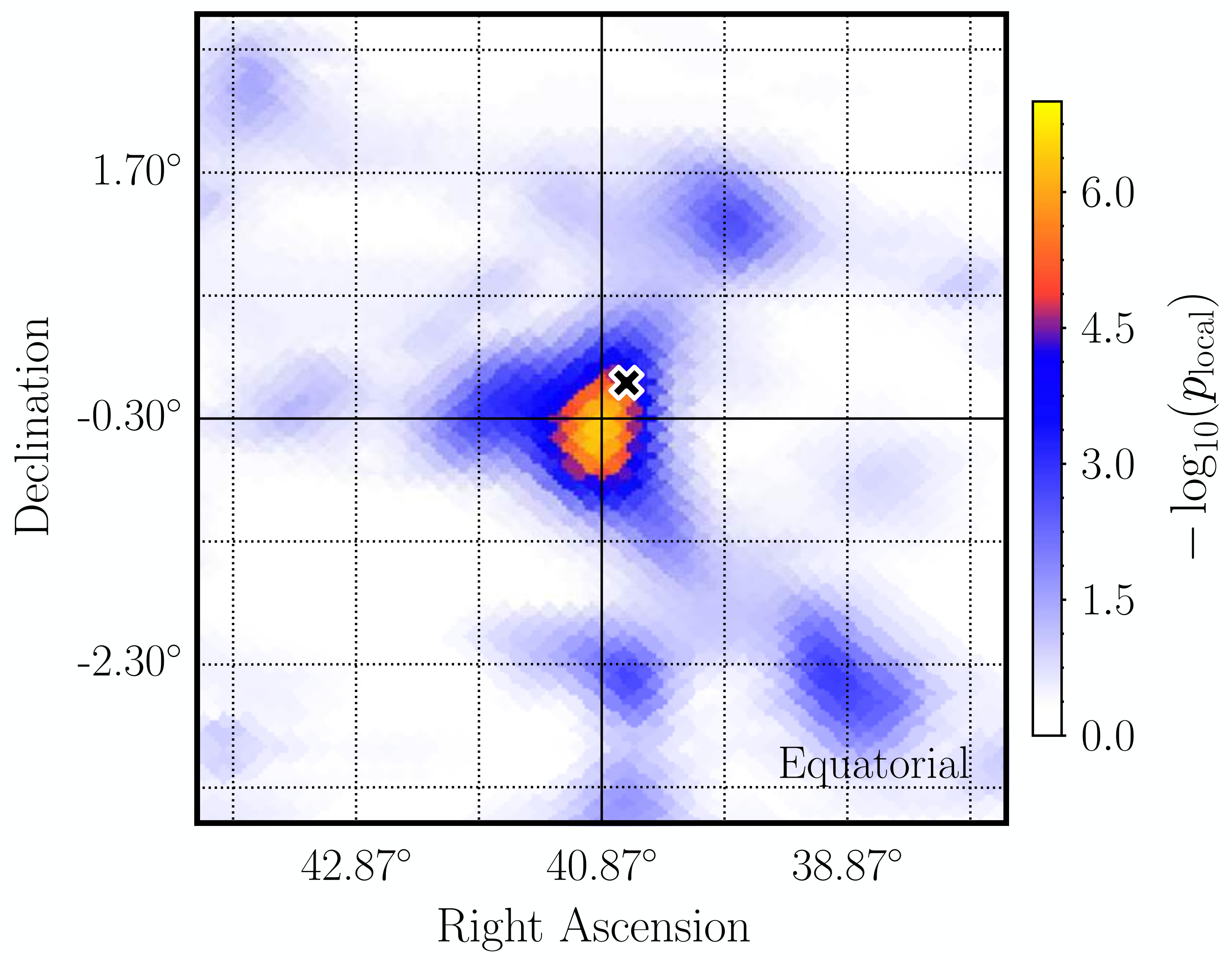

FIG. 2. Local pre-trial p-value map around the most significant point in the Northern hemisphere. The black cross marks the coordinates of the galaxy NGC 1068 taken from *Fermi*-4FGL.

でも、冪は -3.4 とsoft

F. Halzen in ICRC 2019

IceCube collaboration, PRL 124, 051103 (2020)

極高エネルギー宇宙線に拘らず…

スペクトルと化学組成の"Global Fit"

$E^{2.6}$ J(E)

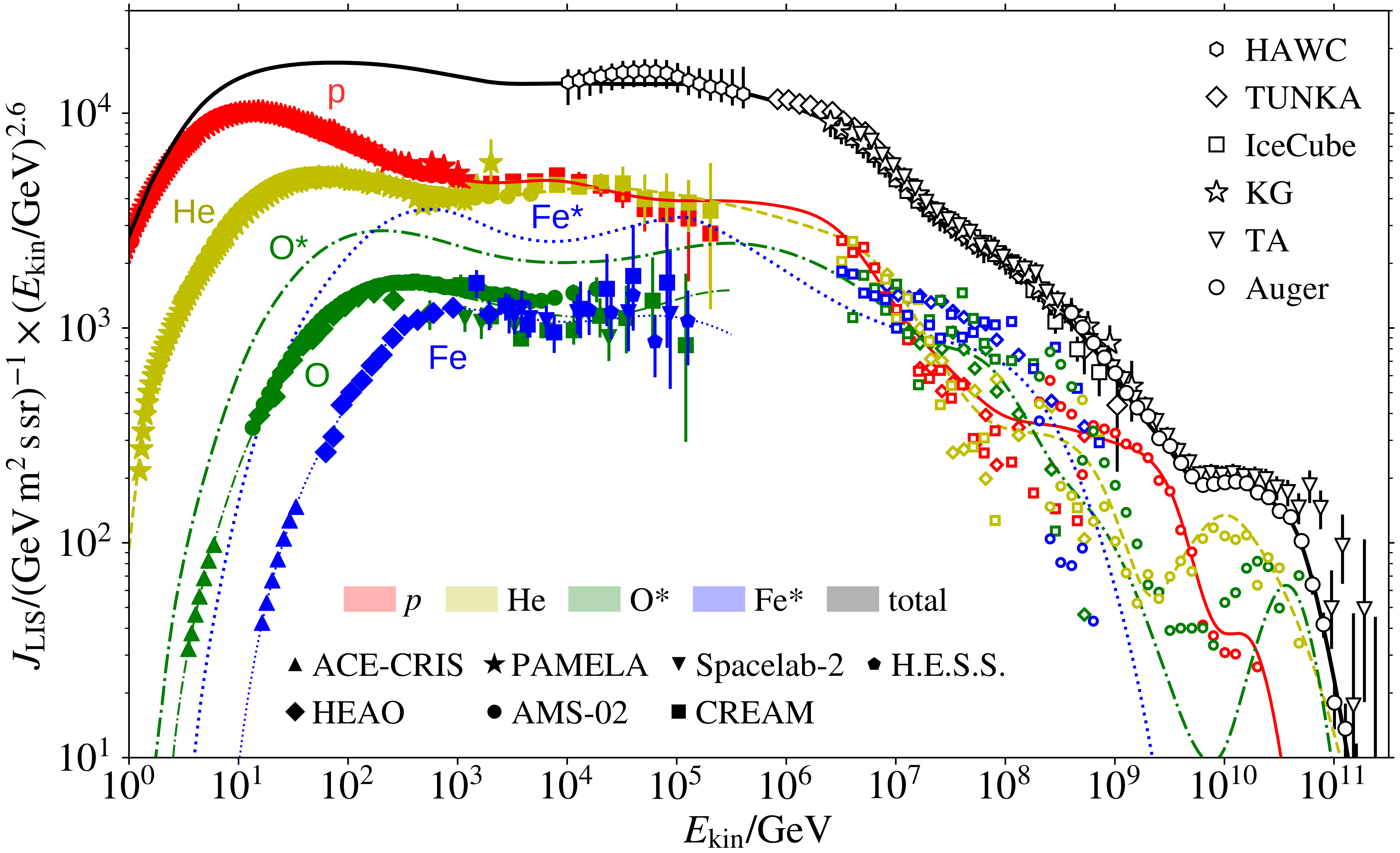

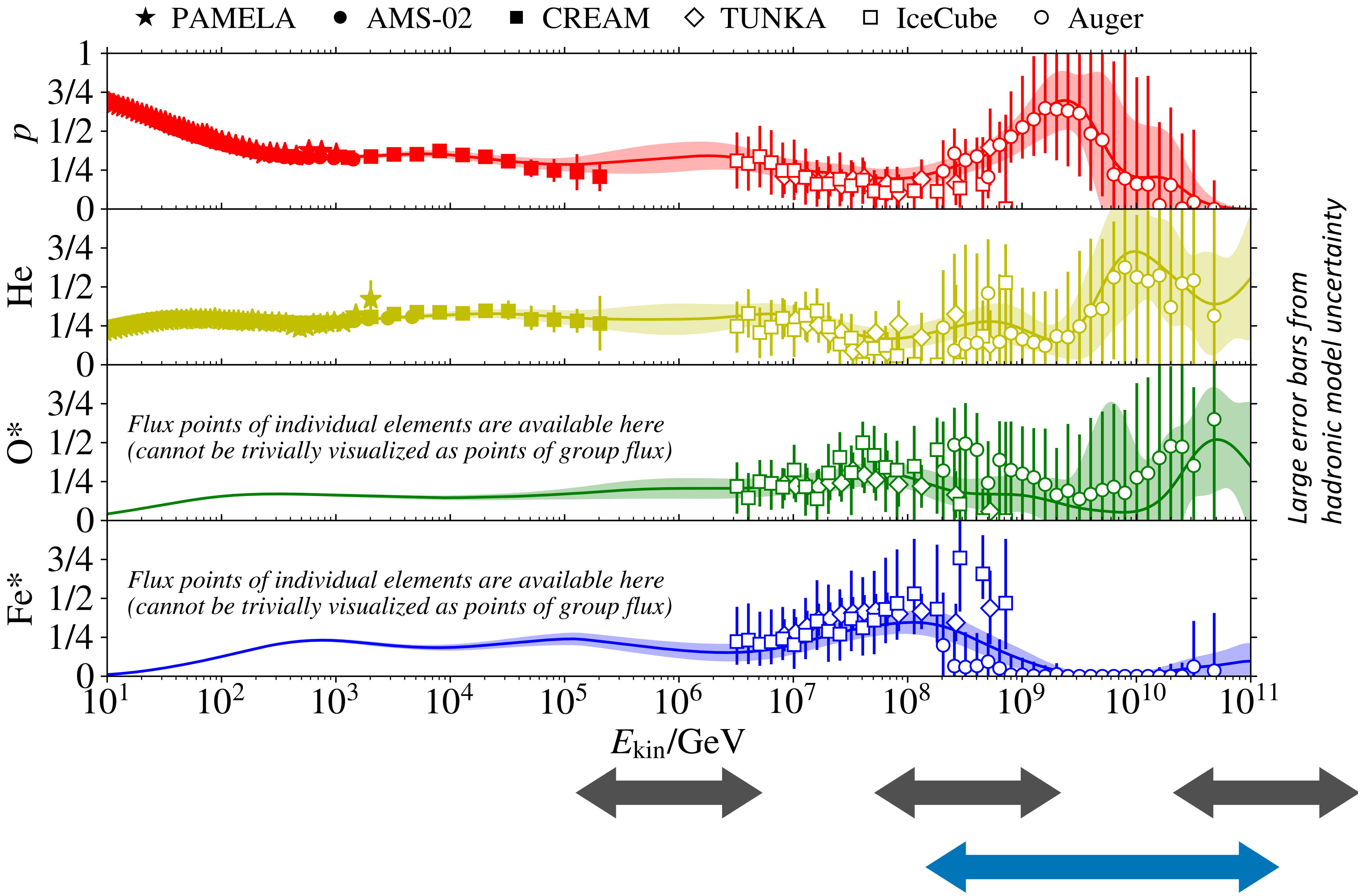

Hans Dembinski et al., UHECR 2018

O* : O Group (from Li to F)
Fe* : Fe Group (from Ne to Ni)

- 今後、精密測定すべきエネルギー領域
- ハドロン相互作用モデルの改善の必要性

広いエネルギー領域の質量組成

X_{max} by traditional techniques: fluorescence, air-Cherenkov, rise time

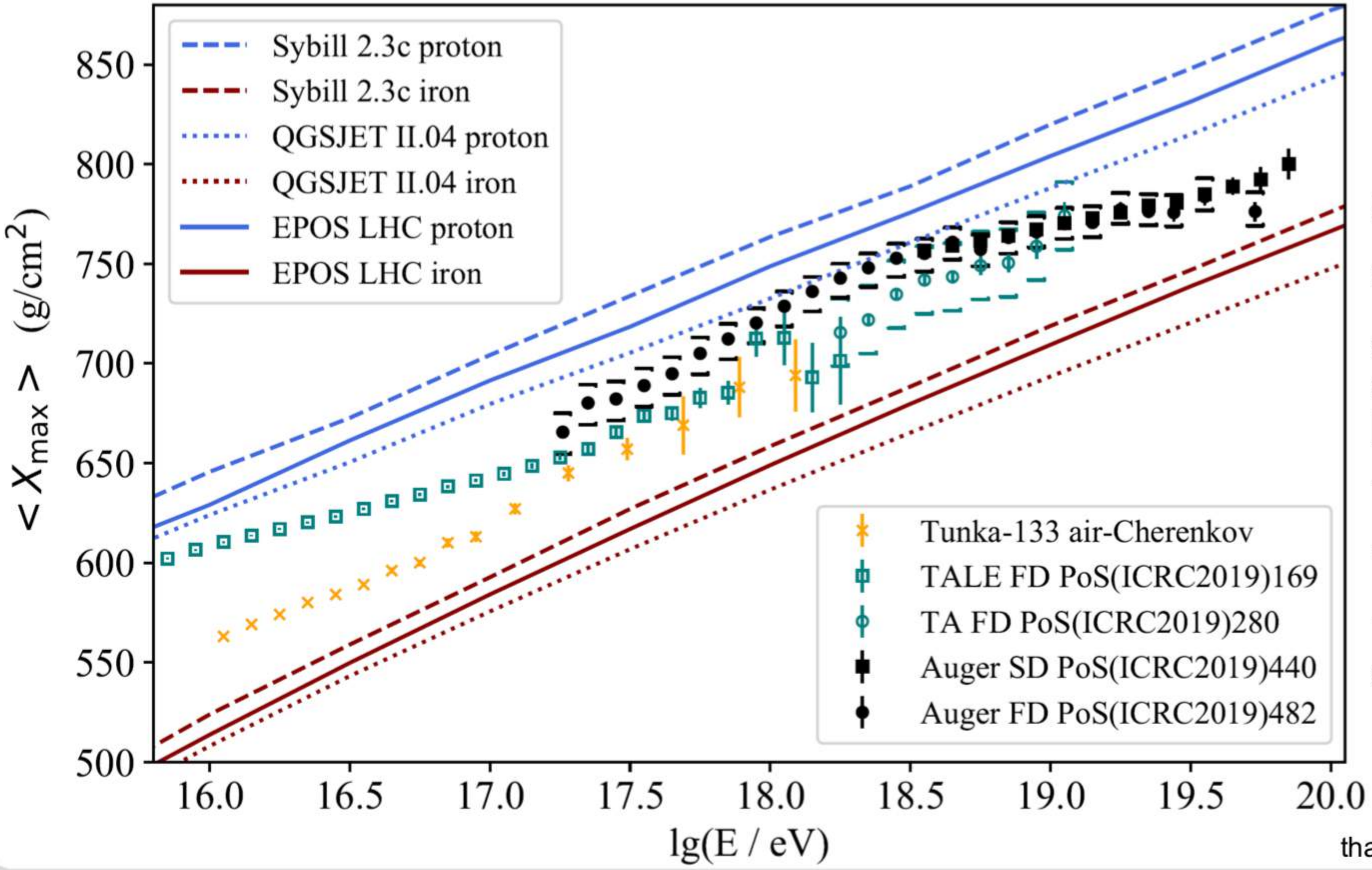

Caveats:

energy scale uncertainties

some experiments have acceptance biases, but model lines are without bias

TA acceptance bias: 11 g/cm^2

TALE bias not fully known

Tunka-133 biases and systematics not fully known

thanks to T. Pierog for model X_{max} values

fgs@udel.edu
frank.schroeder@kit.edu

Frank G. Schroder in ICRC 2019

銀河系内の宇宙線の加速限界は？

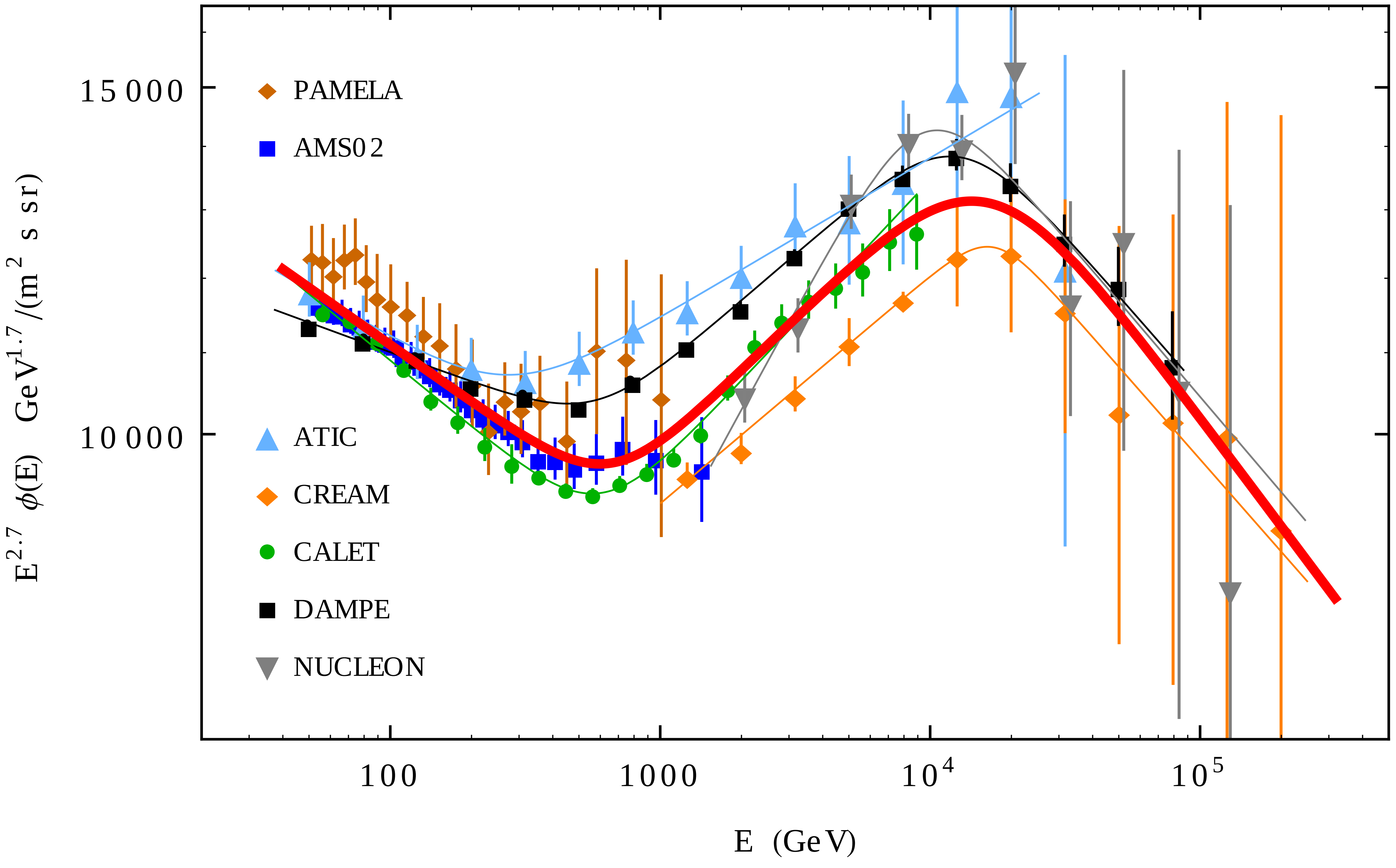

Figure 1: Direct measurements of the CR proton spectrum. The flux is shown in the form $E^{2.7}\,\phi(E)$ versus E to enhance the visibility of the spectral features. The points are the data of PAMELA [2], AMS02 [4], ATIC [5], CREAM [6], CALET [7], DAMPE [10] and NUCLEON [8]. The thick (red) solid line is a fit of the combined data of all the experiments using the two–break expression (1). The thin lines are fits of the data of individual experiments. The parameters of all fits are listed in Table 1.

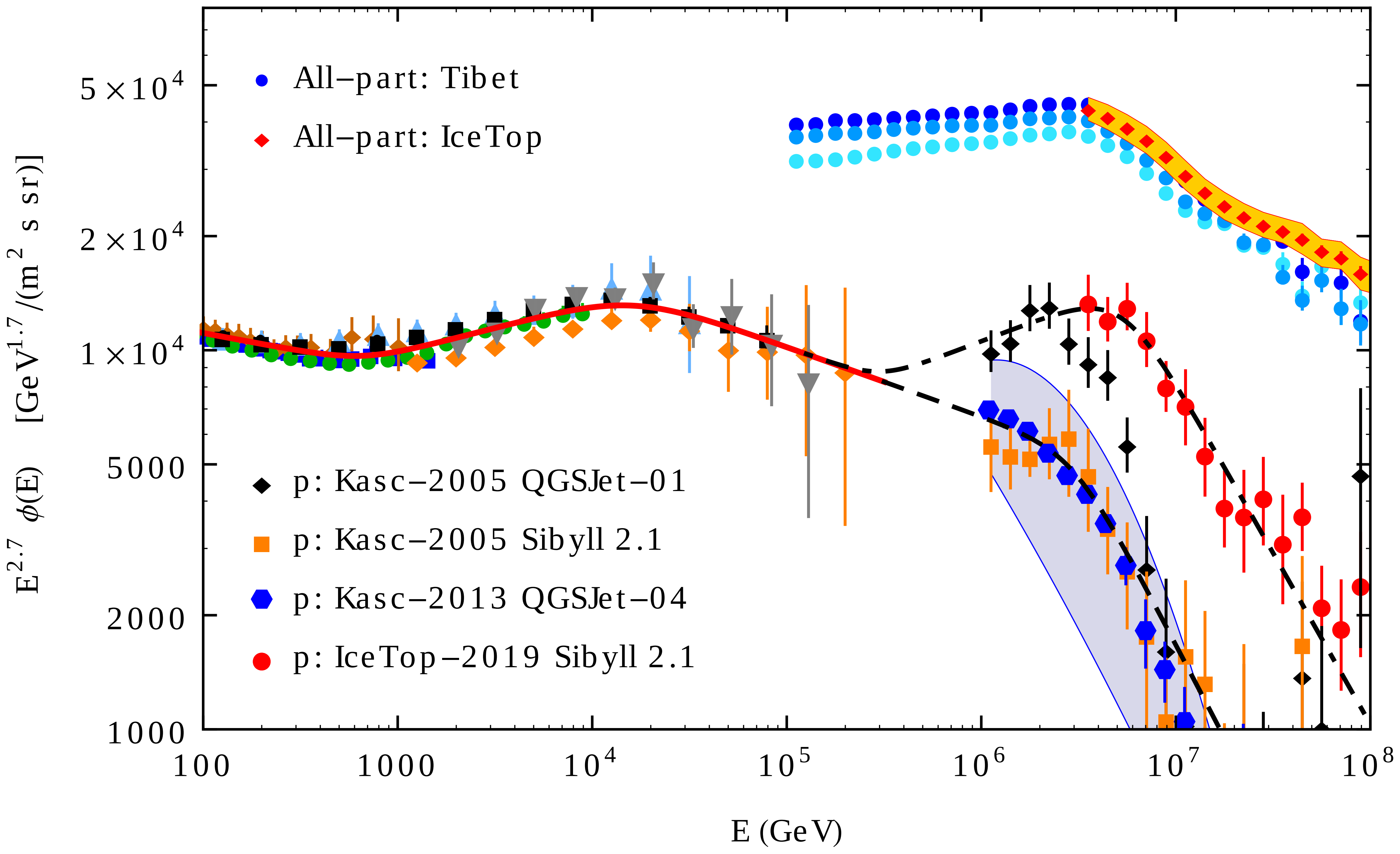

Figure 2: All–particle and proton spectra obtained by direct measurements and EAS observations. The all–particle data are by the Tibet experiment [12] (with three sets of data points obtained with different assumptions for the CR composition and shower development models), and by IceTop/IceCube [13] (with the shaded area indicating systematic uncertainties). For the proton direct measurements the symbols are identical to those in Fig. 1. The EAS proton spectra are by Kascade–2005 [15], Kascade–2013 [19] (with the shaded area indicating systematic uncertainties) and IceTop/IceCube–2019 [13]. The thick solid line is a fit to the direct measurements of the proton flux (with the parameters given in Table 1). The dashed and dot–dashed lines are extrapolations to higher energy (see main text).

Paolo Lipari, Silvia Vernetto, Astroparticle Physics, in Press (2020)

10^{16} eVでも陽子が主？

TALE FD monocular reconstruction

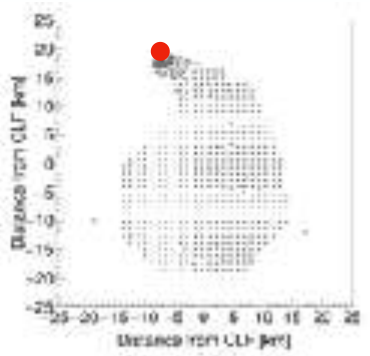

T. AbuZayyad

TALE FD monocular spectrum (2 years)
Ap. J., 865, 74(2018), arXiv: 1803.01288

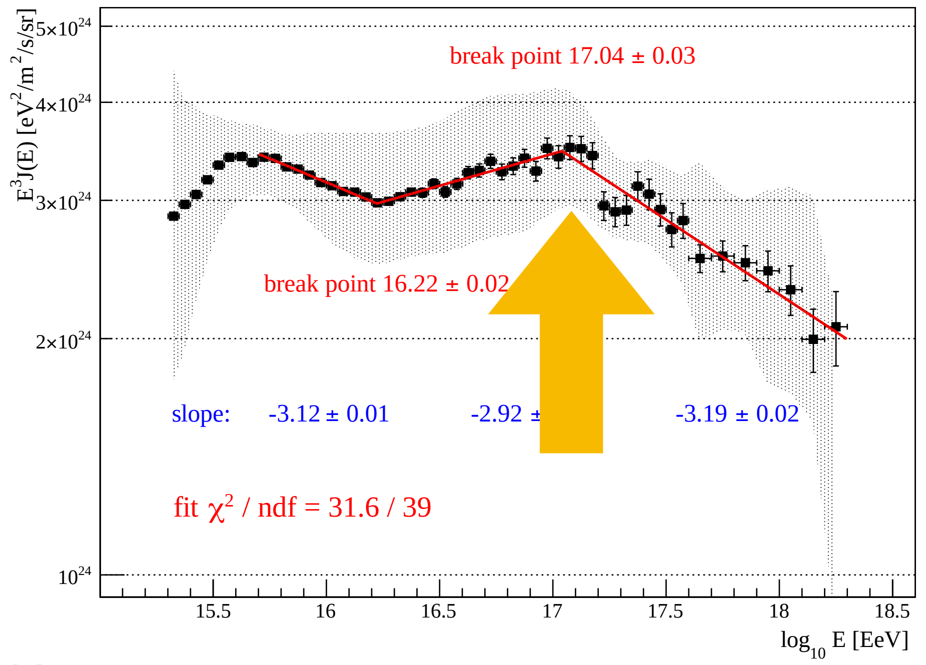

Xmax measured by TALE FD with monocular reconstruction
4 years of data (Jun. 2014 - Nov. 2018)

Change in Xmax elongation rate at an energy of ~10^{17} eV
(It is likely correlated with 2nd knee in the energy spectrum)

Smooth connection of the low(TALE) and the high(BR/LR hybrid) energy rails.

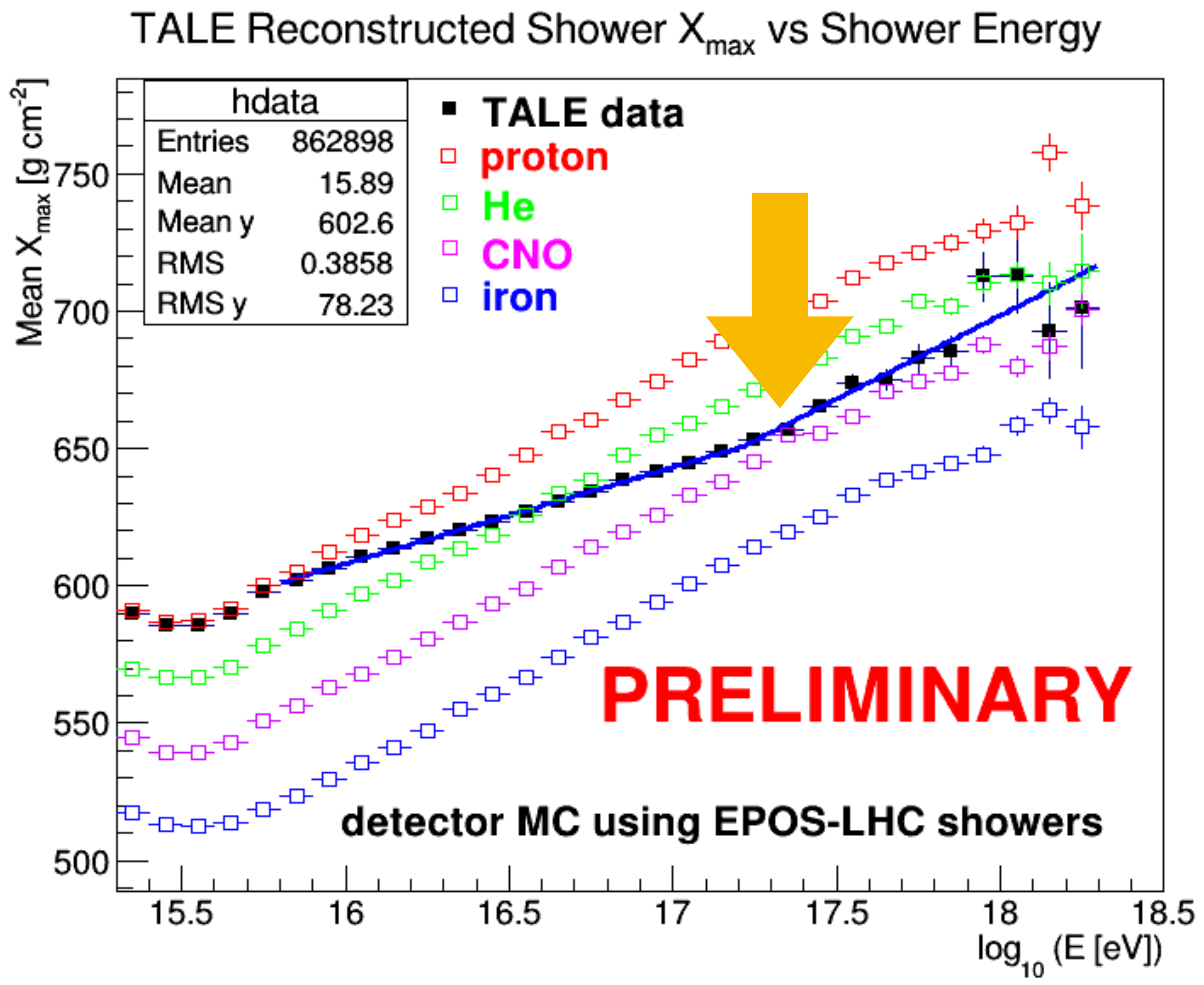

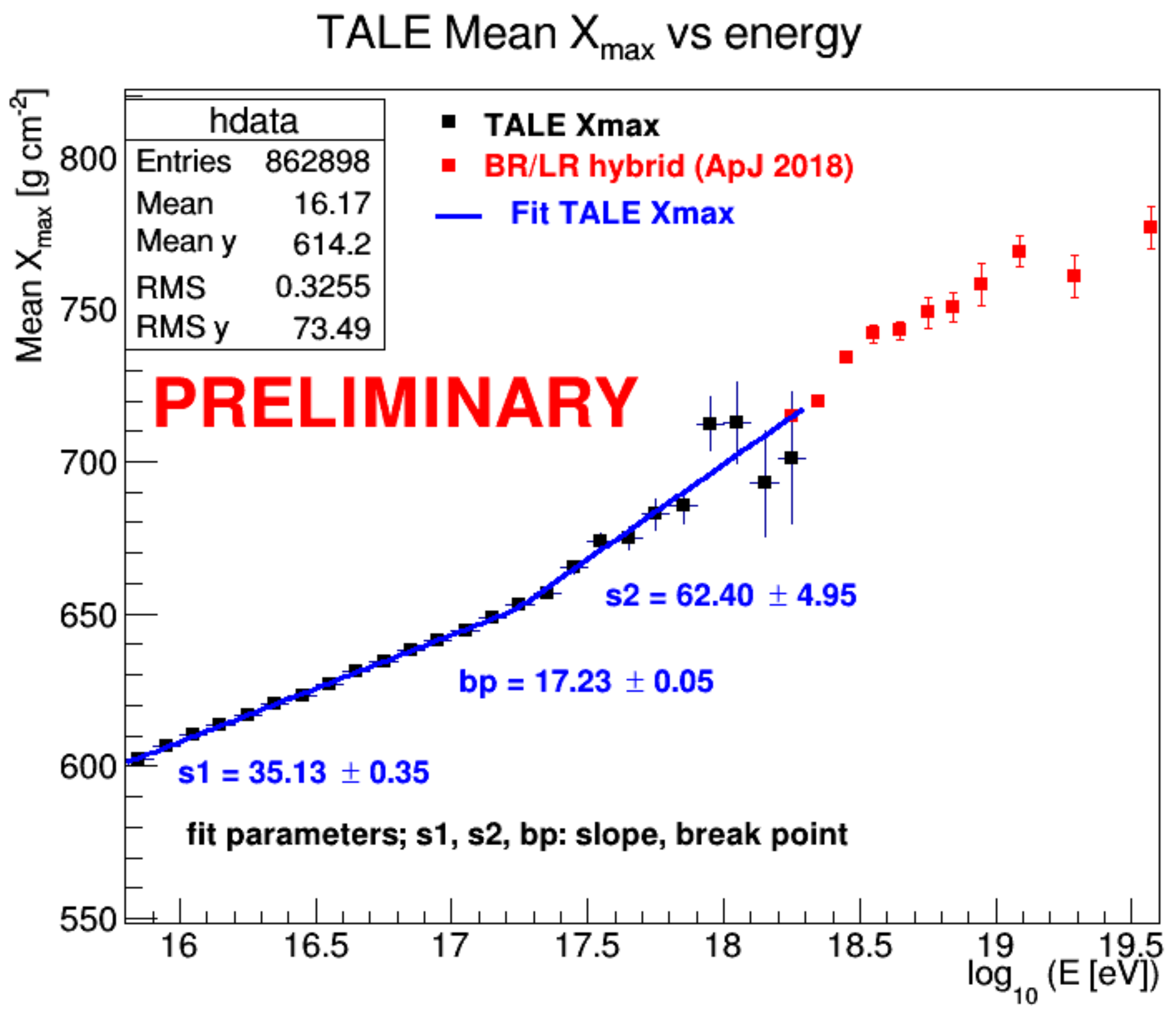

20

S. Ogio, ICRC 2019

銀河系内外起源の遷移は？

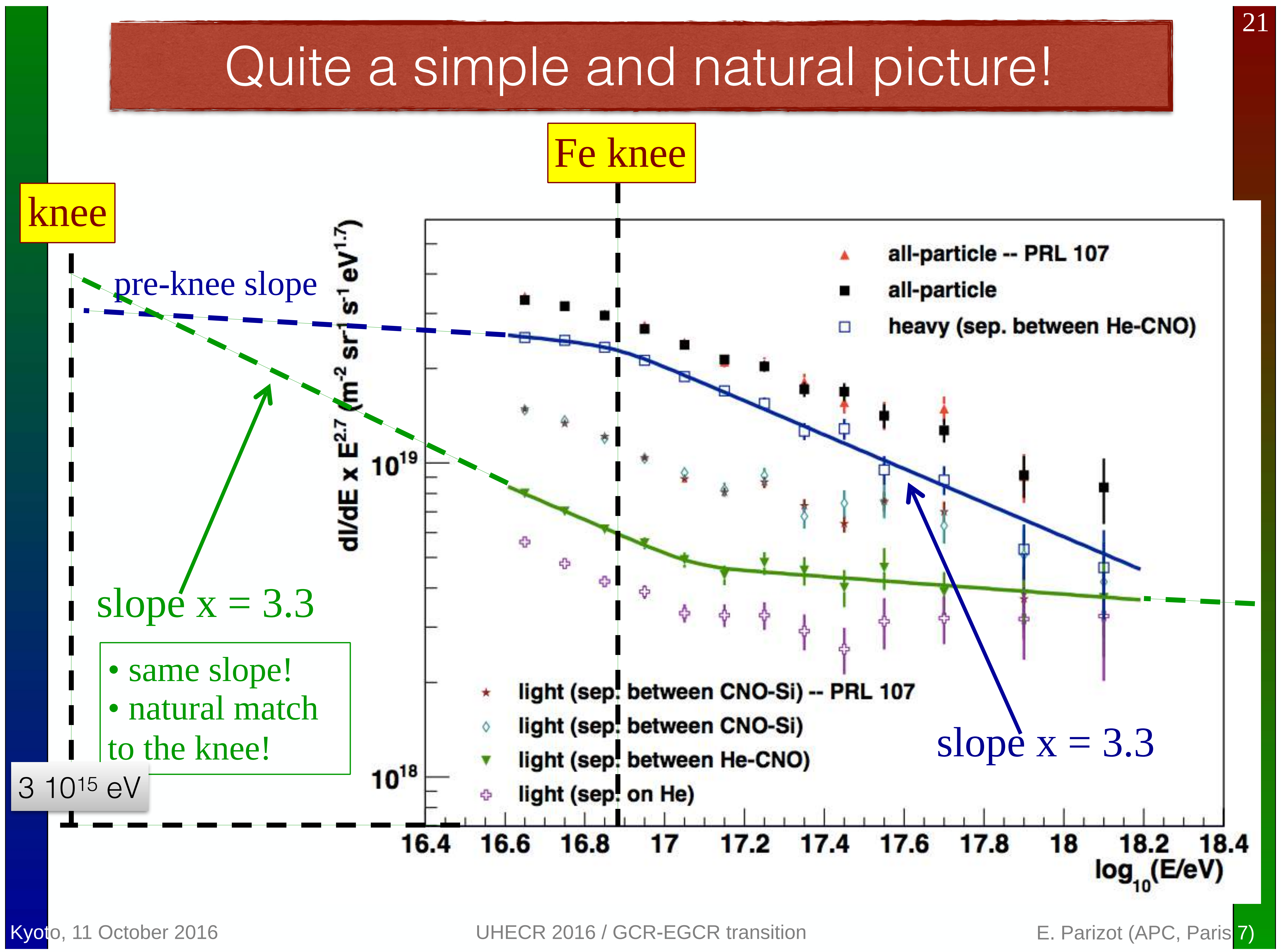

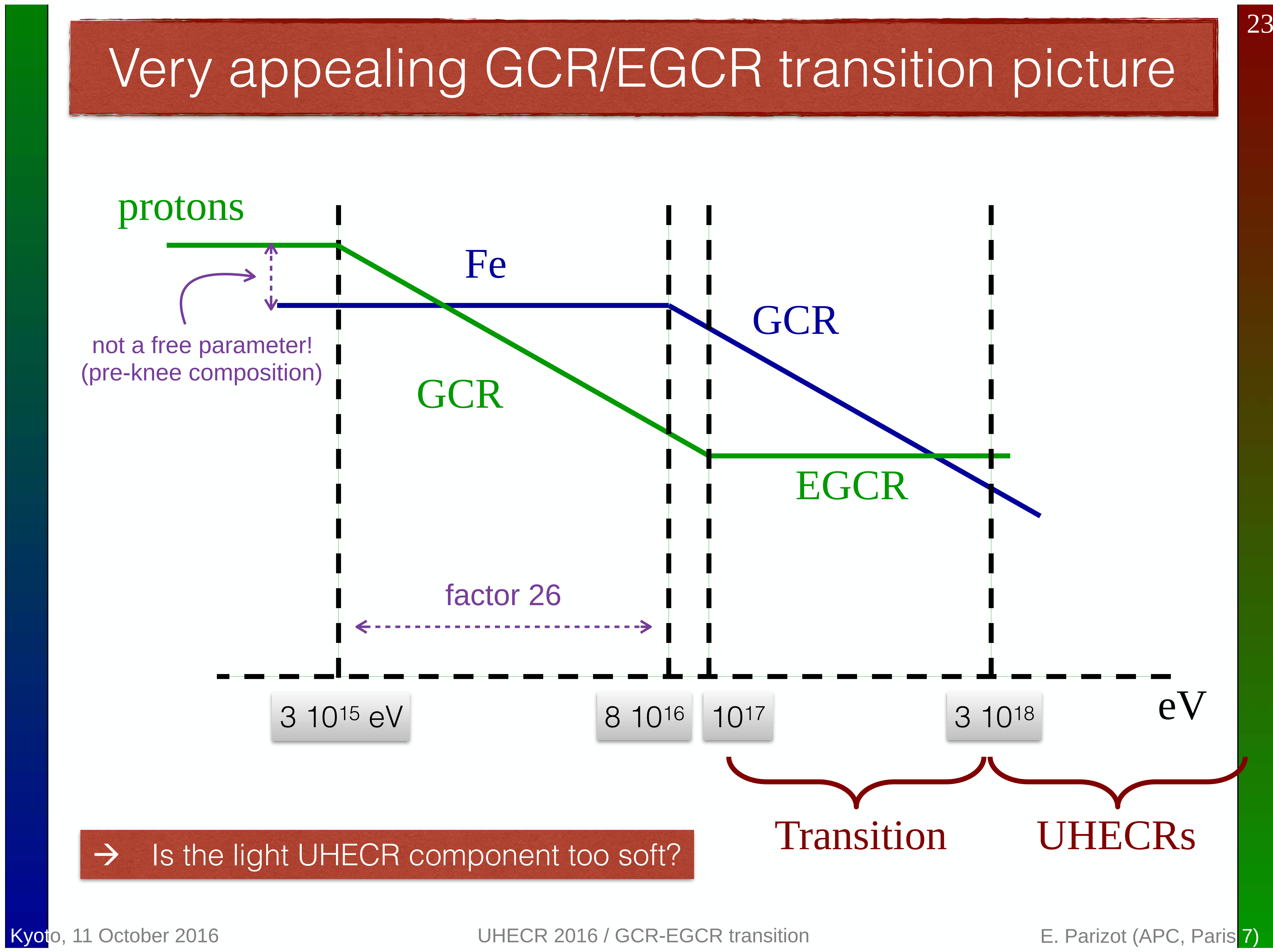

E. Parizot in UHECR 2016

10^{14} eVで位相が銀河中心へ向かっていく

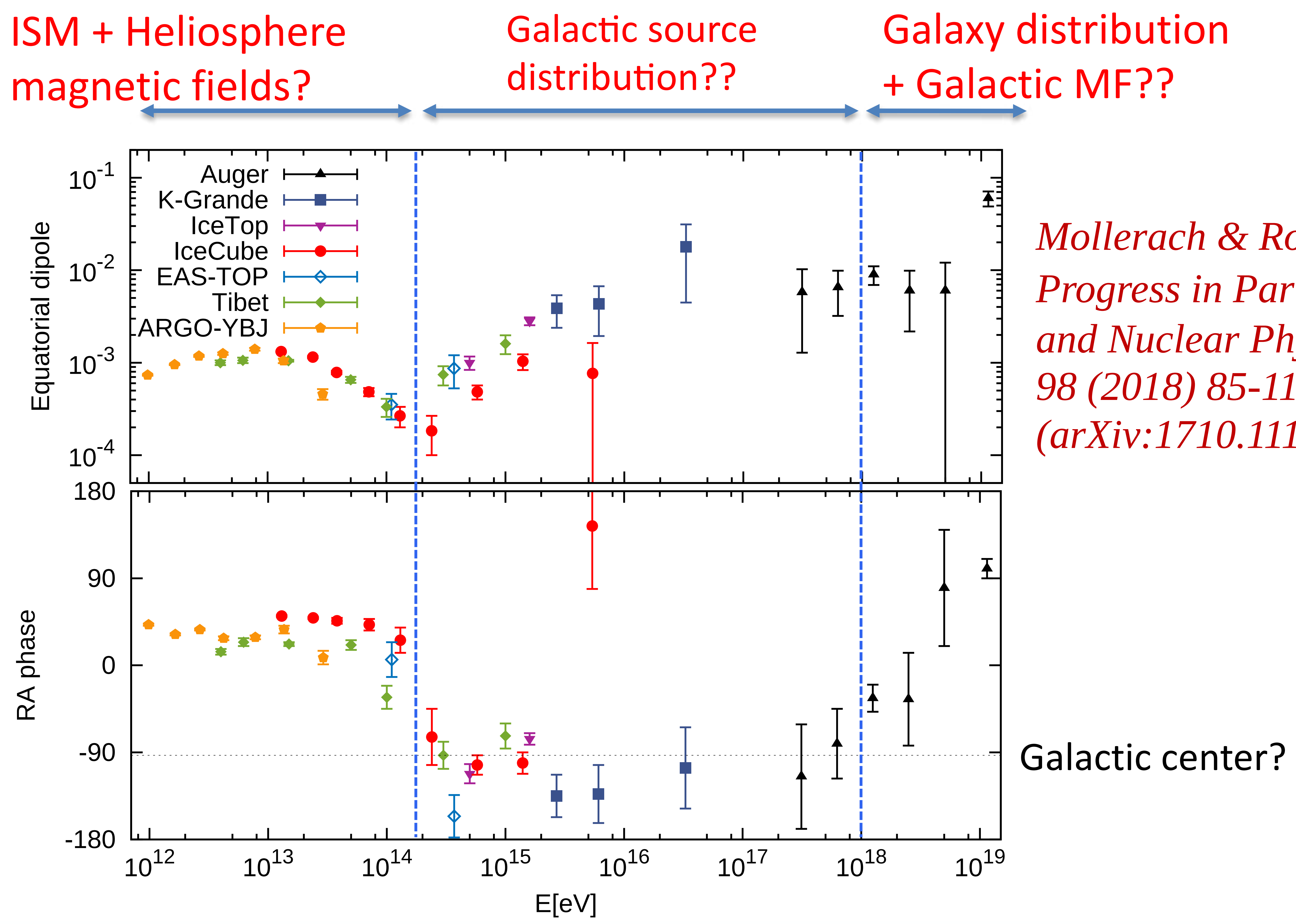

Mollerach & Roulet Progress in Particle and Nuclear Physics 98 (2018) 85-118 (arXiv:1710.11155)

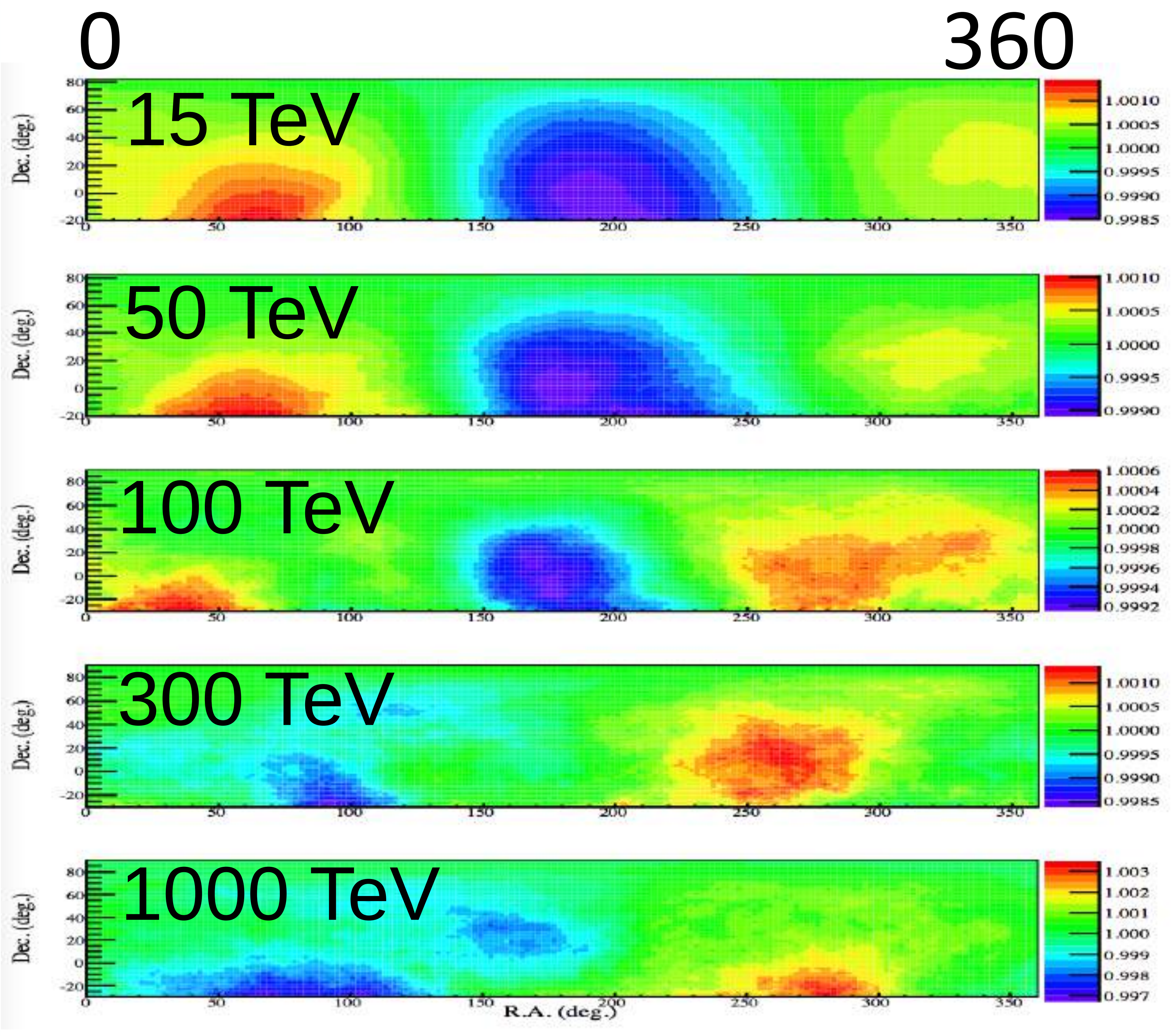

M. Amenomori et al, ApJ, 836, 153-1-7, (2017)

K. Kawata in ICRC 2019

多波長・多粒子観測の連携

X-ray MeV GeV - TeV

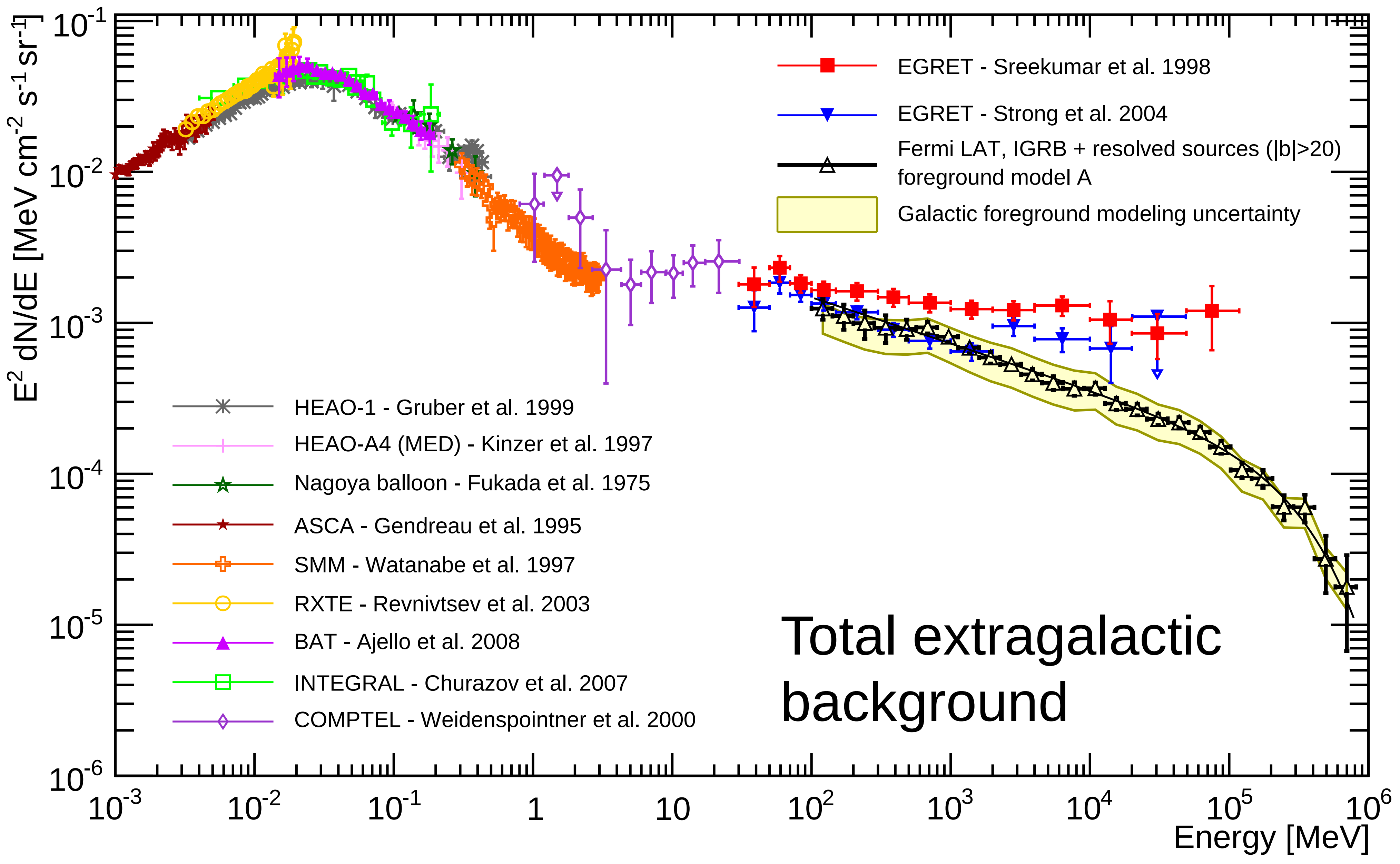

Fig. 10.— Comparison of the derived total EGB intensity (foreground model A) to other measurements of the X-ray and γ-ray background. The error bars on the LAT measurement include the statistical uncertainty and systematic uncertainties from the effective area parametrization, as well as the CR background subtraction. Statistical and systematic uncertainties have been added in quadrature. The shaded band indicates the systematic uncertainty arising from uncertainties in the Galactic foreground. (Note that the EGRET measurements shown are measurements of the IGRB. However, EGRET was more than an order of magnitude less sensitive to resolve individual sources on the sky than the *Fermi*-LAT.)

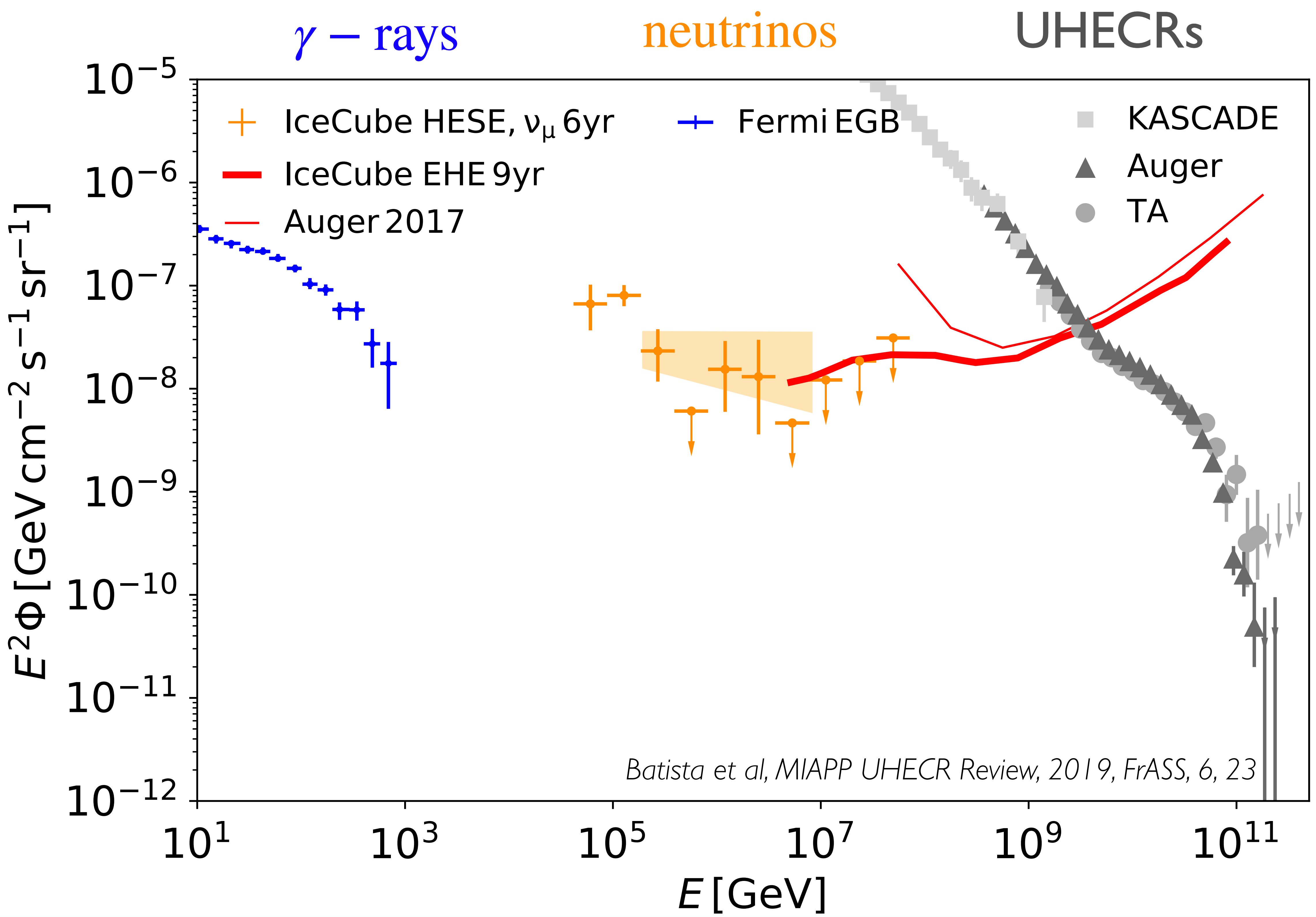

Fermi-LAT collaboration, Astrophys.J. 799 (2015) 86

R.A. Batista et al., Front.Astron.Space Sci. 6 (2019) 23

多波長・多粒子観測の連携

Seyfert galaxies ??? Blazers

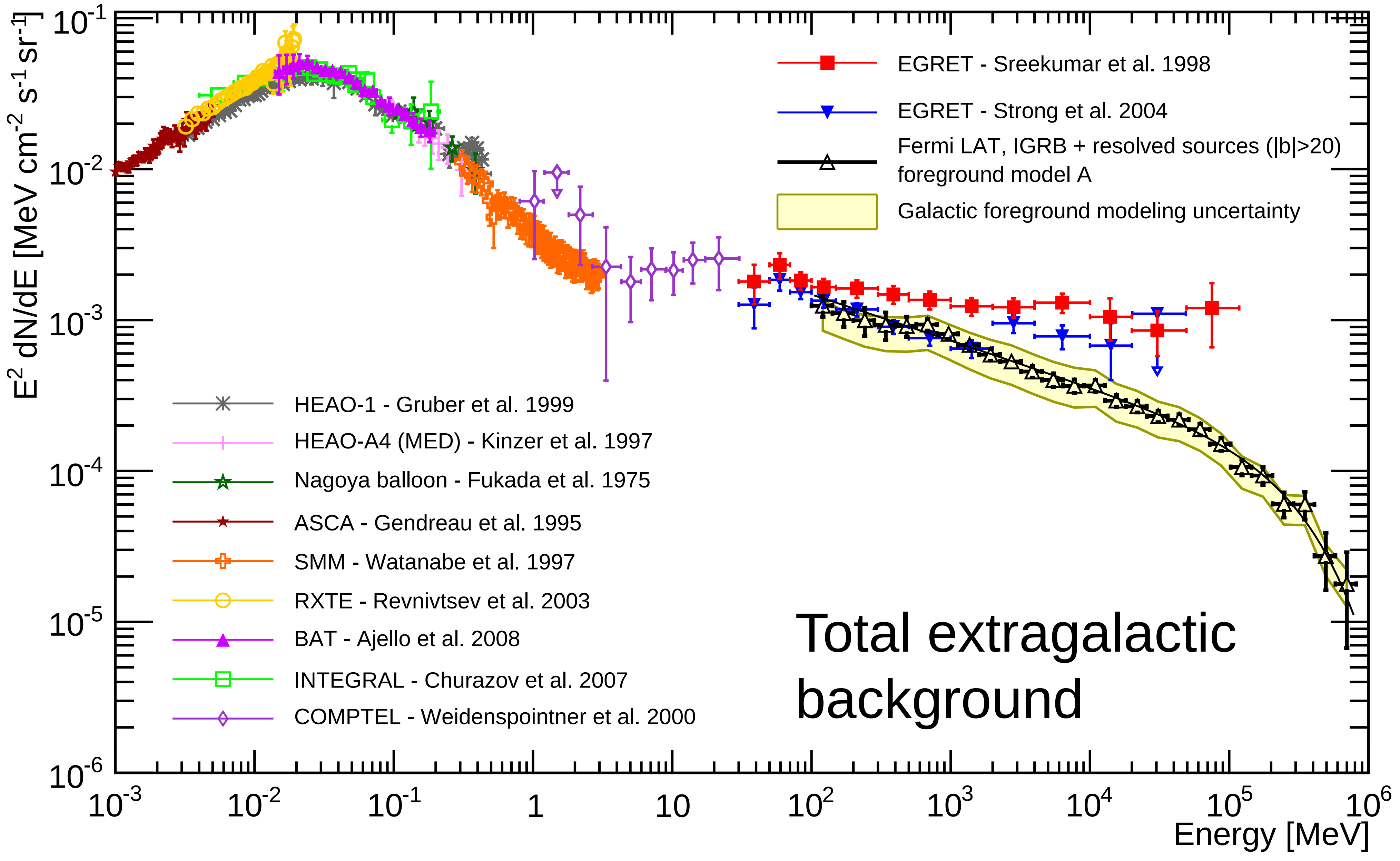

Fig. 10.— Comparison of the derived total EGB intensity (foreground model A) to other measurements of the X-ray and γ-ray background. The error bars on the LAT measurement include the statistical uncertainty and systematic uncertainties from the effective area parametrization, as well as the CR background subtraction. Statistical and systematic uncertainties have been added in quadrature. The shaded band indicates the systematic uncertainty arising from uncertainties in the Galactic foreground. (Note that the EGRET measurements shown are measurements of the IGRB. However, EGRET was more than an order of magnitude less sensitive to resolve individual sources on the sky than the *Fermi*-LAT.)

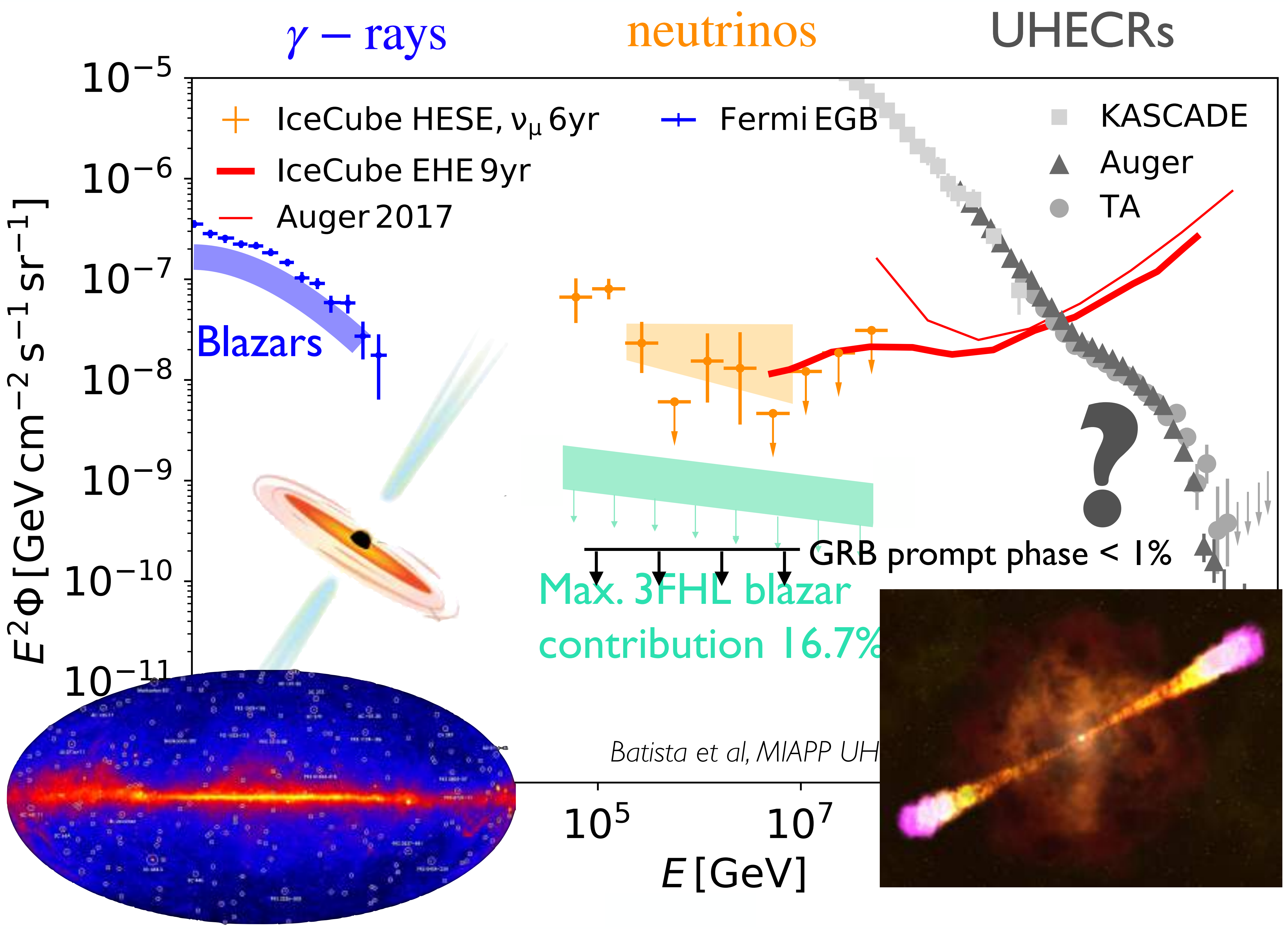

現状の観測結果を説明する理論モデルは？
その理論モデルを証明（棄却）するための測定量は？

Fermi-LAT collaboration, Astrophys.J. 799 (2015) 86

R.A. Batista et al., Front.Astron.Space Sci. 6 (2019) 23

ニュートリノ観測

Astrophysical neutrino detections by IceCube

8 years (ICRC 2017)

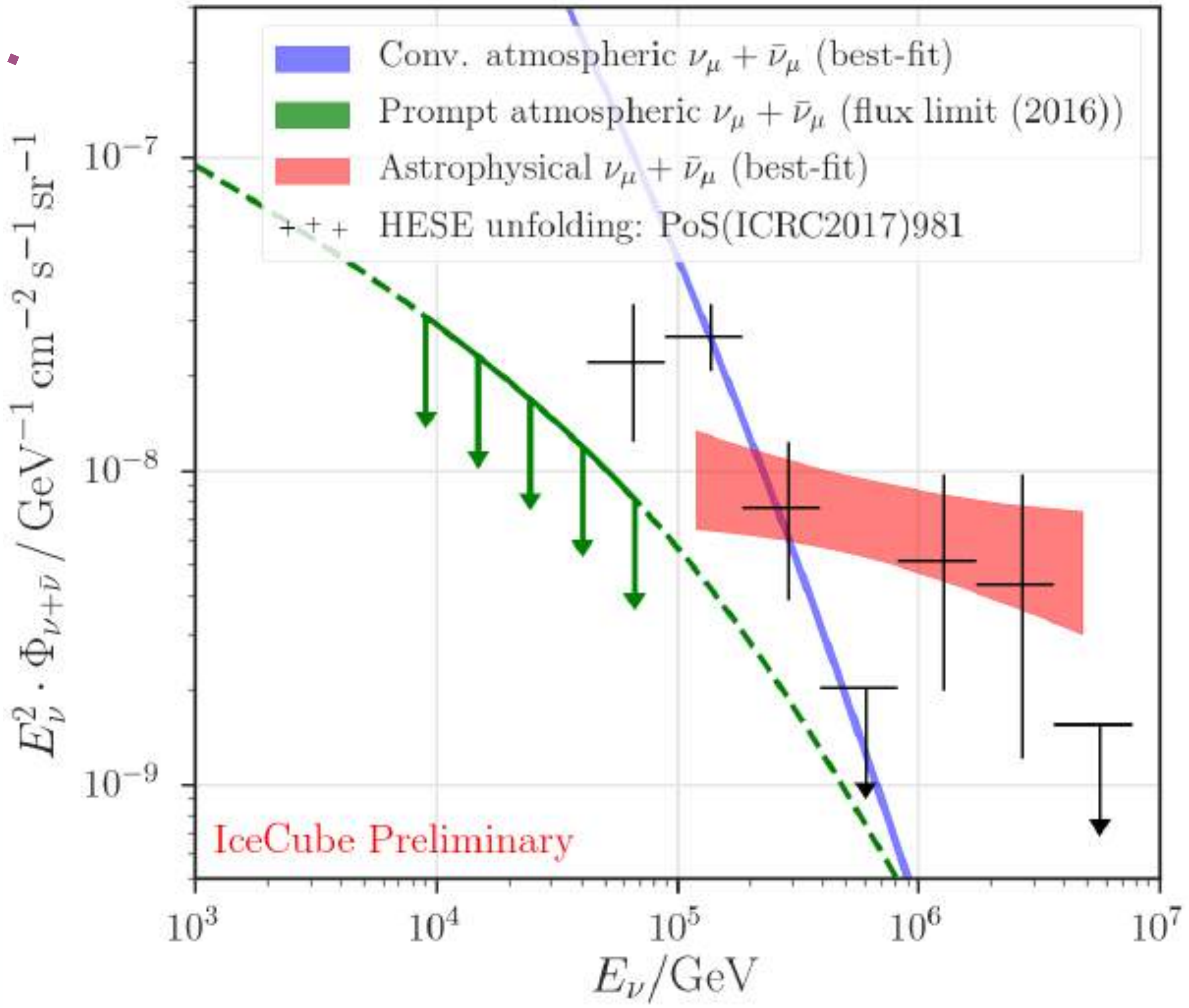

J. Santen in ICRC 2017

A high energy neutrino in coincidence with a flaring blazar

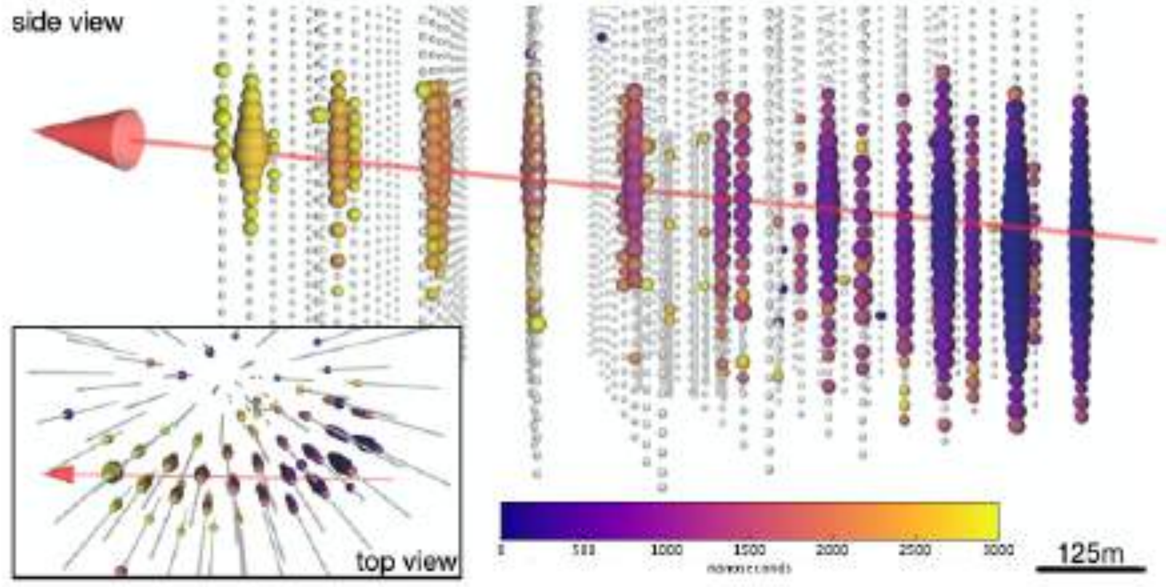

Science 13 Jul 2018: Vol. 361, Issue 6398

Science 13 Jul 2018: Vol. 361, Issue 6398

D. Williams in ICRC 2019

Correlation of IC170922A with TXS 0506+056 preferred to chance at 3σ level

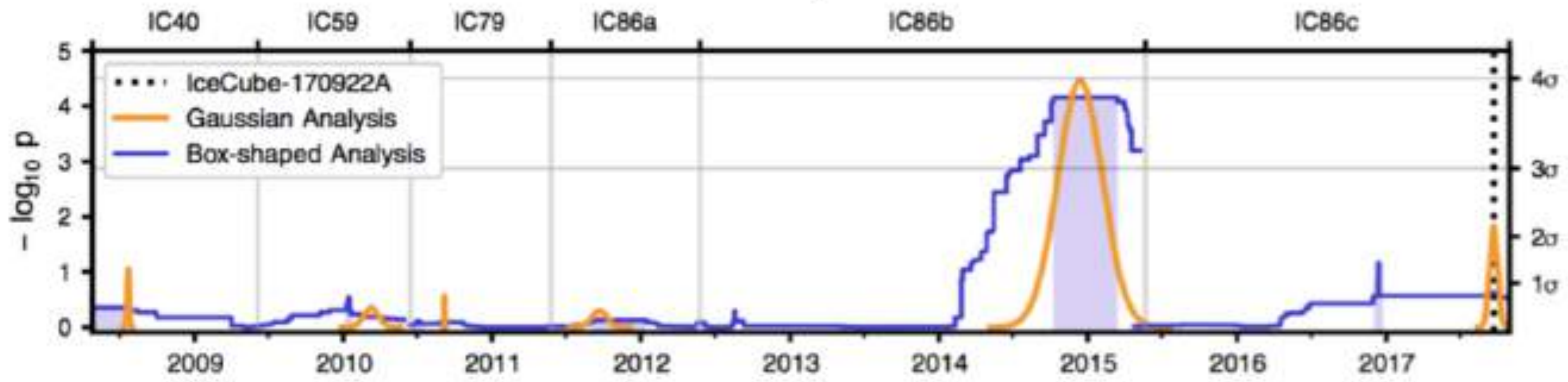

Excess of neutrinos observed between September 2014 and March 2015
Background only hypothesis rejected at 3.5σ

>300 MeV gamma-ray (Fermi-LAT)

Garrappa et al 2019

Neutrino-driven multi-messenger

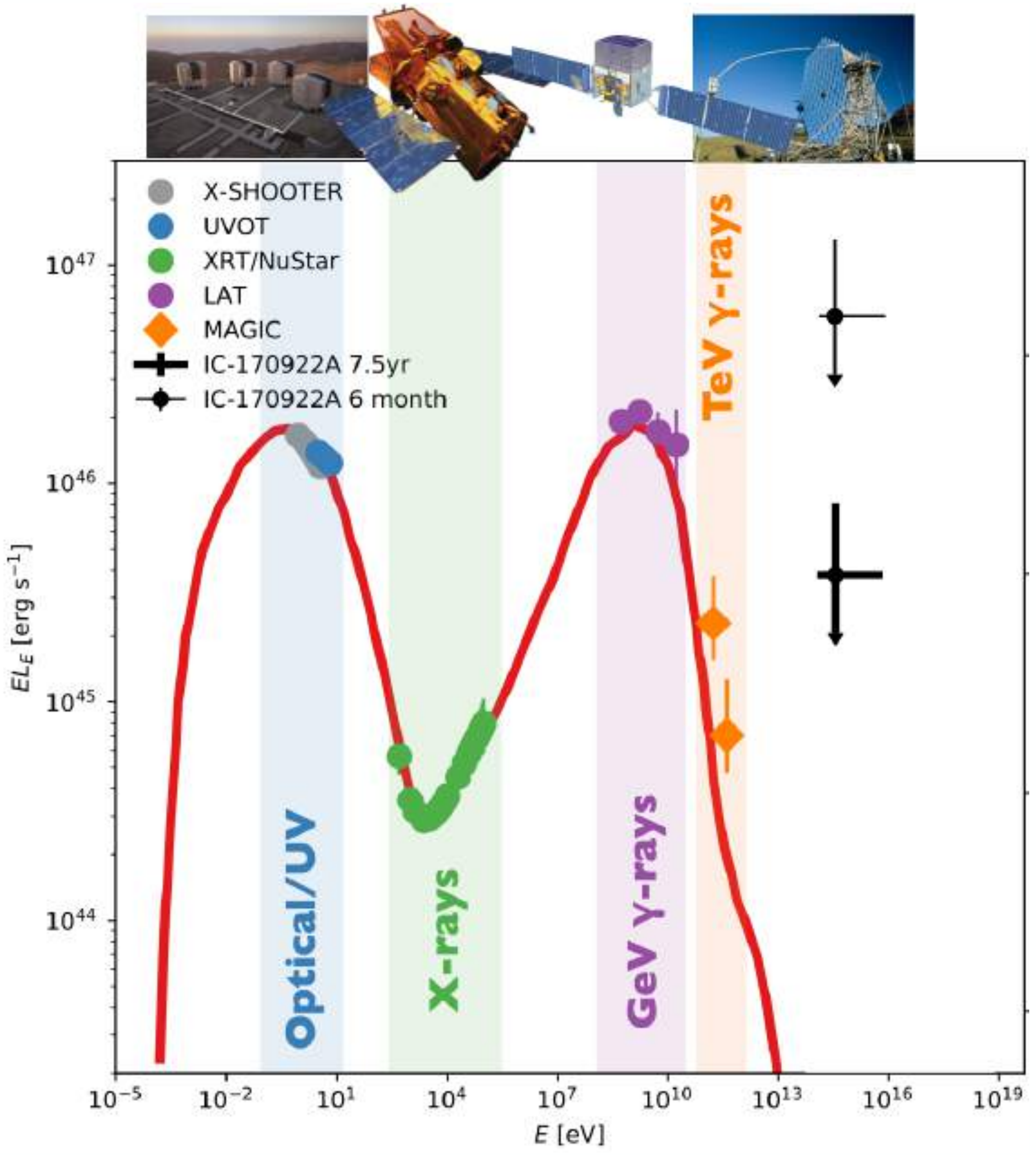

F. Oikonomou in 20-years Auger symposium

ニュートリノも点源が見えてこない

IceCube high-energy events > 30 TeV (2010 - 2016)

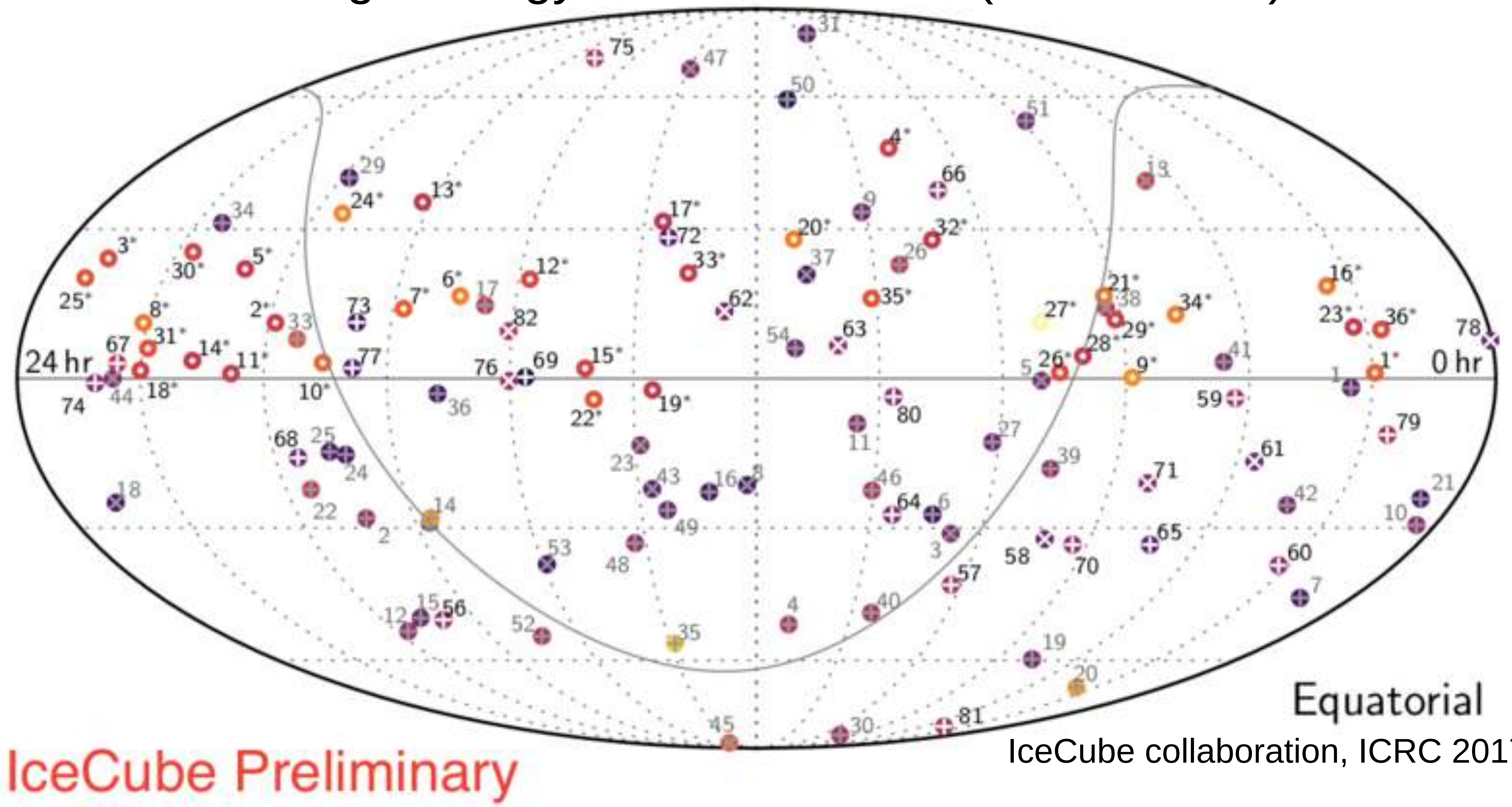

IceCube collaboration, ICRC 2017

UHECRとneutrinoの相関解析

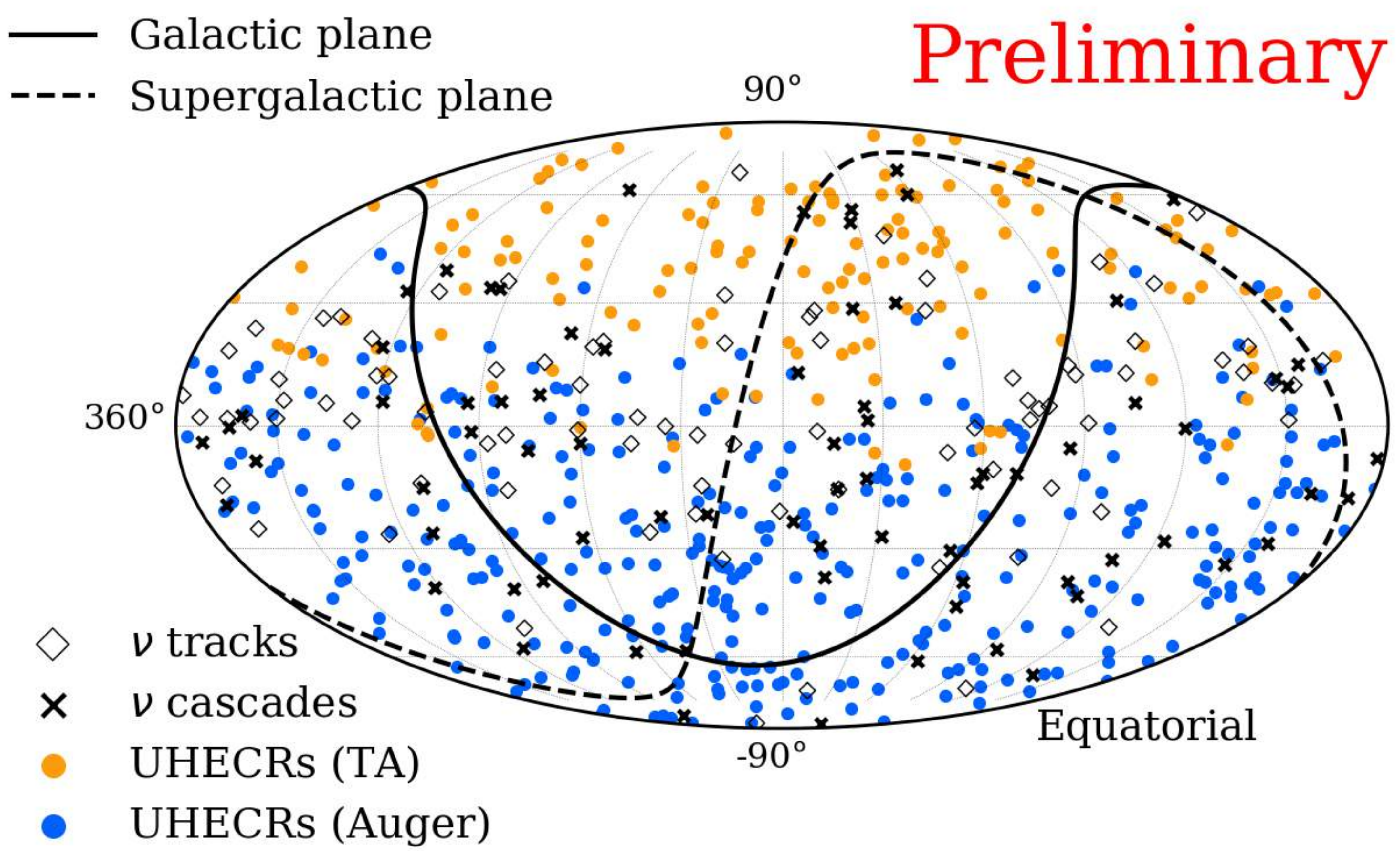

Figure 1: The UHECR events from TA and Auger are shown as orange and blue dots, respectively. The neutrino track- and cascade-like events from IceCube (HESE [10], EHE [11], 7-year through-going muons [12] samples) and ANTARES [20] are shown as black empty diamonds and crosses, respectively.

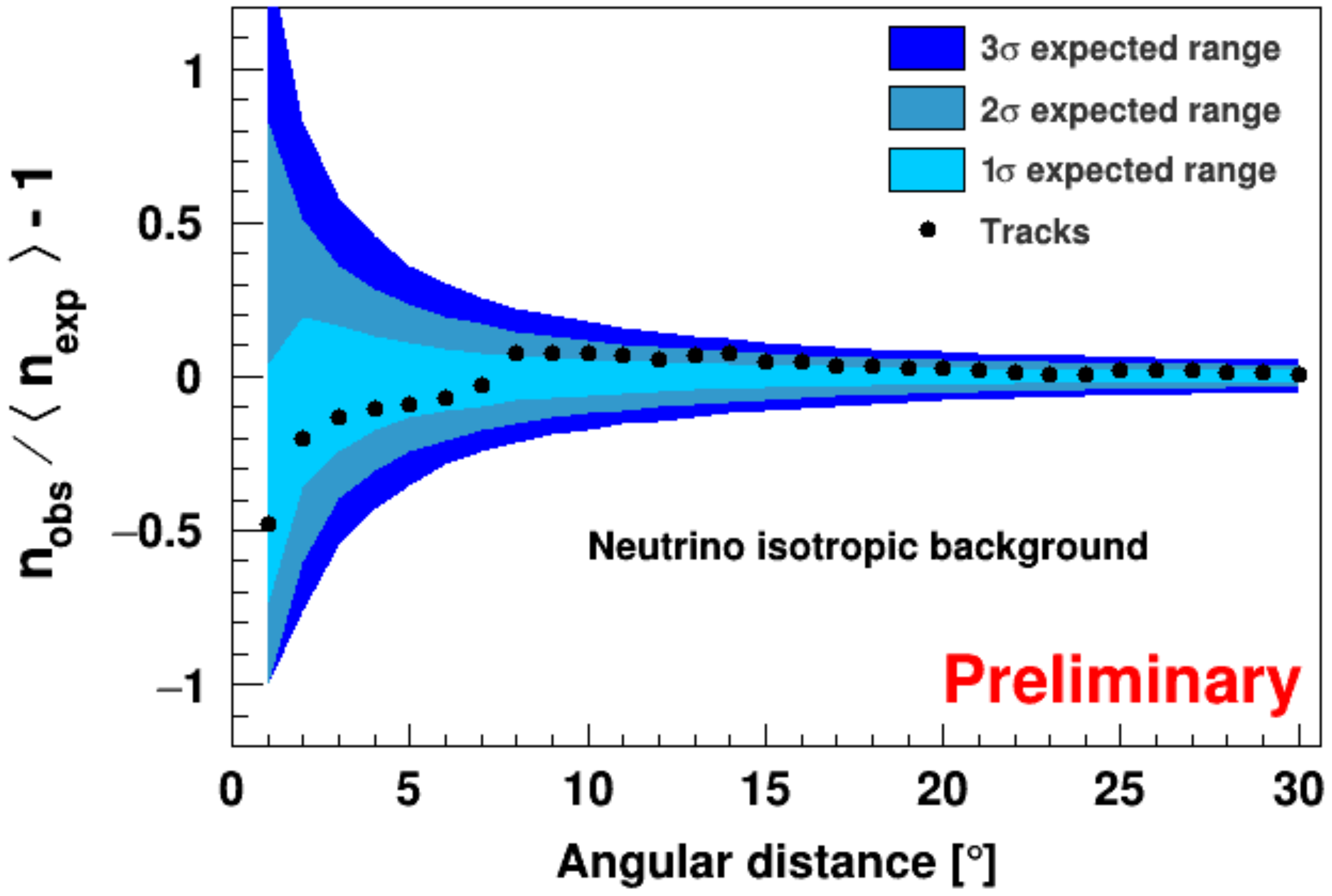

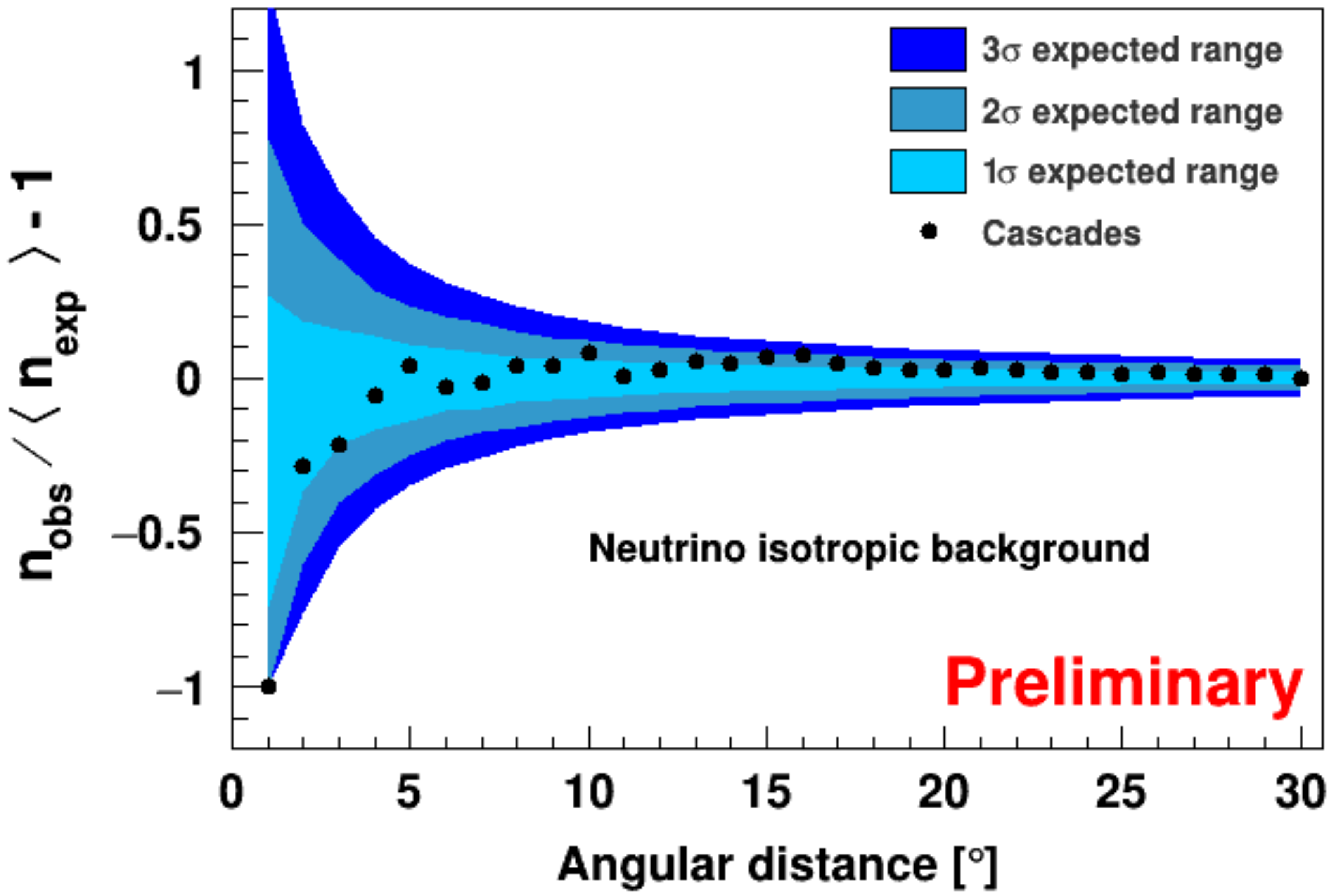

Auger: 324 events, TA: 142 events (A. Barbano et al., ICRC 2019)

宇宙線の点源が見えてこない

高エネルギーニュートリノ (>$10^{13.5}$ eV)

IceCube high-energy events > 30 TeV (2010 - 2016)

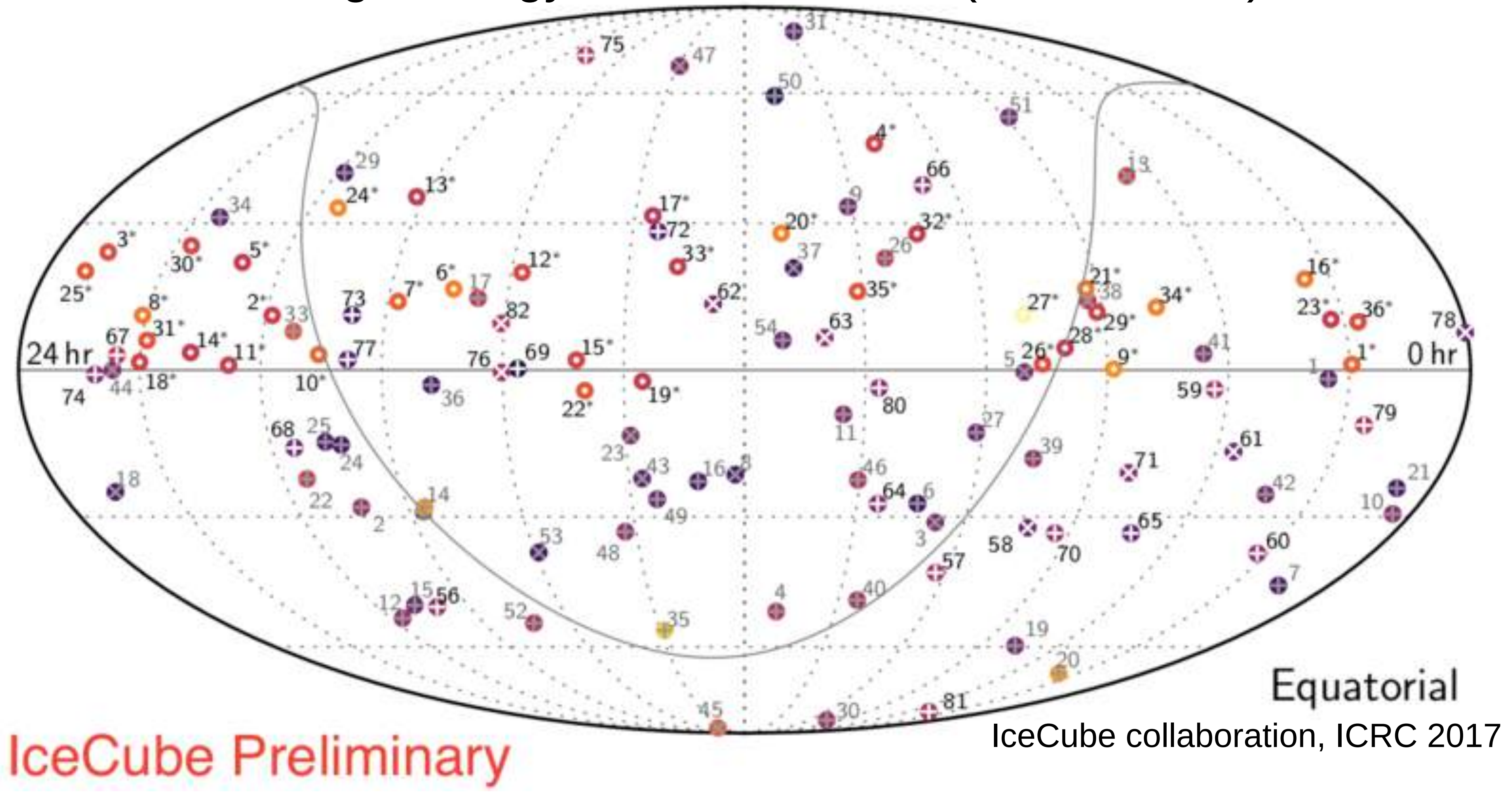

IceCube collaboration, ICRC 2017

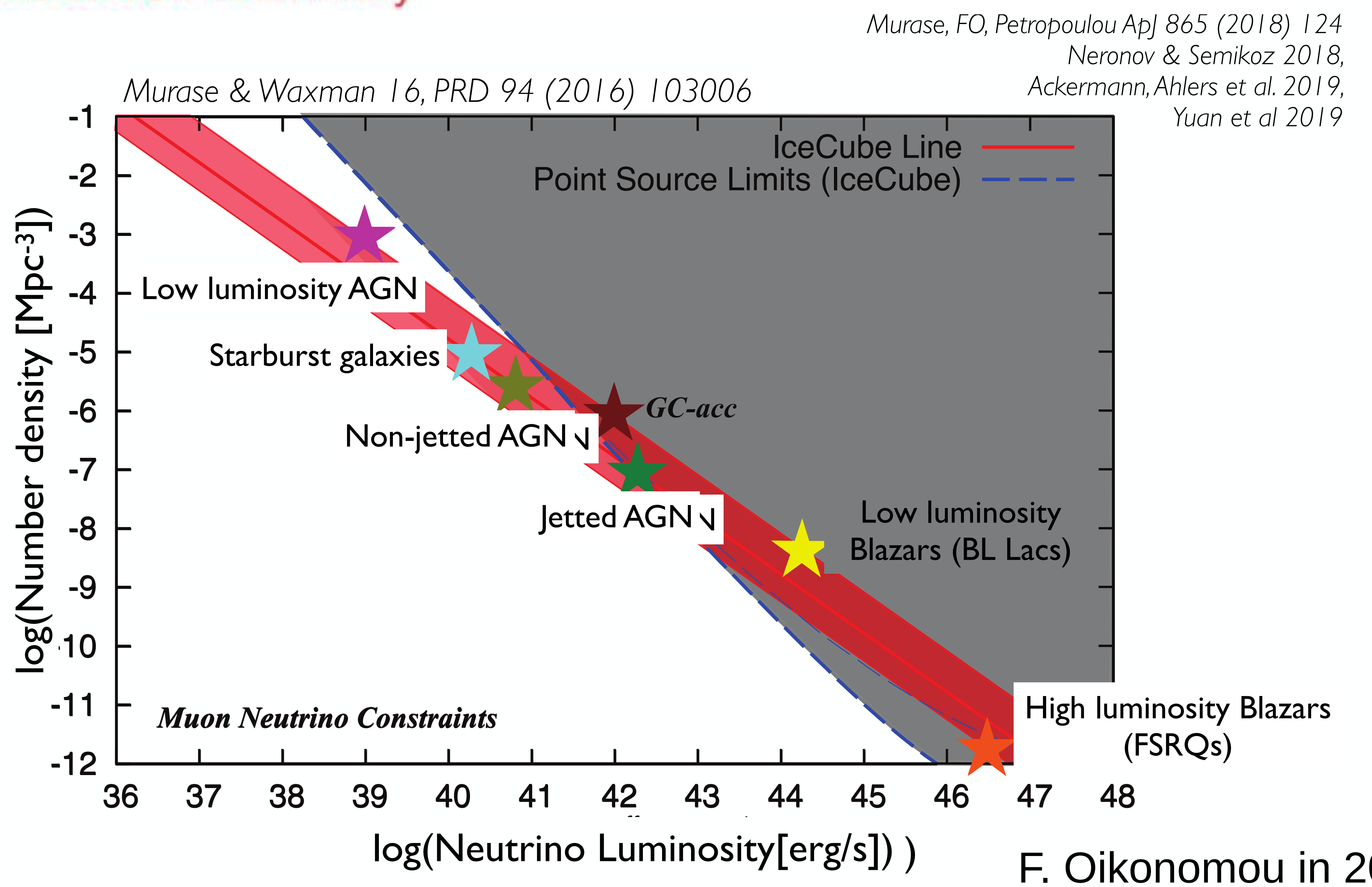

最高エネルギー宇宙線（>$10^{19.7}$ eV）

Confidential

Data from EPJ Web of Conferences **210**, 01005 (2019)

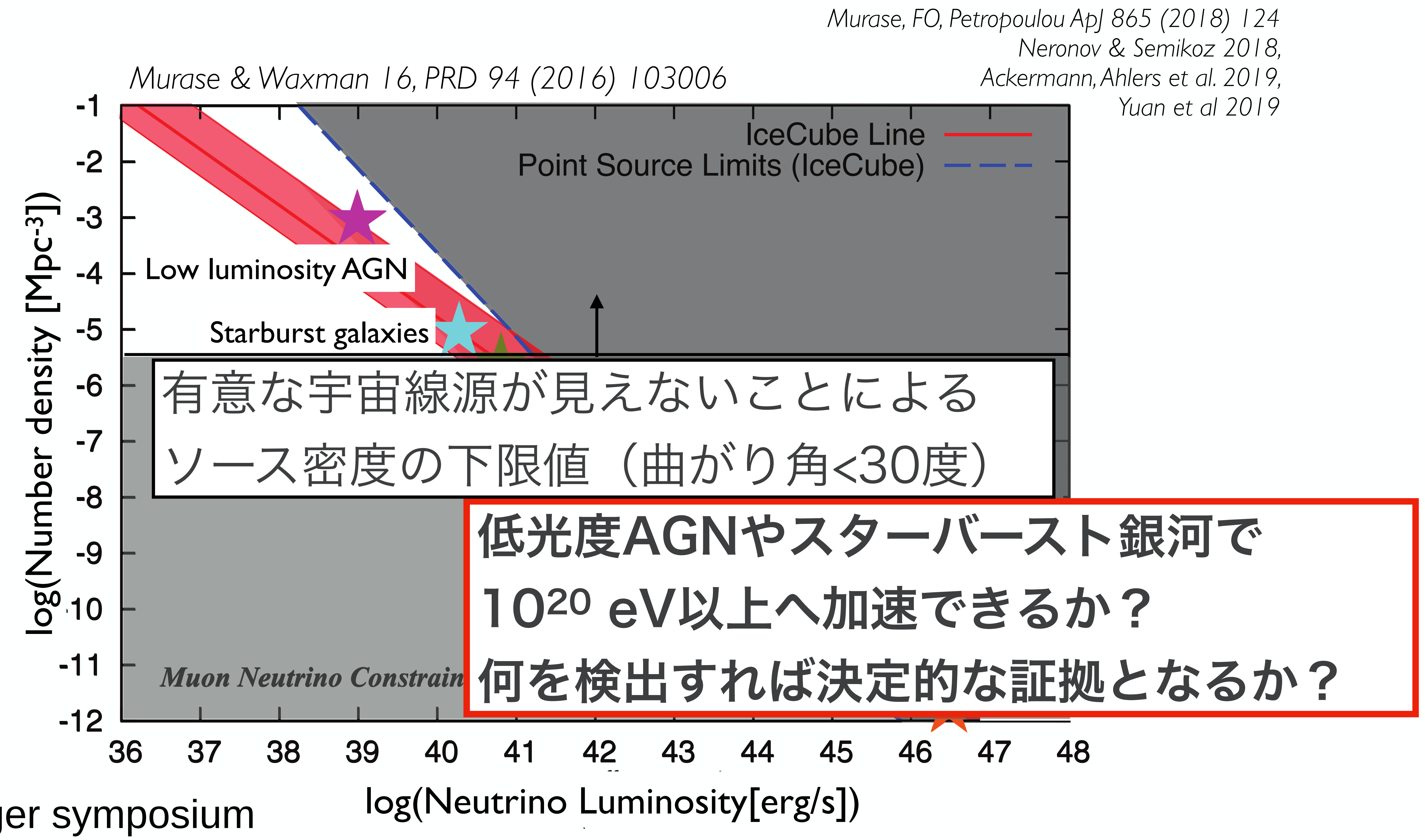

F. Oikonomou in 20-years Auger symposium

ガンマ線観測？

陽子起源　**超新星残骸**

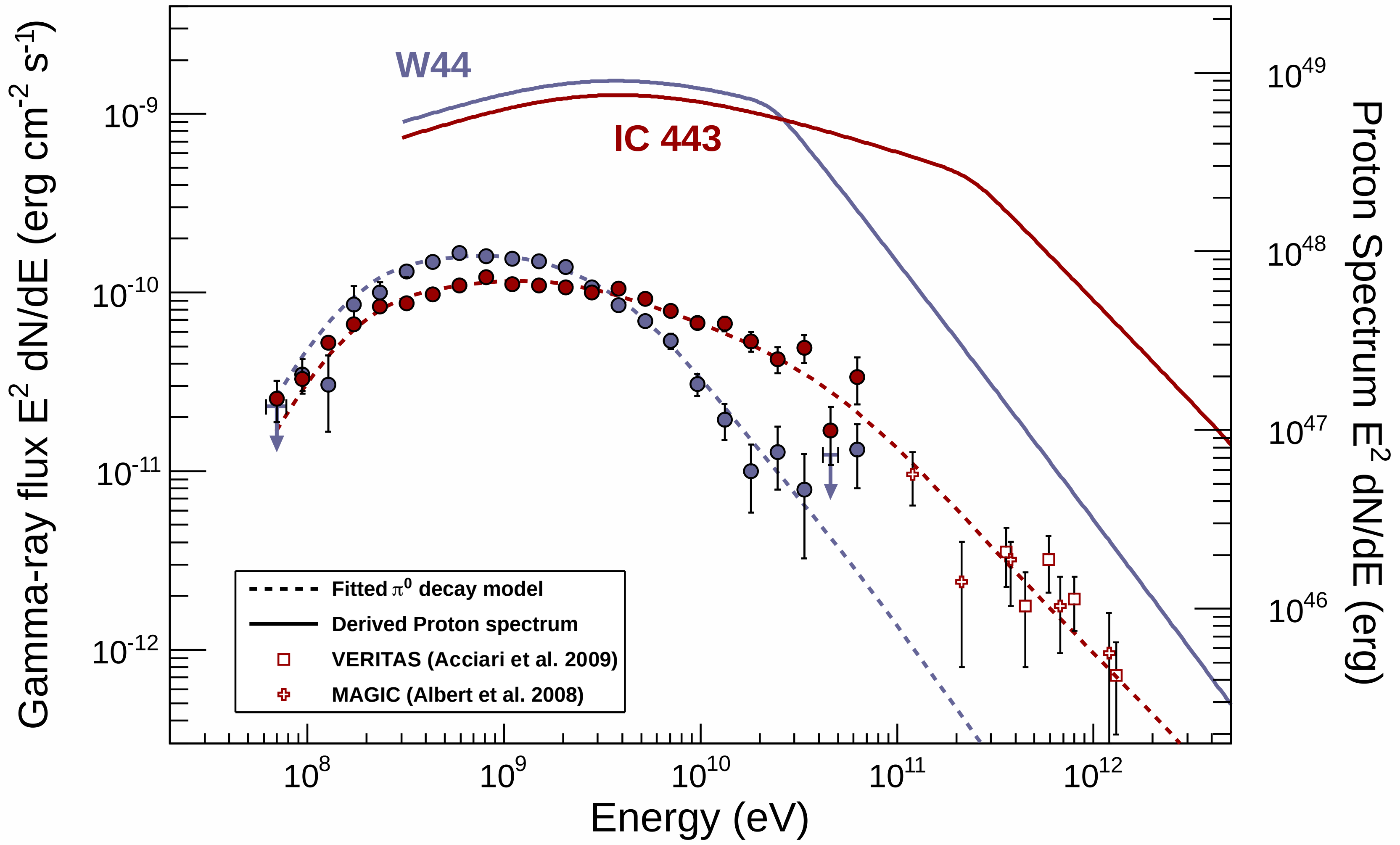

Fermi-LAT collab. Science 339, 807 (2013)

陽子起源？　銀河中心

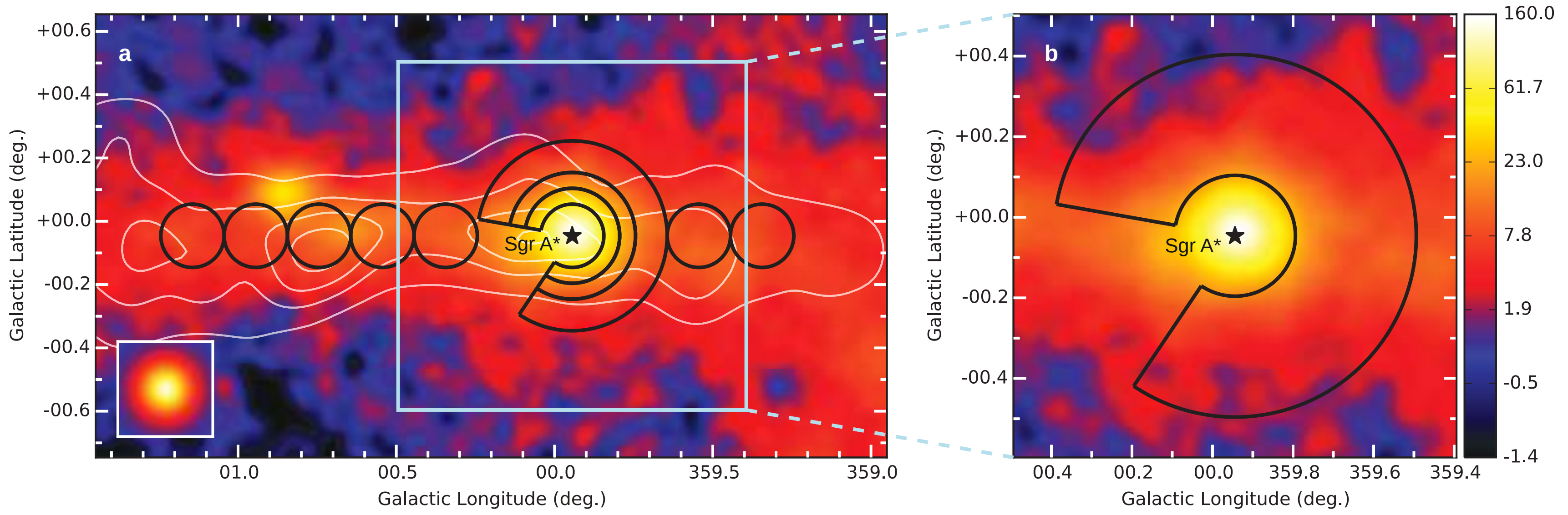

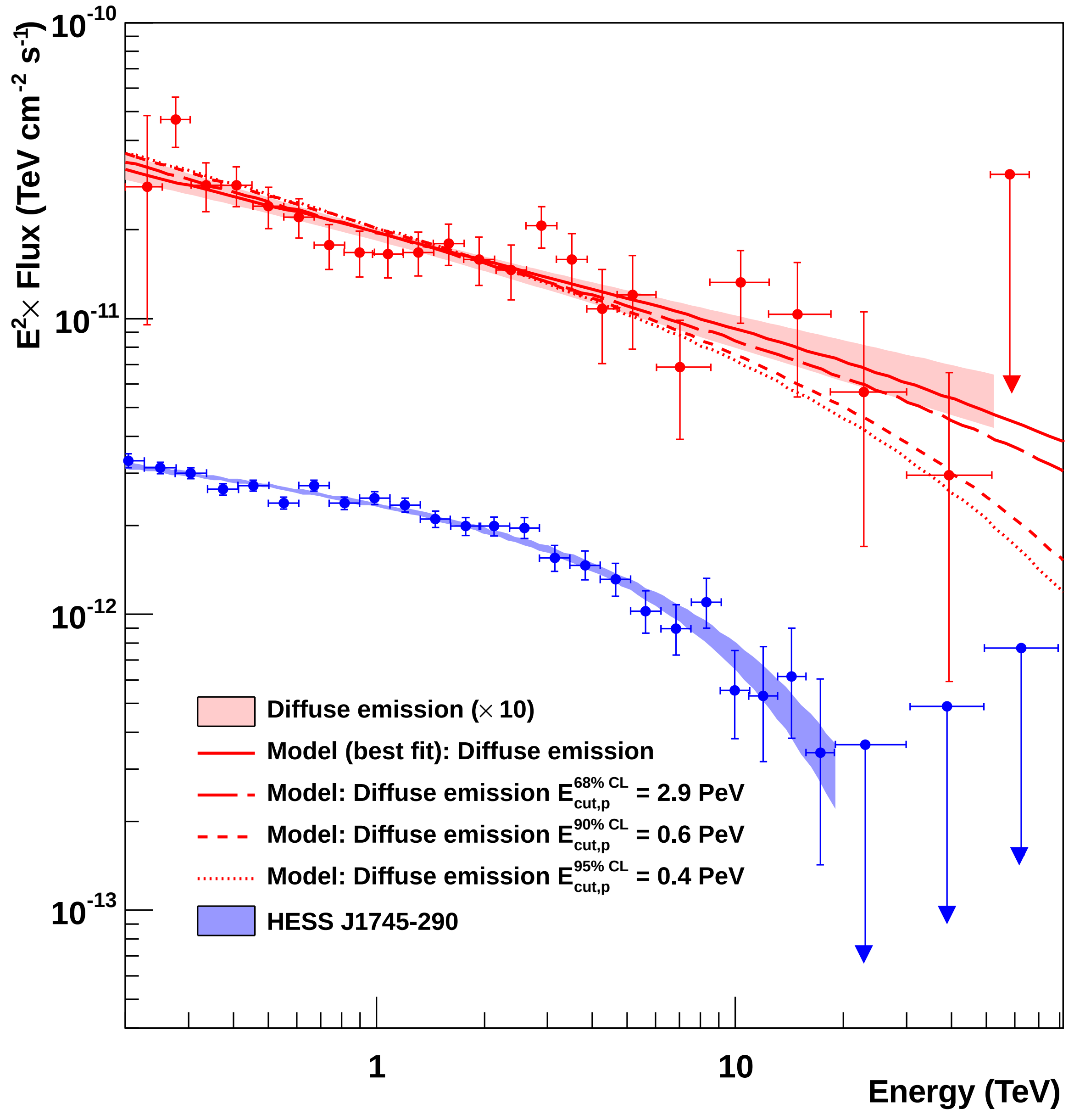

H.E.S.S. collab., Nature 531 (2016) 476

電子起源　ガンマ線バースト190114C

MAGIC collaboration, Nature 575 (2019) 459

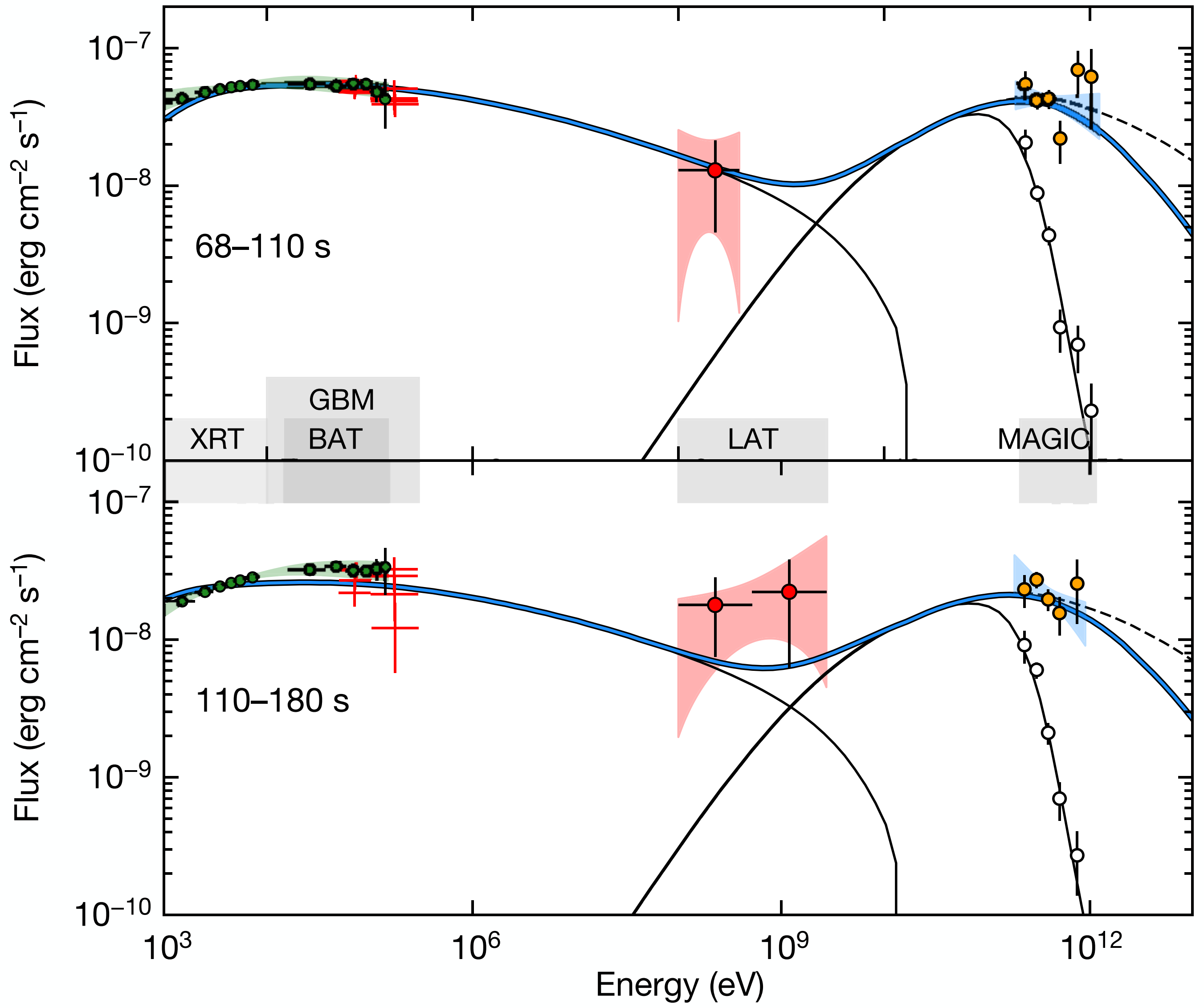

電子起源　カニ星雲からの100 TeV放射

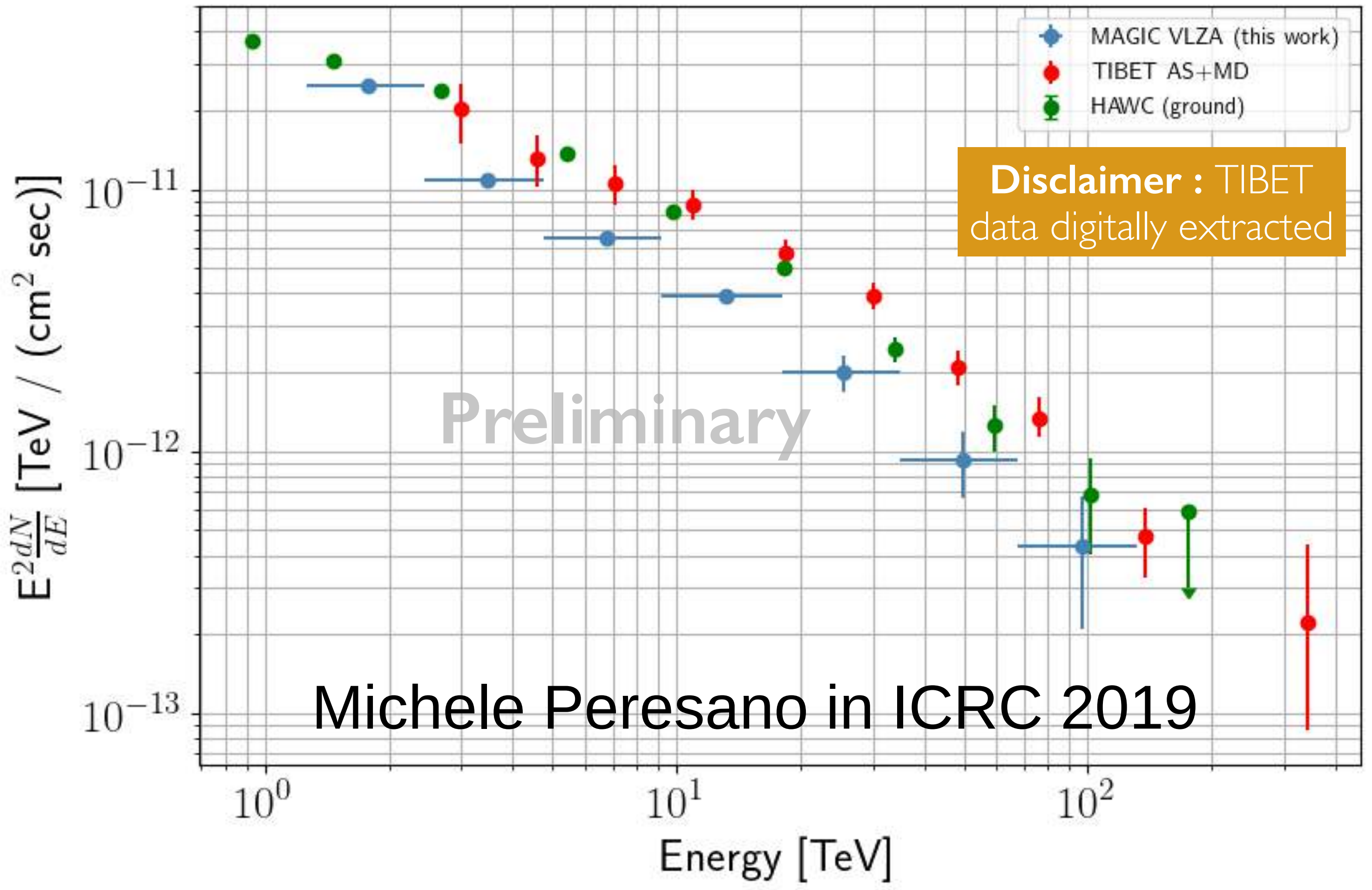

Michele Peresano in ICRC 2019

- 超新星残骸以外では陽子加速の決定的な証拠は見つかっていない。

銀河磁場と質量組成に依存しない測定量の予言

0 - 50 Mpc

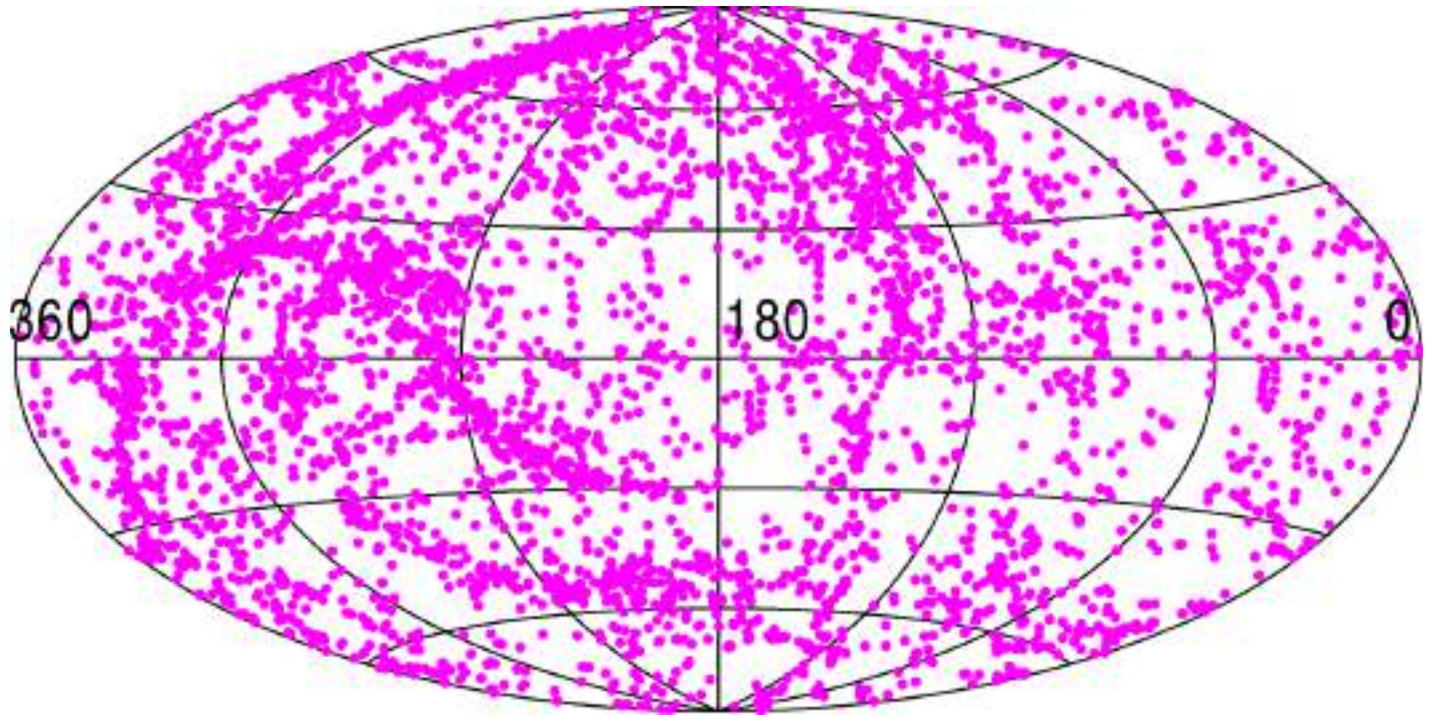

50 - 100 Mpc

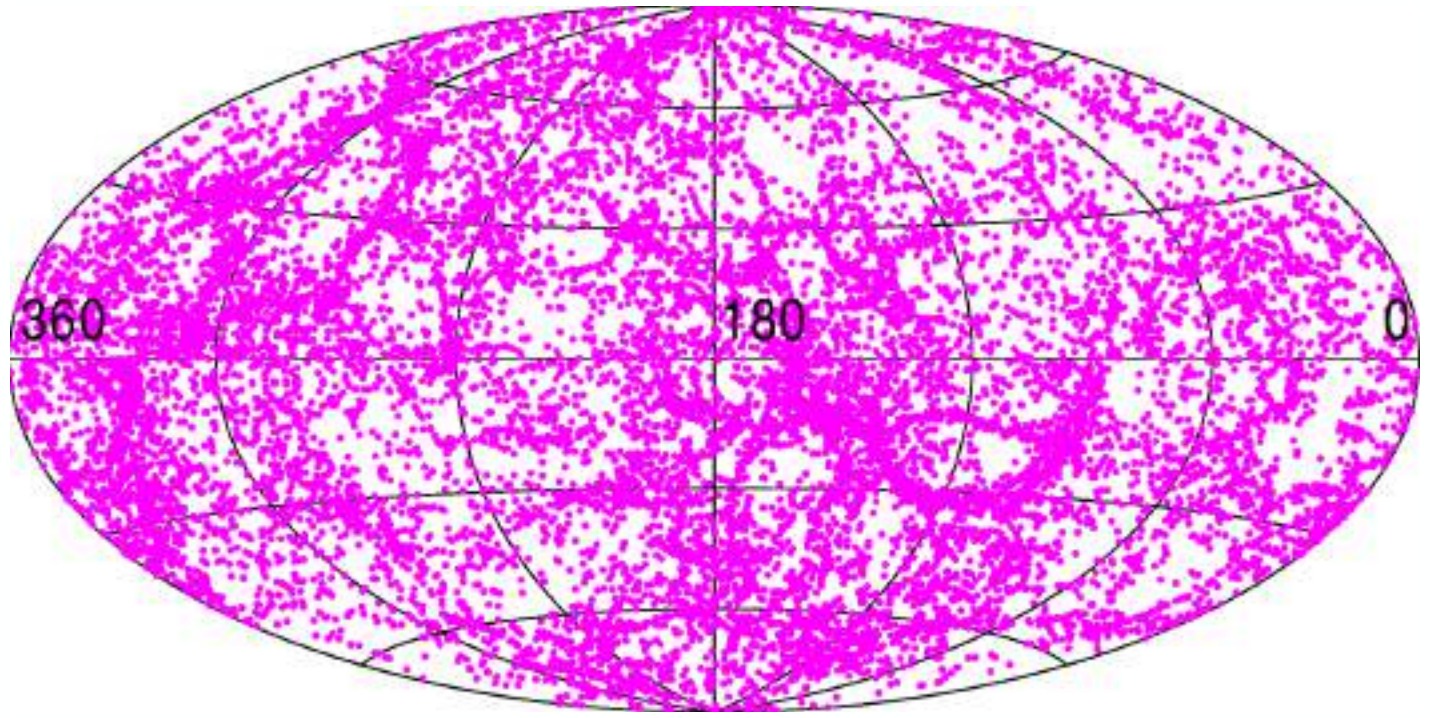

100 - 250 Mpc

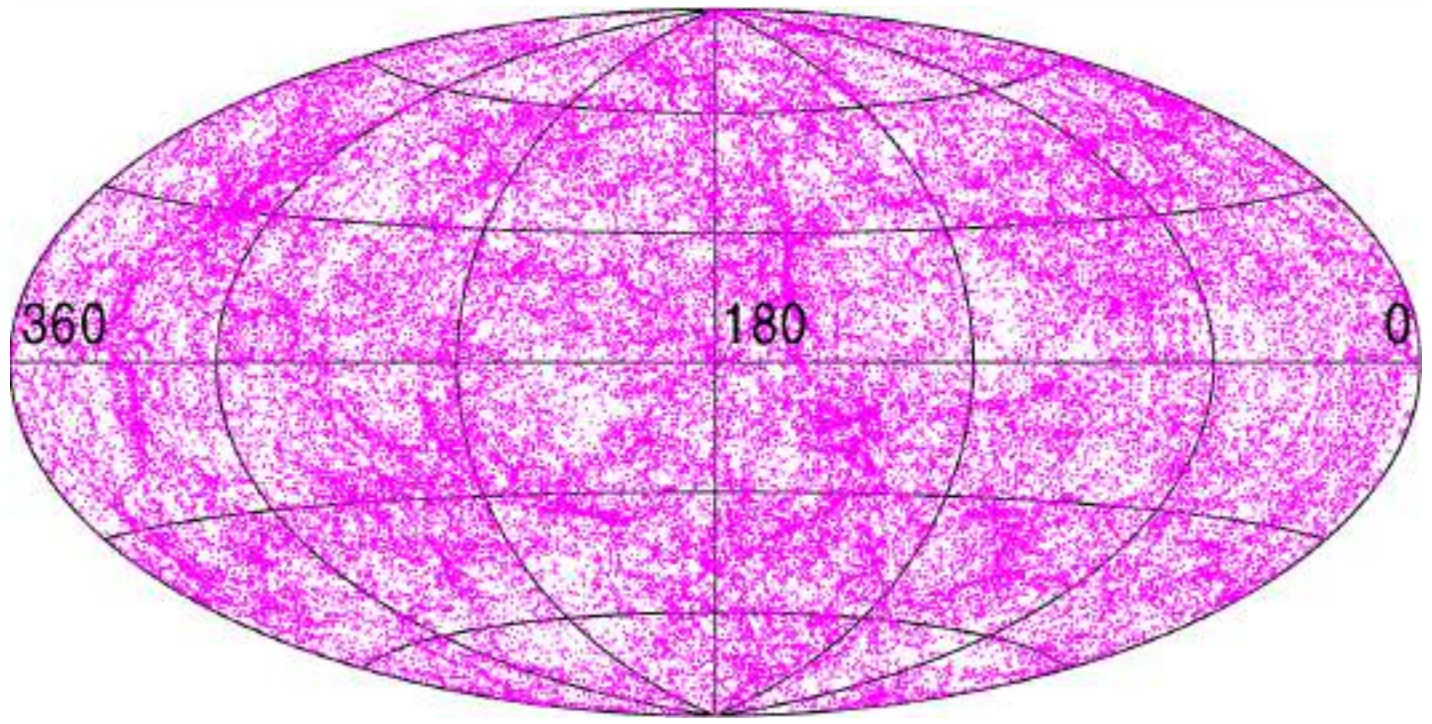

A. di Matteo and P. Tinyakov, Mon.Not.Roy.Astron.Soc. 476 (2018) 715

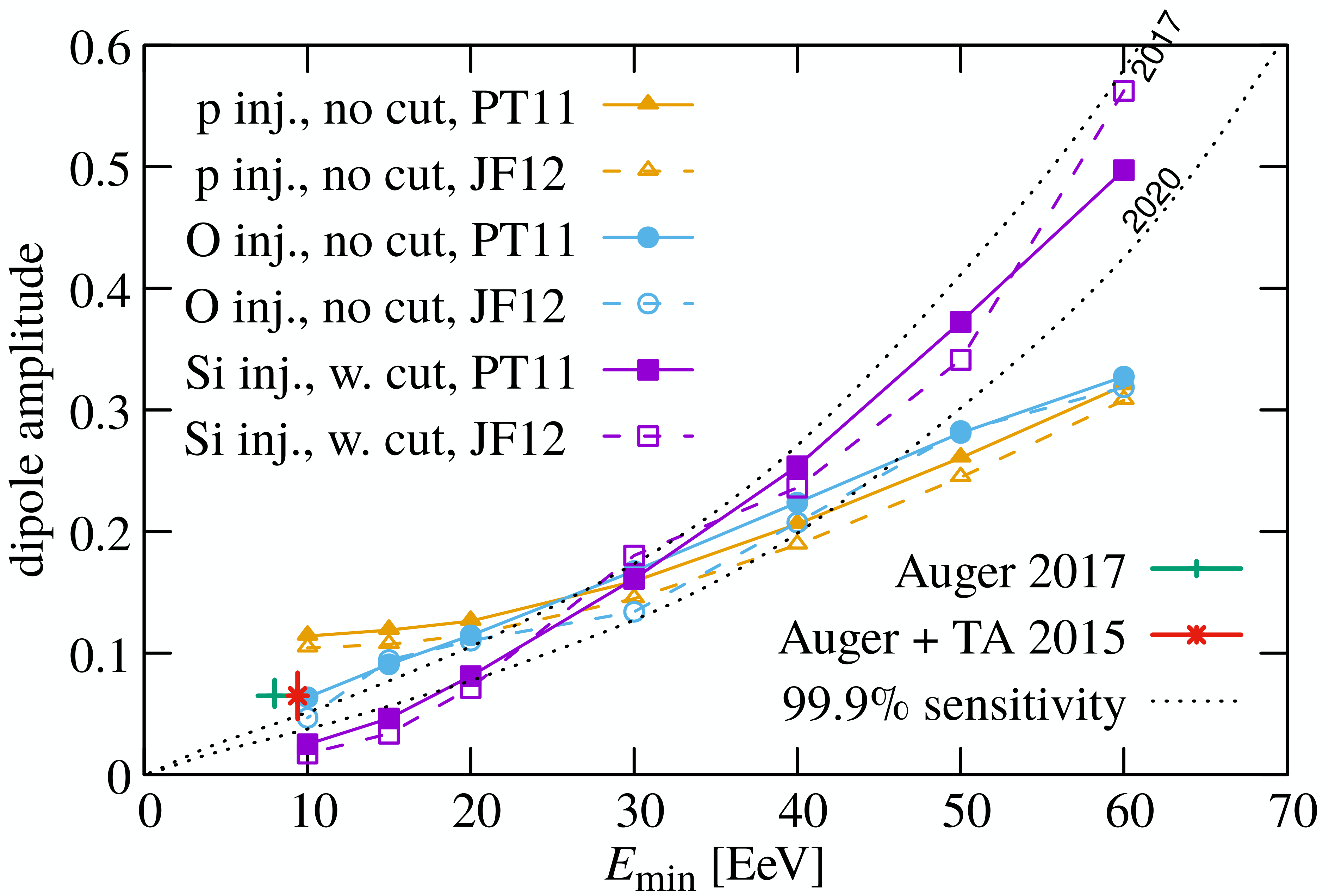

Figure 6. The magnitude of the dipole as a function of the energy threshold $E_{\rm min}$ for the three injection models and two GMF models we considered. The points labelled "Auger + TA 2015" and "Auger 2017" show the dipole magnitude reported in Deligny (2015) and Taborda (2017) respectively. The dotted lines show the 99.9% C.L. detection thresholds using the current and near-future Auger and TA exposures (see the text for details).

遠くまで見えると等方的に天体が分布
(2MASS Redshift survey galaxies)

30 EeVで磁場・質量組成への依存が小さい
天体起源であるかを検定できる

多波長・多粒子観測の連携

Starburst galaxies?

ニュートリノのホットスポット

(2.9σ)

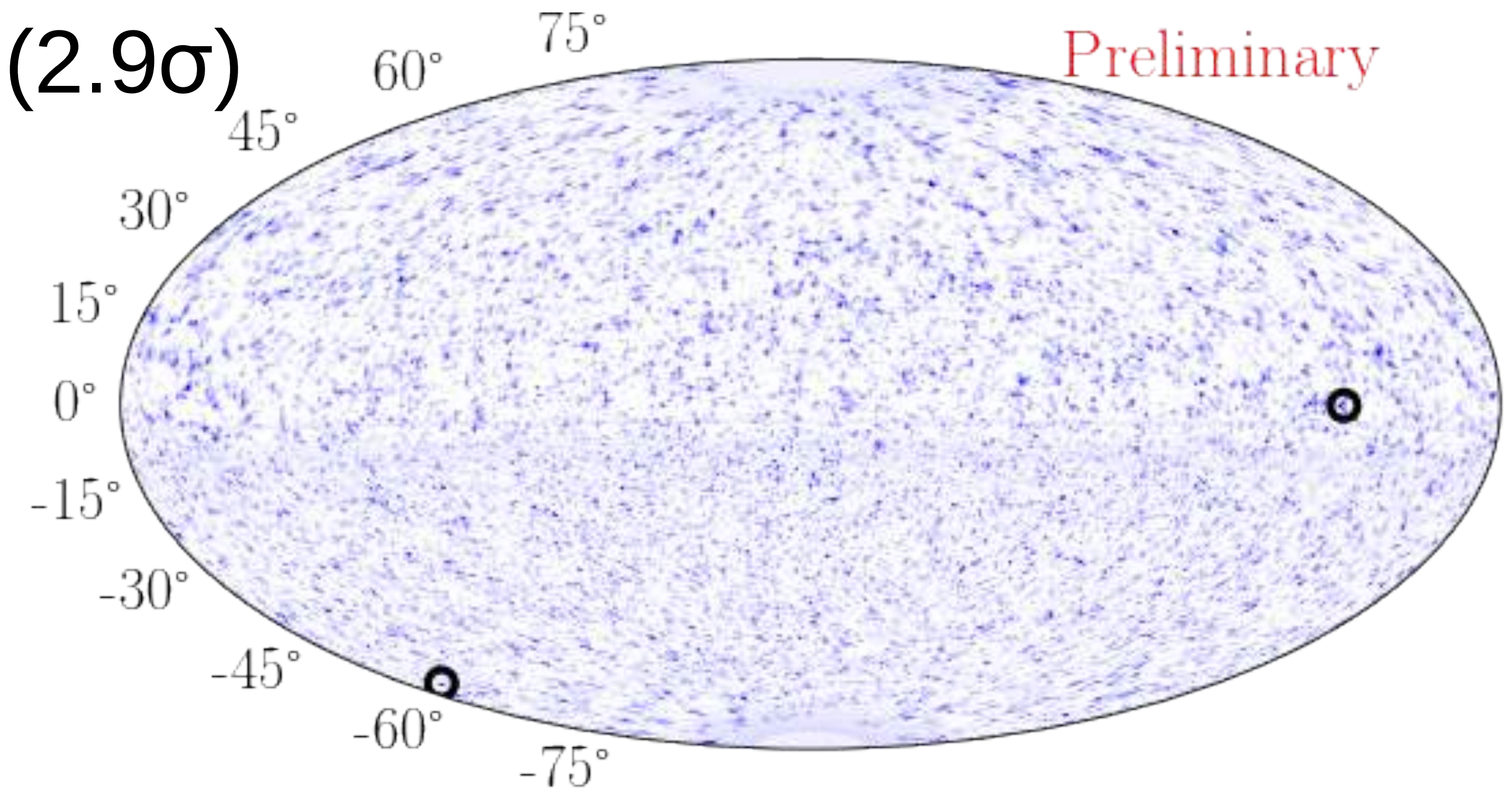

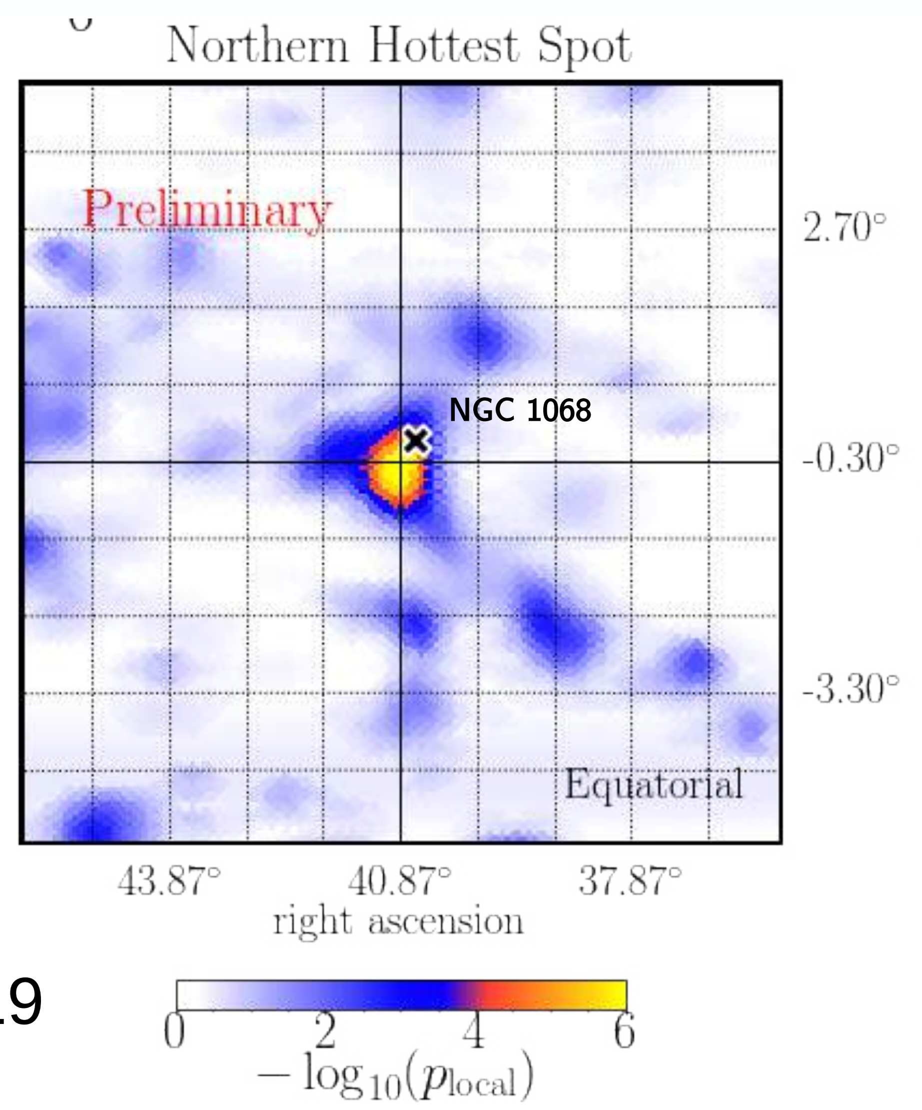

F. Halzen in ICRC 2019

Powerful black hole jet?

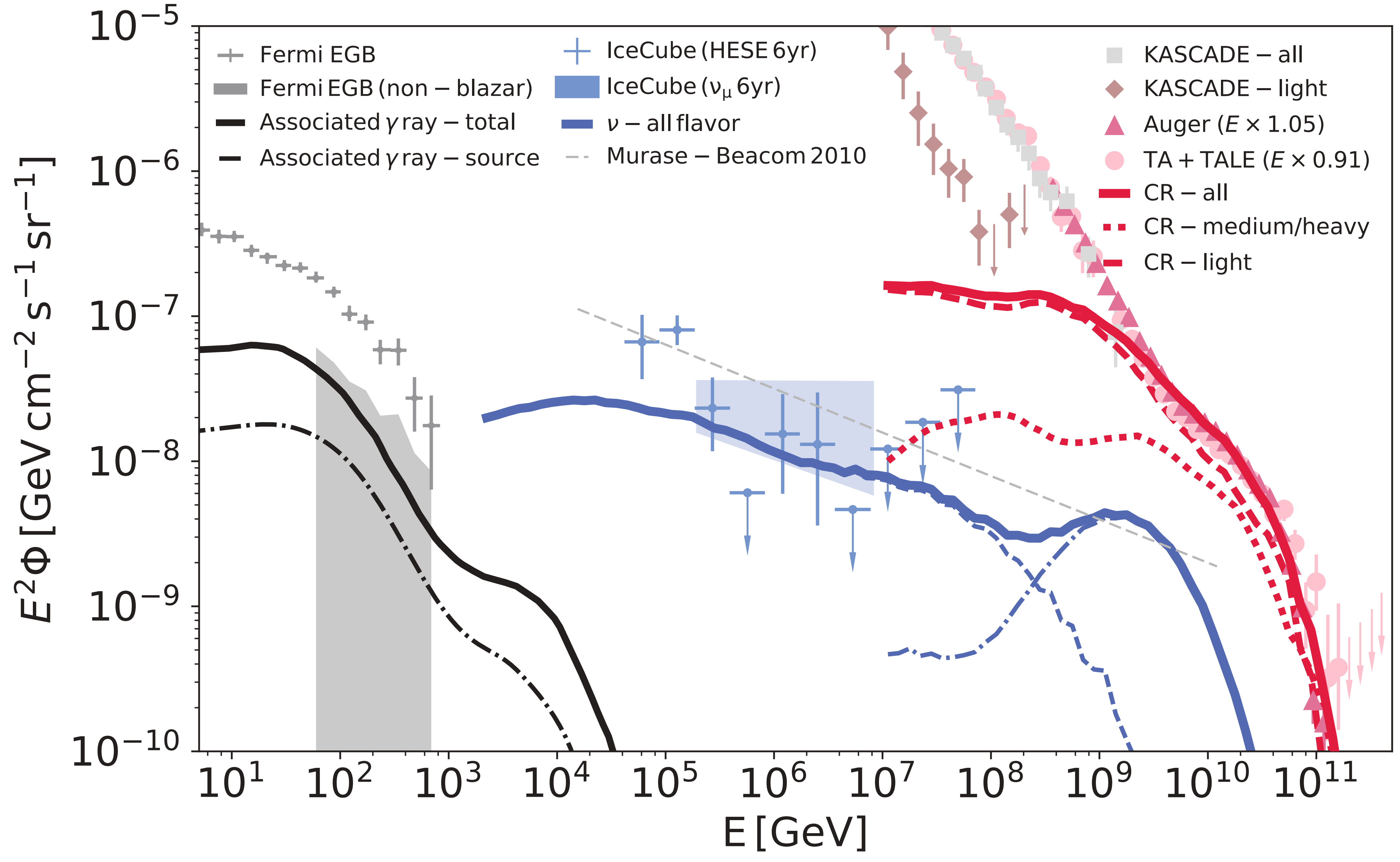

K. Murase, K. Fang, Nature Phys. 14 (2018) 396-398

近傍スターバースト銀河の

電波強度マップ

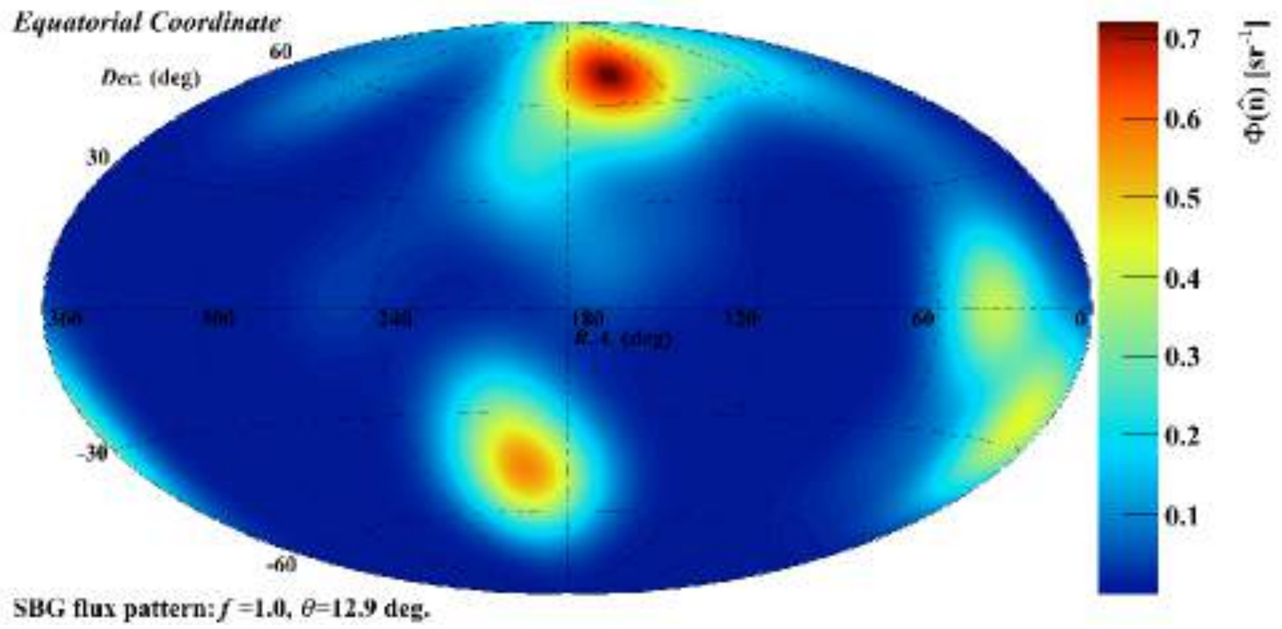

最高エネルギー宇宙線(>$10^{19.7}$ eV)

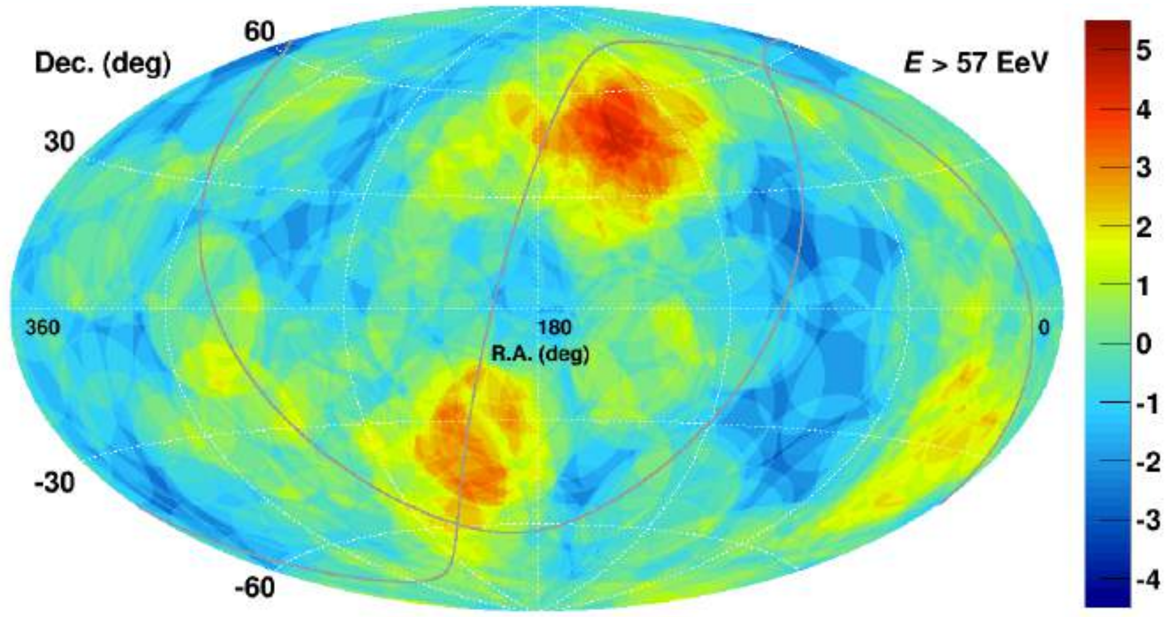

近傍天体との相関解析: 4.5σ (スターバースト銀河11%+

等方分布89%, >$10^{19.6}$ eV)

L. Caccianiga in ICRC 2019

Galactic coordinates

Centaurus A

3.9 σ effect (post-trial)
for E>37 EeV, 28⁰ window

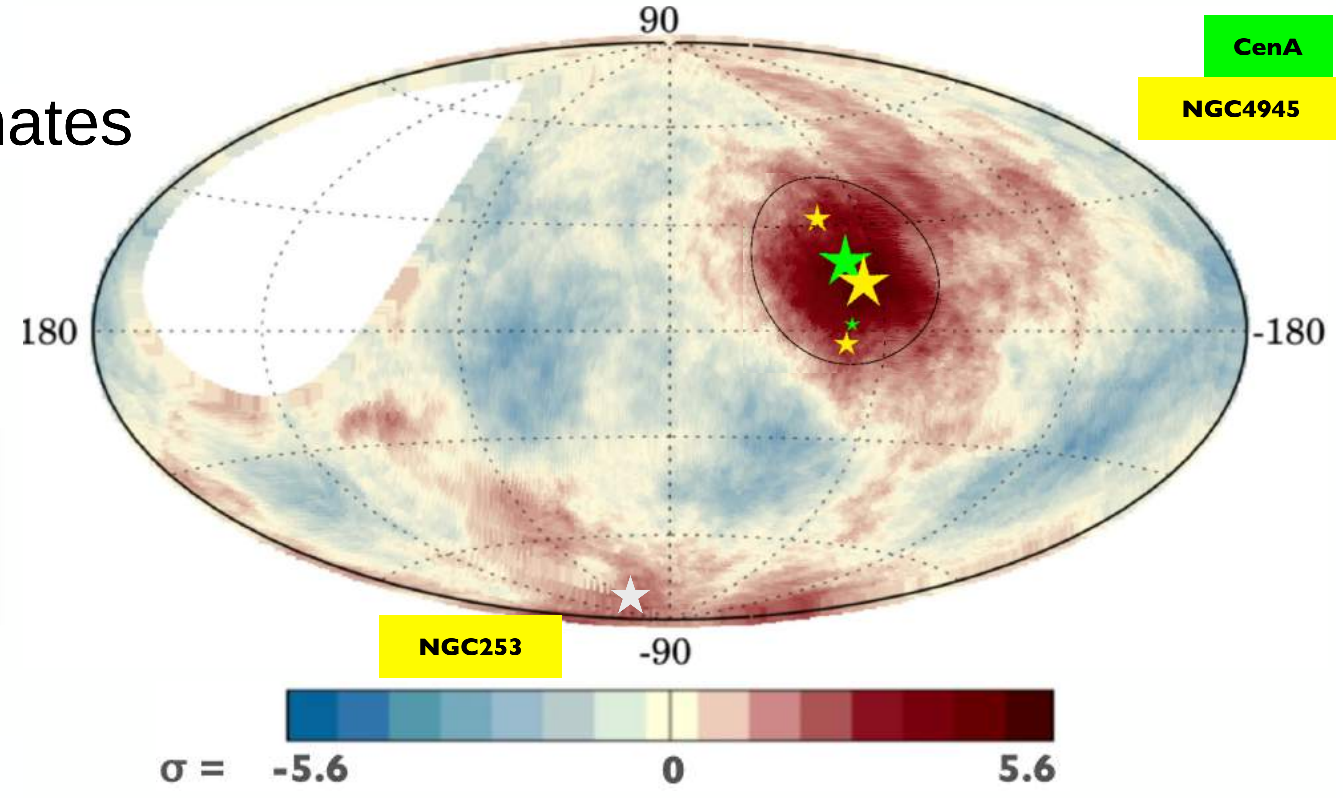

A. Castellina in ICRC 2019

極高エネルギー宇宙線源の検出(>5σ)が近づきつつある

Connecting high-energy astroparticle physics for origins of cosmic rays and future perspectives

December 7 - 10, 2020

Kyoto University, Kyoto, Japan

http://www2.yukawa.kyoto-u.ac.jp/~crphys2020

http://www2.yukawa.kyoto-u.ac.jp/~crphys2020/

系外起源解明へ向けた開発研究

- 極高エネルギー宇宙線の感度を1桁向上し、宇宙線源を特定する
  - 低コスト型の望遠鏡を大量に並べる。Fluorescence-detector Array of Single pixel Telescopes (FAST), https://www.fast-project.org
  - M. Malacari et al., Astropart.Phys. 119 (2020) 102430
  - 京都大学プレスリリース「次世代天文学を拓く新型の宇宙線望遠鏡を開発 ー極高エネルギー宇宙線で極限宇宙を観るー」, http://www.kyoto-u.ac.jp/ja/research/research_results/2019/200123_3.html

「地惑宇宙における物質創生および循環の解明」

- 研究領域
  - 宇宙線の質量組成の精密測定（CALET、TALE、TA）
  - X線観測による組成比測定（超新星）
  - 電波・赤外観測による宇宙塵の組成測定（ALMAによるダスト測定、アルミナダスト形成と進化）
  - NSNS衝突からの元素合成？
  - 銀河磁場の精密測定？